The Jansky-Very Large Array Sky Survey (VLASS)

The VLA Survey Science Group*

January 15, 2015

Contents

*A full list of those who directly contributed ideas and/or writing that led to this proposal can be found in Appendix A.

1 Executive Summary/Overview

The Very Large Array Sky Survey (VLASS) is a community-driven project initiated to develop and carry out a next-generation large radio sky survey using the recently upgraded Karl G. Jansky Very Large Array (VLA). VLASS will open the radio sky to a new exploration of the time and spectral domains. VLASS was developed through unprecedented community involvement and consensus building, including a public workshop at the AAS, the submission of 22 white papers and long competitive debate in the Survey Science Group (SSG), along with its community working groups of more than 200 multi-wavelength astronomers (see Appendix A). A careful internal NRAO scientific and technical review then provided critical additional input, leading to the optimization of the observing plan. The resulting VLASS survey definition is designed to provide a broad, cohesive science program that will both deliver forefront scientific impact in identified science themes and generate unexpected scientific discoveries. VLASS will engage radio astronomy experts, multi-wavelength astronomers and citizen scientists alike, leaving a lasting legacy value for decades to come. The data from VLASS will be available in the NRAO archive immediately with no proprietary period and science data products will be provided to the community in a timely manner. The design of VLASS paid extremely close attention to future Square Kilometer Array (SKA) pathfinders, leading to a survey that will both stand out, and be complementary to those other pathfinder surveys at 1.4 GHz.

The proposed VLASS is a ∼9000 hour comprehensive two-tiered survey, with $\frac{2}{3}$ invested in All-Sky and $\frac{1}{3}$ in Deep, as summarized in Table 1, and detailed in §4 below. Using the VLA to capture the radio spectrum from $2-4$ GHz, VLASS will measure or constrain spectral shapes (e.g. power-law spectral indices), simultaneously providing full polarization parameterization to enable science that showcases the unique capabilities of the Jansky VLA. VLASS as proposed surveys the whole Jansky VLA-accessible sky through the All-Sky component, providing full spectral and polarimetric data for a myriad of targets and source types, addressing a broad range of scientific questions, individually and statistically. At the same time, through the Deep Component, VLASS will address key science themes of our generation including the nature of dark energy and cosmological bias, questions which can only be addressed through very deep systematic observations over a sufficiently large portion of the sky. Neither of these goals can be reasonably achieved through individual PI programs, as the scale of the survey proposed is orders of magnitude more complex than previous programs. Both components make optimal utilization of the Jansky VLA's unique capabilities: *high resolution imaging and exquisite point-source sensitivity*, critical for source identification; *wide bandwidth coverage*, enabling instantaneous spectral index determination; and *full polarimetry* with good performance even in lines of sight with high Faraday depth, enabling instantaneous rotation measure and Faraday structure determinations. VLASS will be carried out in multiple passes, providing a synoptic view of the dynamic radio sky similar to those now available through the new generation of synoptic imagers at other wavelengths. VLASS will provide unique measurements of the radio sky at key epochs and sensitivity levels between that from FIRST and NVSS and the new upcoming radio surveys. This will be a critical enabler for early identification and filtering for the most interesting transient events.

Table 1: VLASS Survey Definition Summary

Tier	Area (deg^2)	Resolution (arcsec)	rms (μJy/beam)	Total Time (hr)	Epochs
(1) – "All-Sky"	33,885 ($\delta > -40°$)	2.″5	69	5436	3
(3) – Deep	10 (COSMOS, ECDFS, ELAIS-N1)	0.″8	1.5	3391	4

Note: Resolution and sensitivities assume robust weighting to achieve near-natural weighted sensitivity with suppressed side lobes.

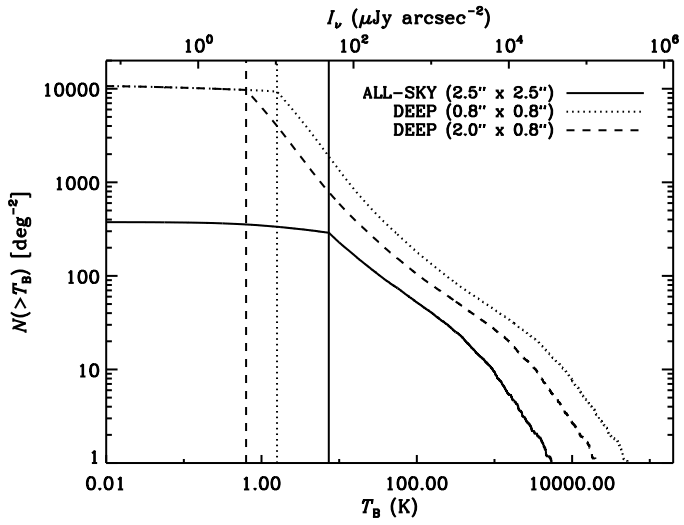

Figure 1: The anticipated cumulative extragalactic source count distribution by VLASS tier using the S^3 simulated radio sky (Wilman et al., 2008). The vertical line indicates the 5σ surface brightness sensitivity of each tier. There are two separate limits for the Deep tier, as the very southern ECDFS field will have an elongated synthesized beam.

Table 2: Expected VLASS Source Statistics

Tier	Area (deg^2)	Density (deg^{-2})	Total Detections
All-Sky	33,885	290	9,700,000
Deep	10	9500	95,000

Note: Sky coverage, expected extragalactic source density, and total number of extragalactic detections per VLASS tier above a 5σ surface brightness limit.

As an indication of the power of VLASS, Figure 1 and Table 2 provide an estimate of the expected extragalactic source counts from VLASS based on the S^3 simulated radio sky (Wilman et al., 2008).

Why is a $2-4$ GHz, high-resolution, synoptic, polarimetry survey able to deliver such high value science?

- High angular resolution is required to not only identify and associate the radio emission with its optical host galaxy, but also to identify the location of the emission within the galaxy.
- The $2-4$ GHz band allows polarimetry on lines of sight with high Faraday depth without depolarization and will enable much broader band Faraday diagnostics in advance of, and complementing, upcoming SKA precursor surveys.
- The $2-4$ GHz band allows for earlier identification of explosive event afterglows when they are brighter, and unlike at $1-2$ GHz, allows for multiple independent epochs occurring within the survey time span.
- Observing at $2-4$ GHz provides the highest yield of flat or inverted spectrum compact sources while still detecting a large number of sources with "normal" modestly steep spectra.
- Employing the $2-4$ GHz band at high angular resolution will result in a survey that will provide maximum complementary utility when combined with the lower-frequency, lower-resolution surveys planned for the SKA precursors and pathfinders later this decade, while additionally *doing* key SKA Phase 1 science years before its completion.
- Even in the era of the SKA Phase 1 science observing next decade, VLASS will provide a reference epoch this decade for transient object identification, as well as coverage of the Northern sky not accessible to those instruments.

This survey approach enables both focused and wide ranging scientific discovery through the coupling of all-sky survey science and a deep focused field, thereby both addressing key science issues and providing a statistical interpretational framework. Such an approach provides both astronomers and the citizen scientist with information for every accessible point of the radio sky, while simultaneously addressing fundamental questions about the nature and evolution of astrophysical objects. VLASS will follow the evolution of galaxies and their central black hole engines, measure the strength and topology of cosmic magnetic fields, unveil hidden explosions throughout the Universe, and chart our galaxy for stellar remnants and ionized bubbles. Multi-wavelength communities studying rare objects, the Galaxy, radio transients, or galaxy evolution out to the peak of the cosmic star formation rate density will equally benefit from VLASS. The **VLASS Key Science Themes** can be summarized as:

- **Imaging Galaxies Through Time and Space** – Following the Ecology of Galaxies, Star Formation, and their Black Hole Engines.
- **Radio Sources as Cosmological Probes** – Tracing the Underlying Dark Matter Density Field.
- **Hidden Explosions** – Unbiased Measurements of Energetic Events.
- **Faraday Tomography of The Magnetic Sky** – Charting the Emergence of Large-Scale Magnetic Fields in Galaxies.
- **Peering Though Our Dusty Galaxy** – Finding and Studying the Tracers of Stellar and Chemical Evolution.
- **Missing Physics** – Enabling the Incorporation of Radio Astrophysics in Multi-Wavelength Astronomy.

These are described in more detail in §3 below, demonstrating that VLASS will have a strong legacy across a broad landscape of astronomical science.

2 VLASS – A Launchpad for the Future

VLASS builds upon the newly upgraded Karl G. Jansky Very Large Array (VLA) to employ its enhanced bandwidth, time resolution, and survey speed to carry out a next-generation sky survey. The Jansky VLA has been in science operation since 2010, with commissioning completed at the end of 2012. Consequently, the capabilities required for VLASS have largely been proven in past and ongoing science programs, making this the ideal time to utilize the VLA for a science survey that will both inform future Jansky VLA PI science for decades to come, while simultaneously planting radio astronomy firmly within the multi-wavelength framework of astronomical research. VLASS will provide an important and unique reference atlas for the science that will be enabled by a new suite of multi-wavelength surveys and observatories coming online now through the end of the decade across the electromagnetic spectrum and beyond – Pan-STARRS, ALMA, DES, JWST, eROSITA, Advanced LIGO/VIRGO, LSST, to name but a few.

VLASS stands on the shoulders of the pioneering NVSS and FIRST surveys carried out with the VLA from $1993-2002$. VLASS additionally sets the stage for future radio surveys and facilities [i.e., Meer Karoo Array Telescope (MeerKAT), the Australian Square Kilometer Array Pathfinder (ASKAP) and the Westerbork Synthesis Radio Telescope (WSRT/AperTIF)], leading to SKA Phase 1 science operations that will commence in $\gtrsim$2020. Each of these facilities include dedicated 1.4 GHz surveys as a prime component of their science programs. The observing band and parameters of VLASS complement these lower frequency programs and provide a foundation for the next decade. The Jansky VLA, with its greatly enhanced and unique suite of capabilities, is well positioned to be at the forefront of this new suite of deep radio surveys. VLASS, as proposed here, provides a qualitative and quantitative improvement in observations of (and understanding of)

the radio sky. It will detect the radio counterparts to the current and emerging multi-wavelength suite of surveys (from the sub-millimeter to γ-rays), and will serve as a technical proving ground for future radio telescopes and their intended surveys. VLASS has been designed with both SKA Pathfinders and the SKA itself in mind, and it showcases the unique capabilities of the Jansky VLA.

A major survey such as VLASS must self-evidently reduce the time available for direct PI science in the short term (by roughly 20% over six VLA configuration cycles). And, on an oversubscribed telescope such as the Jansky VLA, all proposals executed are by definition high quality science. It will, at least, be the lower rated approved proposals, which frequently are only partially completed due to dynamic scheduling, that will be most severely impacted. Furthermore, it is important to note that the survey itself will obviate the need for some fraction of future PI proposals (by providing the data needed directly through the survey itself). At the same time VLASS will provide radio measurements for a broad component of the astronomical community. The existing VLA sky surveys, NVSS (Condon et al., 1998) and FIRST (Becker et al., 1995; White et al., 1997), provide powerful evidence that the telescope time dedicated to these surveys repays the investment. In Appendix B, we provide a detailed analysis that demonstrates the scientific impact of FIRST and NVSS as measured by publications, citations and data utilization. There are a number of key ways in which PI science itself is enhanced by the survey science, including:

- VLA sky surveys have a demonstrably high science impact per observing hour. This is at least partly because surveys expand the usage of radio data beyond the usual radio astronomy community.
- Once VLA sky survey products are available, many science projects that require pointed observations of a sample of objects (e.g., to measure spectral indices for a sample of quasars) can be carried out directly from the catalogs rather than requiring an observing proposal. That reduces the time requested for such observing proposals and so increases the time available for other projects.
- The survey products themselves become a key resource for astronomers in identifying targets and projects for followup proposals. That leads to an increase in the science done by enabling projects that are not possible without the inputs from a sky survey.

The balance between the scientific impact from VLASS for the broad astronomical community and increased competition for PI science time needs to take all these elements into consideration.

3 VLASS Themes and Headline Science

There are six themes that run throughout the VLASS design and science goals. These exploit the unique capabilities of the upgraded Jansky VLA. In each of these themes we highlight the "Headline Science" that will be done with VLASS. These are exemplary key science projects that illustrate both known and unknown science potential for VLASS, a survey we anticipate will open new frontiers for discovery. In Appendix C, we describe extensive additional science areas that VLASS is likely to impact. The lasting legacy value of VLASS in light of future radio surveys on the horizon is discussed in §3.7.

3.1 Imaging Galaxies Through Time and Space

AGN and the Evolution of Accretion Activity:
It is widely thought that AGN activity (particularly radio-loud AGN) may be responsible for switching off star-formation in massive galaxies, but a direct observational link between AGN

activity and star-formation at high redshifts remains elusive. Recent studies from both a theoretical (Silk, 2013) and observational (Kalfountzou et al., 2012, 2014) perspective have shown that powerful radio-loud AGN may actually provide a positive form of feedback. On the other hand, there is little evidence for any type of feedback from radio-quiet objects based on the latest studies using *Herschel* (e.g., Bonfield et al., 2011; Rosario et al., 2013). Moreover, the interplay between jets (also rare AGN–requiring a large survey area) and associated satellite galaxies is even more poorly understood. As *Herschel* studies are limited due to resolution and confusion noise, and optical surveys miss all of the obscured galaxies, radio is again the best line of attack. However, current radio surveys are unable to probe radio emission from star formation over the epoch where AGN activity is having an impact on the environment. Given that different forms of AGN feedback are invoked in current semi-analytic models of galaxy formation (e.g., Croton et al., 2006; Bower et al., 2006; Hopkins, 2012), it is essential that we understand such processes if we are ever to understand the evolution of galaxies.

Indeed, there is now strong evidence that the standard AGN unification paradigm (e.g., Antonucci, 1993; Urry & Padovani, 1995) does not give a complete picture. For example, observational evidence (e.g., Hardcastle et al., 2007; Herbert et al., 2010; Best & Heckman, 2012) suggests that many or most low-power ($P < 10^{25}\,W\,Hz^{-1}$) radio galaxies in the local universe (the numerically dominant population) correspond to a distinct type of AGN. These sources accrete through a radiatively inefficient mode (the so-called "radio mode"), rather than the radiatively efficient accretion mode typical of radio-quiet optically or X-ray selected AGN [sometimes called 'quasar mode'; see Heckman & Best (2014) for a recent review covering these feedback processes]. The role of these two accretion modes appears to be strongly influenced by the environment (e.g., Tasse et al., 2008) while the presence or absence of a radio-loud AGN appears to be a strong function of the stellar mass of the host galaxy (e.g., Best et al., 2005; Janssen et al., 2012). Deeper radio surveys covering areas of sky with the best multi-wavelength data are required to probe the evolution of these relationships and the accretion mode dichotomy over cosmic time; this is key information for any attempt to incorporate mechanical feedback from radio-loud AGN in models of galaxy, group and cluster formation and evolution.

Furthermore, the details of the mechanism(s) of interaction between radio-loud AGN and their environments, on all scales, remain unclear; such basic questions as whether the most powerful sources are expanding supersonically throughout their lifetimes (e.g., Begelman & Cioffi, 1989; Hardcastle & Worrall, 2000) or what provides the pressure supporting the lobes of low-power objects (e.g., Bîrzan et al., 2008; Croston et al., 2008) remain unanswered. These questions can only be addressed by the accumulation of large, statistically complete samples of radio sources with good imaging and excellent, homogeneous multi-wavelength data. Information on both large and small-scale radio structure is required.

The optimal combination of sensitivity and spatial resolution of VLASS allows the study of the entire AGN population from classical radio-loud sources down to the realm of radio-quiet AGNs ($P \sim 10^{22-23}\,W\,Hz^{-1}$, Jarvis & Rawlings, 2004; Wilman et al., 2008; Kimball et al., 2011a; Condon et al., 2013a), from $z \sim 0 - 6$. This will provide a complete view of nuclear activity in galaxies and its evolution, unbiased by gas/dust selection effects. The All-Sky tier is required to obtain a good baseline of radio AGN at low redshifts, while the Deep tier is needed to push out to $z \sim 1 - 2$, where feedback needs to be most active to prevent galaxy growth. The VLA's high-resolution is crucial for morphologically distinguishing different types of AGN (e.g. FRI and FRII) from star-forming galaxies, and to establish reliable cross-identifications in all tiers.

The wide-band spectro-polarimetry, in combination with the high spatial resolution provided by VLASS, will enable statistical studies of depolarization trends in radio lobes, their dependence on spectral index, and lend insight into the interaction between radio lobes and their environment (e.g., O'Sullivan et al., 2013). The wide bandwidth is important for inferring the physical state of the AGN and surrounding environment as well as constraining the power of jets. Some broader themes that we will explore include:

Why are some AGN strong radio emitters and others not?
Except for the radio, there is nothing in the optical/UV properties of quasars (continuum, emission, absorption) that specifically identifies a quasar as radio-loud or not (e.g., Kratzer, 2014). An important avenue forward to is have better demographics across a broad range of luminosity and redshift, seeking to confirm marginal evidence that objects are more likely to be strong radio sources at lower redshift and higher luminosity. Further insight can be gained from radio demographics across the Eigenvector 1 parameter space (Schmidt & Green, 1983) that maximizes the dispersion of quasar properties.

Even radio-quiet quasars are not radio-silent. Is the radio emission from failed jets, star formation, or shocks (e.g., Kimball et al., 2011b; Condon et al., 2013b; Zakamska & Greene, 2014)? There is evidence that all three may contribute. Again, better demographics – both for high S/N detection and stacking analysis – are key to understanding this question.

Along what line of sight are we viewing individual quasars?
Quasars are not spherically symmetric; however, at least for unobscured quasars, we have very little handle on the line of sight orientation of the systems. Radio spectral indices provide a rare opportunity to further quasar investigations by grouping them by orientation (or marginalizing over orientation). Understanding the orientation has implications for our understanding of quasar continua, emission lines, absorption lines, masses, accretion rates, and bolometric luminosities (e.g., Wills & Browne, 1986; Runnoe et al., 2013).

To investigate quasars as a function of orientation, we need robust spectral indices. Ideally these would be contemporaneous and/or at the same resolution as measurements at other radio frequencies. In that sense, S-band is ideal, as it provides an internal spectral index measurement within a single VLA observation.

The star-formation history of the Universe:
In almost all existing large-scale radio surveys, the vast majority of the sources detected are the accretion-dominated AGN and quasar populations. However, thanks to the well-known correlation between far-infrared (FIR) and radio emission (e.g., Helou et al., 1985; Appleton et al., 2004; Murphy, 2009; Sargent et al., 2010; Ivison et al., 2010; Jarvis et al., 2010) the star-forming galaxy population becomes detectable at flux densities around $S_{1.4\mathrm{GHz}} \sim 1\,\mathrm{mJy\,bm^{-1}}$, growing to dominate the source counts at fainter flux densities (e.g., Windhorst et al., 1985; Wilman et al., 2008; de Zotti et al., 2010). The radio is a particularly important tracer for this population, as it is relatively immune to dust extinction, providing an unbiased view into the basic features of galaxy formation across the history of the universe, including the volume-averaged star formation rate, its distribution function within the galaxy population, and its variation with environment.

Surveys of the cosmic star-formation rate as a function of epoch suggest that the star-formation rate density rises as $\sim (1+z)^4$ out to at least $z \sim 1$ (e.g., Lilly et al., 1996; Hopkins & Beacom, 2006; Behroozi et al., 2013) and then flattens, with the bulk of stars seen in galaxies today having been formed between $z \sim 1-3$ in the so-called epoch of galaxy assembly. However, the effect of dust on the traditional optical and UV measurements of the star-formation rate means that the behavior of the cosmic star-formation rate density at redshifts above $z \sim 1$ is still uncertain (e.g., Bouwens et al., 2012), as is the importance of downsizing (Cowie et al., 1996). These uncertainties are exacerbated by the effects of cosmic variance in the current samples (multi-wavelength surveys such as COSMOS and GOODS typically cover only modest-sized areas, $\leq$1 deg^2, corresponding to just $\sim$30 Mpc at z$\sim$2), as well as small sample sizes. Given that star-formation is environmentally dependent (e.g., Lewis et al., 2002), any investigation on the evolution of star-forming galaxies requires the ability to detect them over the full range of cosmic environments (e.g., from rich clusters to voids).

VLASS is ideal for tracing the cosmic history of star-formation, free from cosmic variance (e.g., Heywood et al., 2013) or dust extinction biases. The Deep tier will detect star forming galaxies out to $z \lesssim 4$, and the large area of the All-Sky tier will provide a baseline sample of relatively nearby

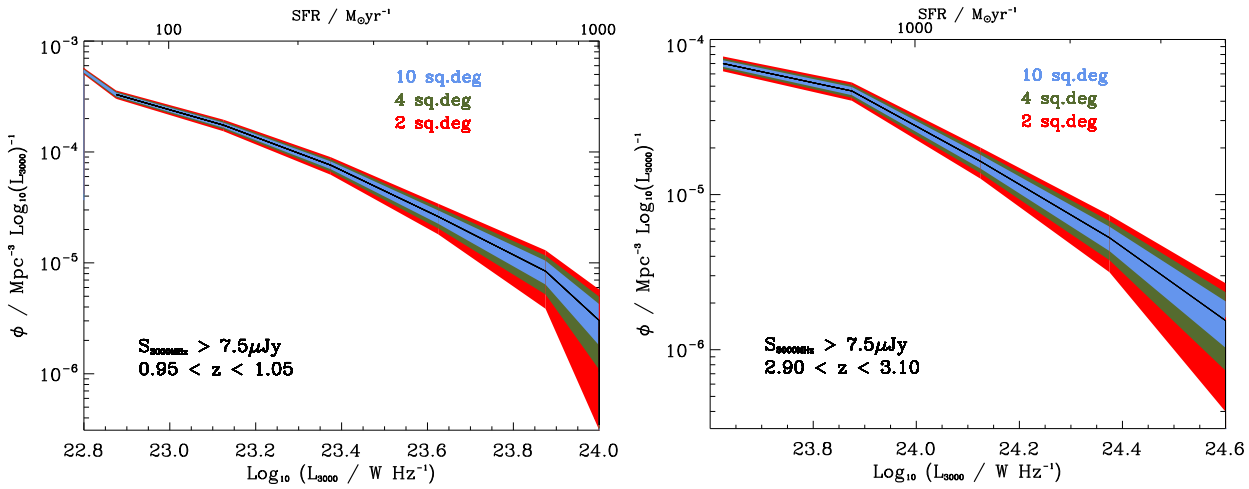

Figure 2: Predicted luminosity function at $0.95 < z < 1.05$ (left), and $2.90 < z < 3.10$ (right) for star-forming galaxies in the deep continuum survey [based on the simulations of Wilman et al. (2008, 2010)]. The red region shows the Poisson uncertainty for a 2 deg^2 survey, the green region is for a 4 deg^2 survey and the blue region is for the proposed 10 deg^2 survey. The equivalent star-formation rate is given on the upper x-axis.

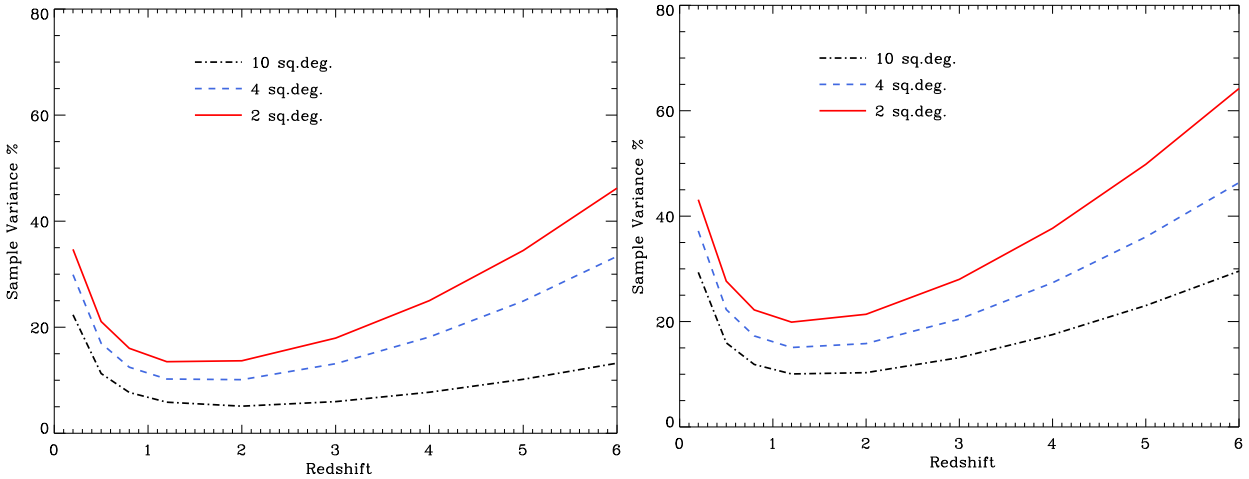

Figure 3: Sample/cosmic variance for galaxies of mass $10^{10}\,M_\odot$ (left) and $10^{11}\,M_\odot$ (right) for different survey areas. Moving from a 2 deg^2 area to 10 deg^2 reduces the sample variance from ∼15% to ∼5% at the crucial epoch around $z \sim 2$ for $10^{10}\,M_\odot$, and from ∼30% to ∼10% for $10^{11}\,M_\odot$.

($z \lesssim 0.5$) objects of similar luminosity with which to compare them. The targeted deep fields have the best multi-wavelength data available over the few deg^2 areas of interest for VLASS, making the VLA's angular resolution essential for establishing reliable counterparts in these crowded fields, as well as measuring the sizes of star-forming disks at such early epochs. In addition to the overall star-formation history of the Universe, such a large-scale survey is necessary for answering closely-related questions regarding the dependence of star-formation on host galaxy mass (e.g., Peng et al., 2010, 2012) and the emergence and growth of large-scale magnetic fields in the star-forming ISM of these galaxies – the latter of which is ideally obtained using wide-band spectro-polarimetry with the VLA's S-band (see §3.4). In Figure 2 we show the predicted constraints on

the radio luminosity function for star-forming galaxies in three redshift bins of width dictated by the expected photometric redshift error of $\delta z/(1+z) \sim 0.05$. One can see that moving from 2 deg^2 (the area covered by the COSMOS survey) to 10 deg^2 greatly reduces the Poisson uncertainty on the luminosity function for star-forming galaxies. Figure 3 shows the sample variance due to large-scale structure in various survey areas for different galaxy masses, demonstrating again that the move towards larger areas/volumes is key to developing understanding of the link between star-formation, galaxy mass and environment.

It is worth stressing that VLASS Deep takes a transformational step for studies of galaxy evolution by moving beyond the point of simply counting galaxies and measuring the average luminosity function. To properly understand galaxy evolution requires a clear understanding of the role played by environment and AGN activity. This requirement forces the need to cover a wide enough area that is sensitive to galaxies in all environments over the epoch of peak activity (i.e., $0.5 < z < 3$). With 10 deg^2, VLASS Deep is able to achieve this by having enough volume to study 10's of clusters with masses $> 10^{14}\,M_{\odot}$. In doing so, astronomers will be able to start addressing the question of quenching and downsizing with a measure of star formation rate that is free from dust obscuration, and also does not suffer from the resolution problems of existing *Herschel* surveys – *VLASS Deep is actually as sensitive to obscured star formation as the deepest Herschel far-infrared survey data, but covers a factor of ≈100× more area with ≈10× higher spatial resolution*. Smaller area surveys, such as the existing area in COSMOS, simply cannot significantly address these science goals.

3.2 Radio Sources as Cosmological Probes

Cosmology and Large Scale Structure:
Over the past few years there has been an increasing focus on using radio continuum surveys to address the fundamental issues related to the cosmological model, including determining the equation of state of dark energy and whether we can find evidence for departures from General Relativity on the largest scales (e.g., Raccanelli et al., 2012; Camera et al., 2012). Three key tests where one can use radio continuum sources as cosmological probes are: the Integrated Sachs-Wolfe effect (e.g., Raccanelli et al., 2008); the power spectrum of the radio source populations (e.g., Blake et al., 2004); and the cosmic magnification bias (e.g., Scranton et al., 2005). However, one of the key unknowns in our understanding of how well radio sources can help determine the underlying cosmological model is their bias, i.e. how they trace the underlying dark matter density field.

It is actually very difficult to determine this quantity directly from radio continuum surveys alone, although some progress has been made by measuring the angular two-point correlation function of radio sources cross-correlated with optical imaging and spectroscopic surveys (e.g., Lindsay et al., 2014a) and by assuming a redshift distribution (e.g., from the S^3 simulation of Wilman et al., 2008, 2010). Such studies are hampered by only the low-redshift sources having reliable optical counterparts, thus limiting the redshift range over which the bias can be measured to $z < 0.5$. Given that the unique niche occupied by radio continuum surveys for determining the cosmological model lie in the fact that their redshift distribution peaks at $1 < z < 2$ (depending on the precise flux-density limit), our lack of knowledge of the bias at $z > 1$ hampers our ability to use these sources as tracers of the universe on large scales.

This problem can be tackled through a deep VLA continuum survey, such as the VLASS Deep tier, by measuring the two-point correlation function of the sources in the survey directly. This is analogous to what has been done at low redshifts, where the optical counterparts can be used in these deep fields to determine redshifts, using either photometric or spectroscopic redshifts. Such an experiment requires the necessary volume to determine the clustering of dark matter haloes, and with a single field of around $\sim$1 deg^2 such a measurement is extremely difficult. However, by

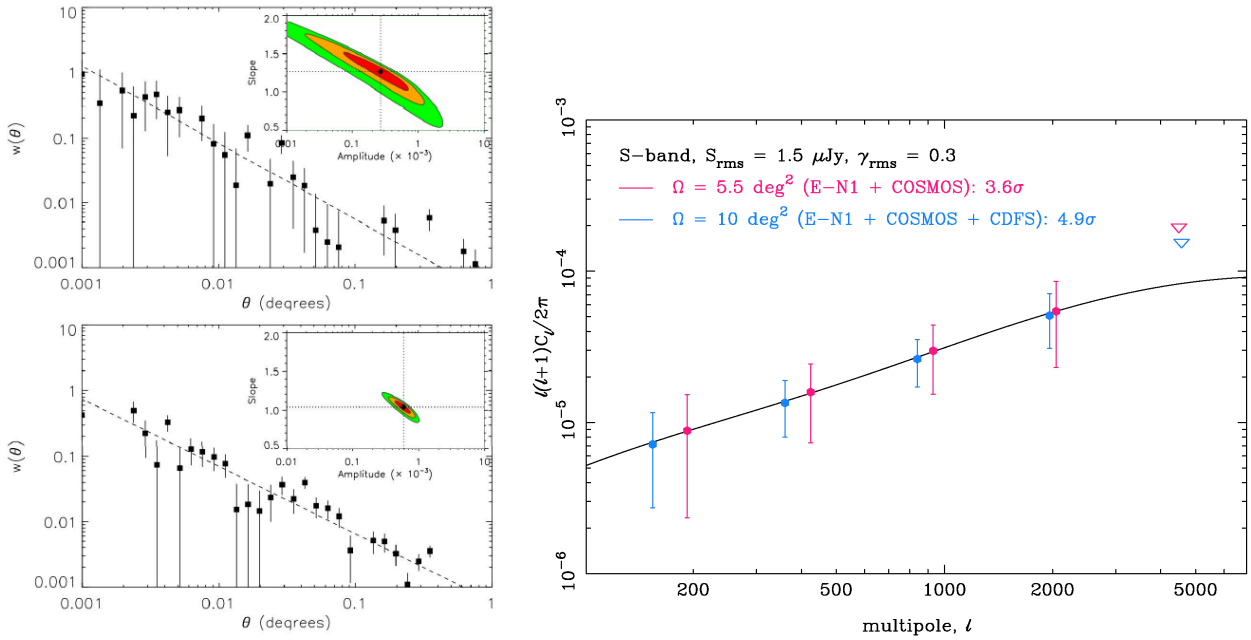

Figure 4: *Left:* The angular two point correlation function for a $S_{3\,\mathrm{GHz}} > 30\,\mu$Jy radio source (top) 1.5 deg^2 and (bottom) 4.5 deg^2. The inset shows the uncertainty contours on the slope and normalization of the power-law fit (Lindsay et al., 2014b). *Right:* Forecasted constraints on the cosmic shear power spectrum from the VLASS Deep tier observations assuming a survey depth of 1.5 μJy and assuming a total shape noise error of $\gamma_{\mathrm{rms}} = 0.3$. Two sets of forecasted errors are plotted to represent the two scenarios in which useable shape measurements can or can not be extracted from the ECDFS observations (which will suffer from an elliptical beam due to the low declination of the ECDFS field). The predicted signal-to-noise of the cosmic shear detection in each case is also indicated. Even with this limitation, ECDFS is still preferred as it has the best multi-wavelength dataset over such a large area.

moving to $\sim$4 deg^2 patches of sky (i.e., as is the case for two of the VLASS Deep fields), the two-halo term in halo-occupation distribution models begin to be measured at > 1 Mpc scales. The left panels of Figure 4 shows the constraints that can be achieved by moving from a 1.5 deg^2 survey to a 4.5 deg^2 survey based on the clustering model prescribed in the S^3 simulation (Wilman et al., 2008). Additional information can also be used, such as the full galaxy catalog from optical and near-infrared data. By measuring the cross-correlation of the much more abundant optical/near-infrared sources with the radio sources one can obtain much tighter measurements of the clustering of radio sources over all luminosity regimes, i.e. even for the rarer AGN (e.g., Lindsay et al., 2014b).

Probing the dark Universe with VLASS:
The nature of dark energy remains the most outstanding question in cosmology. Weak gravitational lensing – the effect whereby images of faint, distant background galaxies are coherently distorted by intervening large scale structures – is recognized as one of the key probes that will allow us to constrain dark energy in future surveys (Albrecht et al. 2006; Peacock et al. 2006). The Deep tier of VLASS offers an exciting opportunity to extend this science area to radio surveys. Its combination of excellent sensitivity and high angular resolution (both of which are essential for weak lensing) will remain unsurpassed until the advent of the SKA (i.e., $>>$2020) and will make it the worlds premier resource with which to spearhead the development of radio weak lensing in preparation for the SKA. Even more impressive, with its combination of area and depth, VLASS Deep sits poised to make the first statistically significant radio weak lensing detection years before

SKA Phase 1 is in full science operations (see right panel of Figure 4).

The radio band offers unique and powerful added value to the field of weak lensing. Firstly, deep radio surveys will probe the lensing power spectrum at significantly higher redshift than most of the planned optical lensing surveys. The addition of radio can therefore offer a more powerful redshift "lever arm" with which to measure the effects of dark energy on the evolution of structure. Secondly, instrumental systematic effects are a serious concern for weak lensing studies for which a very accurate representation of the beam or point spread function (PSF) of the telescope is required. The highly stable and deterministic beam response of radio interferometers could therefore prove a major advantage for weak lensing science. Radio observations offer unique advantages over traditional lensing analyses by enabling fitting of galaxy shapes directly from *uv*-visibility data (Chang & Refregier, 2002; Chang et al., 2004). Another unique aspect comes from the VLA's wide bandwidth at S-band which allows direct measurement of the frequency dependence of the beam. This is a potential major advantage over optical broad-band photometry since while galaxy optical-uv SEDs vary wildly, in the radio galaxies typically exhibit smooth power-law type spectra. Perhaps most importantly, the radio offers unique and novel opportunities to independently evaluate the effects of weak lensing such as through polarization measurements.

Polarization observations of weak lensing provide unique information on the intrinsic (unlensed) shapes of background galaxies. The position angle of the integrated polarized emission from a background galaxy is unaffected by gravitational lensing (Brown & Battye, 2011). If the polarized emission (which is polarized synchrotron emission sourced by the galaxy's magnetic field) is also strongly correlated with the disk structure of the galaxy then measurements of the radio polarization position angle can be used as estimates of the galaxy's intrinsic (unlensed) position angle. Thus, polarization observations can be used to reduce the primary astrophysical contaminant of weak lensing measurements – intrinsic galaxy alignments (see e.g., Heavens et al., 2000; Catelan et al., 2001; Brown et al., 2002; Hirata & Seljak, 2004) – which are a severe worry for ongoing and future precision cosmology weak lensing experiments. Additionally, depending on the polarization properties of distant background disk galaxies, the polarization technique has the potential to reduce the effects of noise due to the intrinsic dispersion in galaxy shapes. VLASS will allow the first demonstration of these new techniques.

For a quantitative comparison with state-of-the-art (optical) weak lensing surveys, we look at the forecasted detection significance numbers for CFHTLenS, KiDS and DES (Brown et al., 2013). The proposed VLASS Deep ($10\,\mathrm{deg}^2$) is aimed at delivering a $5\,\sigma$ detection of cosmic shear in the radio. Current optical weak lensing surveys, such as CFHTLenS ($154\,\mathrm{deg}^2$), KiDS ($1500\,\mathrm{deg}^2$), and DES ($5000\,\mathrm{deg}^2$), are expected to deliver detections with a significance of 15, 30, and $43\,\sigma$, respectively. As is obvious from comparing these forecasted detection significance estimates, DES will constrain dark energy parameters with nearly an order of magnitude better precision than VLASS Deep. Of course, such precision comparisons tell us absolutely nothing about is the impact of systematics, which is the key strength of radio weak lensing. Systematic errors in lensing measurements dominate the uncertainty, and must be carefully accounted for to ensure that cosmological constraints from lensing are unbiased and as precise as possible. This is indeed the reason why weak lensing is a key science driver of the SKA, and why the weak lensing aspect of VLASS-Deep is potentially a groundbreaking project to provide the first definitive measurement of weak lensing in the radio years before SKA Phase 1 construction has finished.

3.3 Hidden Explosions

The 2010 Astronomy and Astrophysics Decadal Survey (National Research Council, 2010) highlights time domain astronomy as an area with great potential for new discoveries. Like the sky viewed in other wave-bands, the radio sky is dynamic, exhibiting variability on timescales from milliseconds to years. Such radio transients often signal explosive events, in some cases probing

the highest energy particle populations in the known universe. These diverse phenomena include astrophysical blast waves, catastrophic gravitational collapses, magnetic acceleration of relativistic charged particles, shocks in high energy particle jets and in magnetized diffuse interstellar plasma, flaring reconnection events in the atmospheres of low mass stars, and the cosmic beacons of rotating neutron stars, white dwarfs, and black hole accretion disks. While the detection of such events has previously relied on the synoptic survey capability of modern wide-field optical, X-ray and γ-ray observatories, VLASS now also offers the potential to systematically characterize the dynamic sky at radio frequencies, targeting both Galactic and extragalactic transient populations. It so happens that the most numerous radio transients with the greatest potential impact, are actually those populations that have been hidden from view at these other wavebands, being largely detectable only at radio wavelengths.

What is the true rate of explosions in the local Universe?
Phenomena associated with the explosive death throes of massive stars have been studied for decades at all wavelengths. These myriad phenomena include the various classes of supernovae (type Ia, type Ib, Ic and type II), the highly relativistic outflows of γ-ray bursts (GRBs) and the mergers of compact objects (e.g., see Figure 5). As well as providing a window into the life cycles massive stars, such events also probe the formation of compact objects and can provide a standard candle for precision cosmology. However, the true rate of such events is poorly constrained; specifically:

(i) A comparison of the star formation rate and supernova discovery in the local universe implies that as many as half of the supernovae remain undetected in the traditional optical searches, largely due to extinction via dust obscuration, with far reaching consequences for models of stellar and galaxy evolution.

(ii) The relativistic outflows associated with GRBs and compact object mergers are highly collimated. Thus, only those bursts that are collimated in the direction of Earth are detected. Best estimates suggest this corresponds to a small fraction of the true event rate, dependent on the typical opening angle of the collimated jet, with poor constraints on the latter.

VLASS can provide the means to establish an unbiased measure of the true rates of these phenomena. Radio observations, unlike optical, can penetrate the dusty environments of obscured supernovae. Similarly, the late-time, sub-relativistic afterglows of GRBs and compact object mergers are not highly collimated. Thus, while such events are not detectable at γ-ray or X-ray wavelengths, they can be detected at radio wavelengths by VLASS.

VLASS has sufficient sensitivity and area coverage to deliver guaranteed high-impact return for these known classes of transient events — at higher frequencies the emission from these blasts arrives earlier, and has shorter rise and decay times. For example, supernovae typically reach their peak brightness in $\lesssim$1 yr at 3$\dot{\text{G}}$Hz compared to a few yrs at 1.4$\dot{\text{G}}$Hz Therefore, the VLASS observing at 2–4 GHz over the span of 7 years is ideally suited for finding and triggering follow-up observations of these events compared to surveys in the $1--2$ GHz band over the same timescale. The All-Sky component of VLASS will be the workhorse for this search. To enable such time-domain science, All-Sky will be carried out in three epochs spread through the 7 years of the VLASS observations, with a roughly 32 month cadence set by the fundamental 16 month configuration cycle of the VLA. Each epoch will reach a image rms depth of 120 μJy/beam (limited by the data rate constraints). At its reference frequency of 3 GHz, the light curves from extragalactic explosive events can have a characteristic span as long as 1 year (e.g. supernovae), and thus these will essentially be three *independent* epochs, thereby maximally leveraging the observing time of the VLASS towards the identification of independent transient events. In contrast, future transient surveys at 1.4 GHz will be densely sampling light curves that have in some cases a characteristic scale of a few years, longer than the entire duration of the planned survey.

Confirmation and classification of VLASS transients will rely on follow-up observations with

the VLA, as well as triggered follow-up from the community at optical and NIR. The former will sample the light curve of the event and, more importantly, will allow confirmation of the broad SED of the radio transient (1-50 GHz), **a capability unique to VLA among current among planned radio instruments capable of synoptic surveys**. The triggering of optical/NIR follow-up allows detailed characterization of the host, which is the primary tool in classification of a radio transient. Confirmation of distance, and thus energetics, together with the radio transient SED and location within a galaxy, will provide a means to routinely distinguish between the various classes of explosive events (cf. Fig 7 of Frail et al. 2012). In this regard the shallow depth of individual epochs of the VLASS is well suited to the task. At these depths, a transient event should be identified with a known optical/infrared host galaxy and there should be no "hostless" events for the known classes discussed below. Furthermore, the high angular resolution of VLASS allows identification of the location *within* the host galaxy, a capability not possessed by the proposed surveys from upcoming lower frequency arrays. This discriminator allows us to assess the likelihood that the event is due to AGN variability or a tidal disruption event (if located at host galaxy center), or a supernova or NS-NS merger associated with a catastrophic stellar demise.

What is the rate of coalescence of neutron star binary systems?
One of the most exciting prospects of the Synoptic VLASS is the opportunity to find and strongly constrain the rate of merging binary neutron star systems. Advanced LIGO (aLIGO) and Advanced Virgo (AdV) are scheduled to commence collecting data in 2015 and are expected to eventually yield the first direct observations of gravitational waves. The network will not be at full design sensitivity in 2015, but will grow in capacity over subsequent science runs (2016-2019) as detectors improve and with the eventual installation of a LIGO detector in India $\sim$ 2020 (LIGO Scientific Collaboration et al., 2013).

Compact binary coalescences, particularly the inspiral of binary neutron star (BNS) systems, are expected to be the most common source for detection and also the most promising to yield a corresponding electromagnetic counterpart. BNS mergers are thought to be the likely progenitor of short γ-ray bursts (S-GRBs), but only a small fraction of such events are detected in γ-rays due to the narrow beaming of the emission (Fong et al., 2012). The fraction of S-GRBs that are not detected due to this narrow beaming is also poorly constrained. It is likely to be large however with the number of undetected events exceeding detected events by an estimated factor of $10^2 - 10^3$, as evidenced by the lack of detection of a S-GRB within range of aLIGO and AdV during the nine year Swift mission. It is clear that an unbeamed electromagnetic signature is required, both to 1) determine the true rate of BNS merger events to allow well defined predictions for the aLIGO and AdV era and 2) to provide a reliable means to unambiguously identify and localize a counterpart to a gravitational wave (GW) event. The radio emission produced by the mildly relativistic outflows interacting with the surrounding medium in the wake of a BNS merger has recently been highlighted as one of the most promising means to detect such events (Nakar & Piran, 2011). This radio afterglow would be produced in the weeks to months following the merger, peaking at frequencies in the range 1–4 GHz.

VLASS will play a two-fold role in the search for such merger events, 1) determining or strongly constraining the true rate of merger events through identification of an unbeamed radio afterglow population and 2) delivering reference image data on a large fraction of the sky with sufficient depth to allow constraining follow-up observations of potential GW events out to the aLIGO/AdV horizon (200 Mpc). Crucially, we note that the VLASS All-Sky tier is sufficiently deep to provide an unambiguous reference map for searches for counterparts to those first events, based on the range of predicted radio flux densities (Nakar & Piran, 2011) for compact object mergers out to the detection horizon for the early Advanced LIGO and VIRGO runs (LIGO Scientific Collaboration et al., 2013).

A Unique Snapshot in Time:
VLASS is not just an engine for the discovery of radio transients, but also a resource for use by

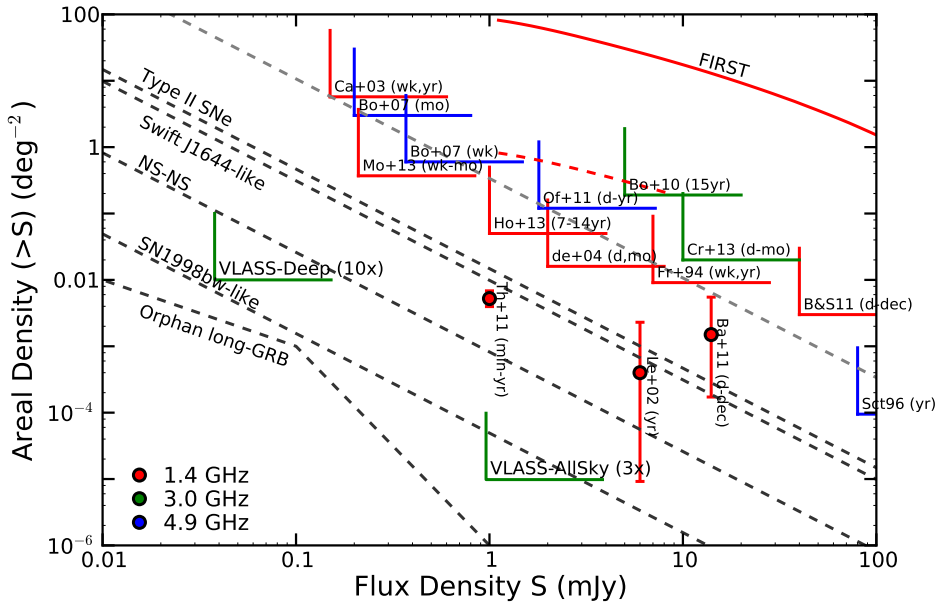

Figure 5: The phase space of explosive extragalactic radio transients. The dashed black lines give the instantaneous source counts for different classes of transients at 3 GHz. The rates for Type II supernovae, neutron star mergers (NS-NS), tidal disruption events (referred to as Swift J1644-like) and for highly luminous supernovae such as SN1998bw are from Frail et al. (2012) and those for orphan long-GRB afterglows are from Ghirlanda et al. (2014). The dashed red line denotes the variable extragalactic source population [1% of the persistent sources; (e.g., Mooley et al., 2013) and references therein]. The solid red line represents extragalactic source counts from FIRST. The dashed grey line is the transient rate claimed by Bower et al. (2007). Wedges indicate upper limits to the transient rates from previous surveys, and errorbars (2-σ) are transient rates for past detections. The markers are color-coded according to observing frequency. The limits shown for the VLASS represent the expected cumulative number of detected transients, with the requirement that a transient event must be detected at $> 10\sigma$ in a single epoch, to overcome thermal noise fluctuations in the data when comparing 2 epochs ($> 10^{11}$ synthesized beams per epoch) as well as image artifacts that masquerade as transients. We note that this is conservative - one can use much lower detection threshold (e.g. 6σ) combined with the requirement that the detected transient must be located in a nearby galaxy ($z < 0.1$) to overcome high-σ thermal noise fluctuations. This alone would increase the detection yield for extragalactic transients by an order of magnitude. It is crucial to emphasize that these rates represents the mean number density of such transient sources at any given time, but the identification of a source as a transient can only be best realized with a reference image taken prior the explosive event. The required separation between reference and detection image depends strongly on frequency, with the mean time to maximum brightness for radio supernovae, for example, varying from weeks at 20 GHz to $>$ 2 years at 1.4 GHz. Thus, to maximize detection sensitivity to transients on all timescales, both short and long, epochs should be separated by gaps greater than the mean time to maximum brightness for all classes transients. This is the strategy adopted by VLASS All-Sky, with epochs spaced by 32 months, and is reflected in the calculated rates.

the whole astronomical community in support of worldwide transient and variable studies at all wavelengths and with all messengers. Providing a new high-resolution standard reference atlas of the 2–4 GHz radio sky, VLASS will constitute a key legacy dataset for opening the time domain astronomy discovery frontier. VLASS will also be a key resource for next-generation synoptic surveys at other wavebands, such as the LSST. The areal coverage and depth of the latter survey (20,000 sq. deg. to a depth of V = 27.5) is such that, of the planned radio synoptic surveys of the

coming decade, only VLASS has the spatial resolution necessary to offer unique identification of radio counterparts with $> 95\%$ certainty.

3.4 Faraday Tomography of The Magnetic Sky

The WIDAR correlator has opened a major new window for wideband polarization work, enabling us to characterize properties of the magneto-ionic medium in AGNs and in galaxies across a wide range of redshifts. This is the **primary** driver for the VLASS polarization science. A **secondary** driver will be the use of the VLASS for studies of Faraday foregrounds. In this area, the VLASS will provide a 6-fold increase in the background polarized source densities that are available today, although this will eventually be superseded by SKA precursor surveys.

Faraday rotation in a magneto-ionic medium produces various external or internal depolarization processes (e.g., Burn, 1966; Tribble, 1991; Sokoloff et al., 1998). These provide a unique and critical diagnostic of the magneto-ionic medium, but only when observed over a wide frequency range with semi-continuous frequency coverage (e.g., O'Sullivan et al., 2012). Almost all studies to date have either relied on a selected number of widely-spaced narrow bands or have observed over a continuous but relatively narrow fractional bandwidth. Both these approaches have severe shortcomings (Farnsworth et al., 2011). **Degeneracies between different types of depolarization behavior, and hence the underlying physical properties of polarized sources and foreground gas, can only be broken by wideband spectro-polarimetry.**

Figure 6 shows the Faraday depth response function for Faraday Tomography with the non-RFI contaminated sections of the JVLA 2-4 GHz (S-band, 2.0-2.128 GHz + 2.384-3.6 GHz). In terms of detecting sources, a S:N=10 criterion of yields uncertainties of 10 rad m^2. For more detailed examination of Faraday structures, we would target polarized intensities above 1.5 mJy beam^{-1}, for which the All-Sky VLASS will provide precisions better than 5 rad m^{-2}. At the angular resolution of VLASS, most objects in the mJy regime will be resolved allowing tomographic exploration of the structure of AGN and radio galaxies, which will enable the statistical characterization of complex and interesting cases in compact and extended AGN regions, absorption line systems and galaxies, where magnetized relativistic and thermal plasmas are mixed. Examples of Faraday-complex sources can be seen in the compilation by Farnes et al. (2014a) (Figure 7); while the full complexity in these examples is seen over larger wavelength ranges, sampling these distributions over the 8-15 cm range will allow valuable statistical characterizations of different AGN populations.

Based on the NVSS we expect over 10^5 sources with polarized fluxes $>$0.75 mJy (S:N$>$10; 5% [0.5%] for I = 15 [150] mJy). We will be able to produce the first large-scale depolarization catalog and statistically evaluate the origins of the depolarization. Of course, this number will dramatically increase in the future, when we can combine the VLASS with the results of SKA precursor surveys.

The relatively high frequencies of the VLASS S-band polarization survey will also uncover previously unknown populations of sources with extremely large Faraday depths and those that are heavily depolarized *and hence missed in the lower frequency catalogs*. For many sources, we will be able to combine these data with 1–1.5 GHz polarization measurements from MeerKAT, ASKAP (POSSUM/EMU) and AperTIF (WODAN), when these data become available, for even higher Faraday precision and exploration of complex Faraday structures.

Using the broadband VLASS data, we can uniquely address such questions as:

(1) What is the magneto-ionic medium in AGNs, galaxies and their immediate environments? Feedback from AGN is important in galaxy formation: it is intimately linked to the star formation history (e.g., Hopkins & Beacom, 2006), and could suppress cooling in massive galaxies, producing the bright-end cut-off of the luminosity function (e.g., Best et al., 2006; Croton et al., 2006). The nature of this AGN feedback is very much under debate: it has been shown that energy deposited by radio jets can either trigger or quench star formation (e.g., Wagner et al., 2012). AGNs are also

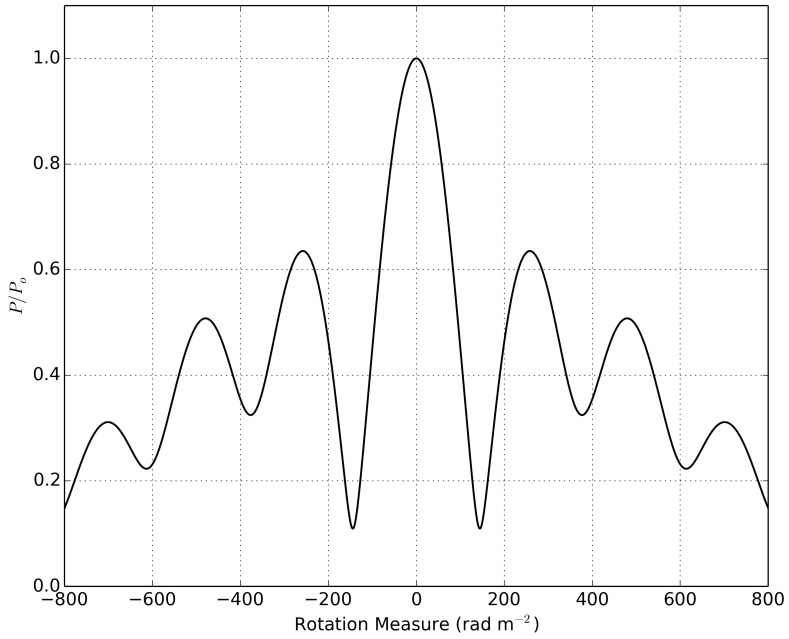

Figure 6: Faraday depth response function. The available non-RFI contaminated frequencies at S-band provides a FWHM response of $\sim$200 rad m^{-2}.

thought to influence their surrounding intergalactic medium by enrichment of metals (Aguirre et al., 2001) and magnetic fields (Furlanetto & Loeb, 2001). Thus, investigating how radio galaxies impart energy into the ISM/IGM is crucial.

While minimal interaction between radio lobes and the environment would lead to a thin "skin" of thermal material around the lobes (e.g., Bicknell et al., 1990), significant interaction should lead to large-scale mixing of thermal gas with the synchrotron emitting material throughout the lobe, causing internal Faraday dispersion. Recently O'Sullivan et al. (2013) fitted the depolarization trend of the lobes in one such radio galaxy, Centaurus A, and found a thermal gas of density 10^{-4} cm^{-3} well mixed in with synchrotron emitting gas in the lobes. A sensitive wide-band polarization survey allows statistical studies of this phenomenon through estimation of the thermal gas content in a large number of radio galaxies, covering a range of luminosities, redshifts, and environments. One quarter of sources are depolarized by a factor of 2 between 2.7 GHz and 1.4 GHz (Lamèe et al. in preparation), providing large samples of sources with significant depolarization signatures from 2-4 GHz. Most of these polarized sources will be spatially resolved by the VLASS Rudnick & Owen (2014), allowing us, to first order, to separate depolarization along the line of sight from beam depolarization (across line of sight).

Additionally, while we now have new extragalactic source catalogs of rotation measure vs redshift (e.g., Hammond et al., 2012; Xu & Han, 2014), we are severely limited by our inability to correct polarization data for cosmological expansion. A "polarization k-correction" is only possible with wide-band polarization data, with which we can then infer intrinsic rest frame properties of the magneto-ionic medium in AGNs, galaxies and their immediate environments, and can then investigate how all these properties evolve with redshift.

(2) How do large-scale magnetic fields emerge and grow in galaxies? Spatially resolved images of the polarized synchrotron emission from nearby galaxies demonstrate the existence of μG azimuthal

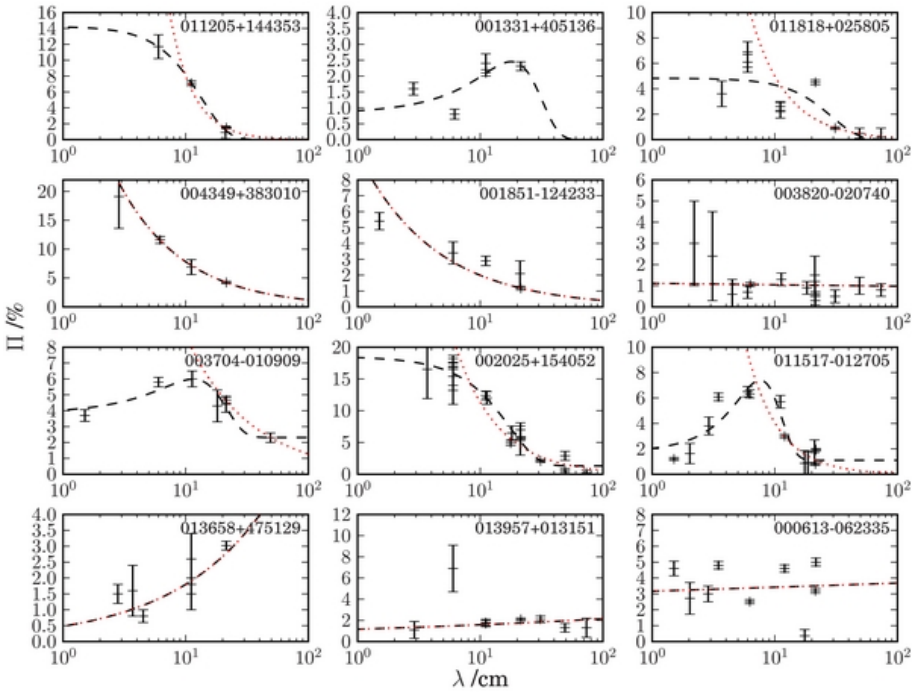

Figure 7: Broad-band spectrum of percent polarization for a sample of radio sources from Farnes et al. (2014a). The diverse complex spectra arise from a combination of internal Faraday depolarization effects (at longer wavelengths) and intrinsic magnetic properties (at shorter wavelengths).

fields (e.g., Beck et al., 1996). However, the evolution of galactic-scale magnetic fields over cosmic time is poorly constrained, because this traditional approach becomes increasingly challenging for distant galaxies. An alternative approach is to utilize the statistics of integrated synchrotron polarization of unresolved galaxies to infer their overall magnetic field properties (e.g., Stil et al., 2009). In the presence of a large-scale galactic field, the position angle of the integrated polarized radiation is aligned with the minor axis of the galaxy for rest frame frequencies above a few GHz.

At lower frequencies the effects of internal Faraday rotation from the galactic ISM both depolarizes the radiation and breaks the global symmetry of the observed field, leading to reduced polarized signal and variance of the correlation between the polarization position angle and the optical axes of the galaxy. On the other hand strong turbulence in starbursts can lead to depolarization that is largely independent of wavelength.

Observations between $2 - 4$ GHz spans the low and high depolarization frequency regimes, and can thus be used to test theoretical predictions from various galactic magnetic field generation mechanisms (see for example, Zweibel & Heiles, 1997), with which we can provide the first constraints on the time scales for galactic magnetic field amplification and the strength of the initial seed fields (Arshakian et al., 2009). Average fractional polarization of unresolved Milky-Way type galaxies is a factor of 3–4 higher at 2 GHz than at 1.4 GHz (Stil et al., 2009; Braun et al., 2010; Sun & Reich, 2012), a 2–4 GHz survey with sufficient sensitivity thus opens enormous potential for characterizing the development of galactic magnetic fields. Star-forming galaxies, which are mostly spirals, polarization reflects the degree of ordering in the intrinsic disk field. The fractional polarization distribution of nearby disk galaxies at 4.8 GHz was measured by Stil et. al. (2009) and Mitchell (2010), who carried out a survey of nearby (within 100 Mpc) but unresolved galaxies using the Effelsberg Telescope. These data show that at at least 60% of unresolved normal spiral galaxies are polarized higher than 1%, and in some cases higher than 10%. Moreover, there is a

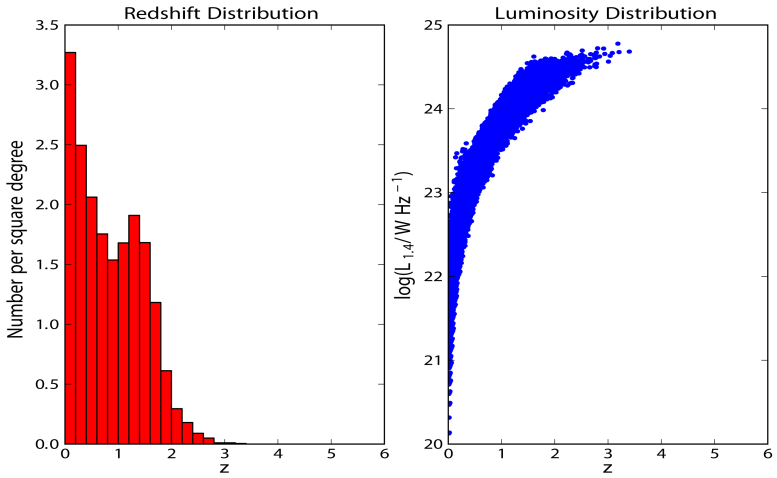

Figure 8: Redshift distribution and radio luminosity versus redshift for galaxies expected to be detected in one square degree with polarized flux density greater than 10 μJy.

strong correlation between polarization position angle and the optical minor axes of the galaxy disk. From predictions based on Monte-Carlo simulations, Figure 8 shows the distribution in redshift of disk galaxies that will be detected in polarized flux density greater than 10 μJy as well as the radio luminosity distribution. Several 10s of galaxies will be detected in each square degree, sampling to redshift $z \sim 2$. The VLASS deep tier will provide direct detection of the presence and properties of ordered magnetic fields in galaxy disks to intermediate redshifts and their relation to star formation and galaxy evolution.

EXAMPLE BACKGROUND EXPERIMENT *(3) What is the covering fraction, the degree of turbulence and the origin of absorption line systems?* Mg II absorbers are associated with $\sim 10^4$ K photo-ionized circum-galactic medium in a wide range of host galaxy types and redshifts (see Churchill et al., 2005, for a review). These systems potentially trace outflows from star formation (e.g., Norman et al., 1996) and cold-mode accretion (e.g., Kacprzak et al., 2010). When seen against polarized background sources, the Faraday depth provides a direct measure of the electron density and the magnetic field strength in Mg II absorbing systems, parameters that are both currently poorly constrained. Bernet et al. (2008, 2013) and Farnes et al. (2014b) have demonstrated the presence of larger values of |RM| associated with Mg II absorbers, and have interpreted this as evidence for μG field at $z \sim 1$, possibly associated with outflows. We can use such data to test models for the circum-galactic gas and the photo-ionization, and to infer the evolution of large-scale magnetic fields over cosmic time. With deep observations and high angular resolution, we can use Mg II catalogs derived from SDSS (Quider et al., 2011; Zhu & Ménard, 2013) to identify sight lines through absorbers (current total number $\sim$ 40,000).

TECHNICAL CONSIDERATIONS The 2-4 GHz band presents a unique opportunity to examine depolarized sources at the expense of lower Faraday resolution than 1-2 GHz. A useful comparison can be made with the bandwidth depolarization present in the NVSS survey. As described in Taylor et al. (2009), the original catalog was significantly depolarized above $|\mathrm{RM}| > 100$ rad m^{-2}, while their split-band analysis was sensitive to a maximum of $\sim$500 rad m^{-2}. By contrast, the sensitivity of the VLASS will extend to $|\max(\mathrm{RM})| \sim$38,000 rad m^{-2}, assuming use of the RFI-free bands of 2000-2128 MHz and 2834-3600 MHz. This coverage also sets the resolution in Faraday space, as shown in the figure 6, where the width of the Faraday transfer function is $\sim$200

rad m^{-2}. At the limit of the VLA survey, Faraday components with separations of $\sim$100 rad m^{-2} that would depolarize the NVSS can be accurately separated by such techniques as Q,U fitting (Sun et al., 2014). For foreground screen experiments, this provides a resolution of 10 rad m^{-2} at the survey limit (S:N=10), sufficiently smaller than the 20 rad m^{-2} difference between MgII populations discussed above and much less than the $\sim 10^2$ rad m^{-2} excesses claimed for the cores of galaxy clusters (Feretti et al., 2012a, and references therein).

For the All-Sky survey with 68 μJy rms, we expect $\sim$6 sources per square degree at a S:N=10, using the results of Rudnick & Owen (2014); Stil et al. (2014) at 20 cm. The loss in polarized intensity at S band due to the total intensity spectrum will be compensated for by the mean depolarization of 1.3 between the two bands (Lamèe et al. in preparation). Note that this result is based on the 9 arcminute resolution SPASS survey (Carretti et al., 2013), so a major reduction in beam depolarization may result in even larger S-band values. Thus, the VLASS All-Sky sensitivity gives at least a factor of 6 above the polarized source density of the NVSS, a major increase in power for targeted foreground experiments, and will, in addition, allow much greater access to the scarce heavily depolarized population. For large-area foreground studies, not otherwise described in this proposal, a fundamental limit to the RM scatter comes from the intrinsic variation in the extragalactic sources themselves, currently estimated at $\sim$5-7 rad m^{-2} (Schnitzeler, 2010). The VLASS can approach this limit for polarized flux densities $\gtrsim$1.5 mJy, providing a source density of $\sim$3 per square degree, an order of magnitude higher than the NVSS for which polarized fluxes of 10 mJy are required for this accuracy.

3.5 Peering Though Our Dusty Galaxy

Dust obscuration and absorption effects are not problematic at radio wavelengths, and there is a rich history of using radio observations to find objects deep within the Galaxy. Further, there have been a host of surveys of the Galaxy from the infrared to γ-ray (e.g., with *Spitzer*, *Chandra*, and *Fermi*) that the VLASS will complement, allowing for a rich multi-wavelength characterization of sources detected.

In the Galaxy, radio source populations include both thermal (e.g., H II and planetary nebulae) and non-thermal (e.g., pulsars and X-ray binaries) emitters. Non-thermal sources tend to have steep spectral indices $\alpha < 0$ ($S_\nu \propto \nu^\alpha$) while thermal sources tend to have inverted spectral indices $\alpha \gtrsim 1$ (Figure 9). Thus, observation frequency of 2–4 GHz, as planned for the VLASS, balances sensitivity to thermal and non-thermal sources, both of which are found in Galactic radio source populations.

The VLASS naturally lends itself to a finding a variety of Galactic radio sources, addressing a variety of Galactic science topics, due to the numerous types of point-like objects producing radio emission (see Appendix C for a broader range of Galactic radio sources that the VLASS might detect). Further, the panoply of Galactic science means that there is a large discovery space for unexpected phenomena. In the remainder of this section, we highlight three classes of objects that will be further illuminated by the Galactic coverage afforded by VLASS All-Sky.

Searching for Exotic Radio Pulsars
Neutron stars are extraordinary laboratories for extreme astrophysics and General Relativity. The VLASS will address well known selection biases that result from traditional large-area, periodicity surveys with single dish telescopes. We first describe the objects or systems that potentially could be discovered from using the VLASS as a finding survey, then describe the specific approach in more detail.

Extreme Double Neutron-Star (DNS) Binaries Compact binary systems have already proven to be powerful laboratories for General Relativity. The DNS with the shortest known orbital period is the double pulsar J0737$-$3039A/B (Lyne et al., 2004), for which $P_{\rm orb} = 2.4$ hr. In principle, DNS binaries could exist down to periods as short as 10 min. The double

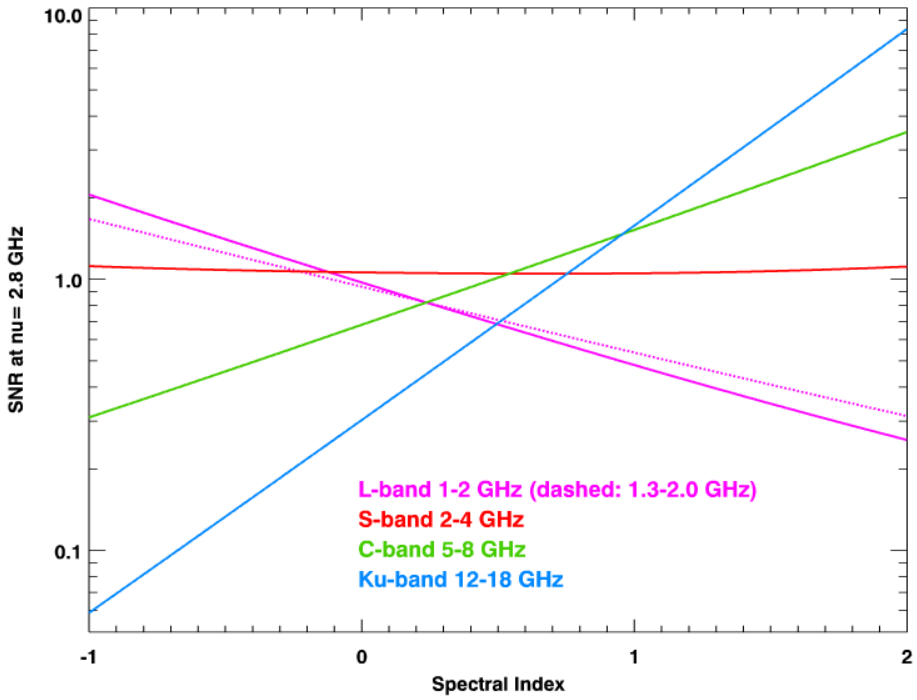

Figure 9: Signal-to-noise ratio sensitivity as a function of spectral index. The figure considers a source with a fixed signal-to-noise ratio (SNR) at a frequency of 2.8 GHz (S band), normalizing sensitivity to it. Higher signal-to-noise ratios can be obtained for non-thermal sources (spectral index < 0) by observing at lower frequencies (L band, pink solid and dashed lines) at the cost of lower sensitivity to thermal sources (spectral index $\gtrsim 1$). Conversely, higher signal-to-noise ratios can be obtained for thermal sources at higher frequencies (C band, green solid line; Ku band, blue solid line) at the cost of lower sensitivity to non-thermal sources. The Galactic radio source population contains both thermal and non-thermal emitters, and the 2–4 GHz observing frequency range for the VLASS provides a balance in the sensitivity for these two classes of sources.

pulsar requires post-Newtonian order 1.5 for its orbital description and has provided tests of GR to 0.05% (Kramer et al., 2006). More compact binaries will test General Relativity to higher order and, with suitable geometries, will provide strong gravity tests from lensing. DNS binaries also provide better calibration of the event rate for LIGO. Based on estimated merger rates, there should be approximately 2000 DNS binaries in the Galaxy with $P_{\rm orb} <$ 10 hr with about 20% of these (400) beamed toward us. The lifetime to GW emission implies a period distribution scaling as $P_{\rm orb}^{8/3}$, so there should be about 10 DNS binaries with orbital periods less than 2.4 hr with favorable beaming.

(Sub-)Millisecond Pulsars (MSPs) Recycled ("millisecond") pulsars with especially high spin stability are being employed in pulsar timing arrays for gravitational wave detection. Standard periodicity surveys using single-dish telescopes will miss some MSPs, including some of the most interesting ones, because binary motion will not be mitigated by acceleration searches in the more extreme cases. Further, our current understanding of the equation of state of nuclear matter allows MSP spin periods as short as 0.5 ms. However, the first discovered MSP (PSR B1937+21; Backer et al. 1982) had a period of 1.56 ms, and even today, the fastest known MSP has a period of 1.4 ms (Ter 5ad; Hessels et al. 2006). Periodicity surveys suffer from selection effects (orbital motion and plasma scattering in the interstellar

medium) that are strongest for the shortest-period pulsars. The VLASS would find objects that could be targeted with intensive periodicity searches, optimized for short-period pulsars. If sub-ms MSPs do not exist, then the combined hybrid approach will provide strong constraints on the evolution and physics of accretion-driven spin-up.

General Relativity Tests in Exotic Systems The recent discovery of a millisecond pulsar in a hierarchical stellar triple system (Ransom et al., 2014) is enabling extremely sensitive tests of the Strong Equivalence Principle, given the large difference in self-gravity between the NS and the inner WD ($3GM/5Rc^2 \sim 0.1$ vs. $\sim 3 \times 10^{-6}$), both of which are falling in the strong gravitational field of the outer WD. Likewise, no pulsar–black hole binary system is known yet, but they should exist on basic binary evolutionary grounds. The discovery of even a single such system will have extraordinary payoffs because timing measurements will probe space-time around a black hole to much higher precision than any other technique.

The value of VLASS is that it will serve as a "finding survey" in which *candidate radio pulsars* can be identified, to be followed by more intensive periodicity searches. A series of "filters" can be used to winnow the large number of radio sources detected in the VLASS to a feasible number on which to conduct a periodicity search. The VLASS is expected to produce a source density of 290 deg^{-2} (Table1). We expect between 25%–50% of these sources to be resolved at the flux density and angular resolution of the VLASS (Coleman & Condon, 1985; Muxlow et al., 2005) and immediately able to be rejected as candidate radio pulsars. With a combination of multi-wavelength counterpart comparisons, polarization, future high angular resolution observations, and other criteria, we expect it to be feasible to reduce the source density to of order 30 deg^{-2}. At this level, there is less than one candidate pulsar per single dish beam (e.g., GBT), and a targeted periodicity search becomes feasible.

The advantage of this hybrid imaging-periodicity search approach is that, for a fixed amount of telescope time in which to conduct a periodicity search, more efficient searches can be conducted by focusing on the relatively few sky positions containing the most interesting candidates rather than spending an equal amount of time on all sky positions. Specifically, for ultra-compact binaries (DNS or PSR-BH systems), it is too expensive to do full acceleration and binary orbit template match searches over the entire sky, whereas it is feasible to conduct such searches on a limited number of compact objects identified in the VLASS. Similarly, rare systems (e.g., PSR-BH binaries) are likely to be deep in the Galactic plane and highly scattered. Periodicity searches at lower frequencies will simply not detect these because they have little to no pulsed flux left, and all-sky periodicity surveys are simply impractical at the required depth. Again, single-dish all-sky searches at higher frequencies (e.g., 8 GHz) are infeasible. Finally, radio frequency interference (RFI) is proving increasingly debilitating to single-dish periodicity searches. The VLASS will provide additional information to enable the identification of true pulsars in a field of contaminating RFI, or to justify deeper targeted periodicity searches of candidate sources.

An early example of this finding survey-targeted periodicity approach was the initial identification of 4C 21.53 West as a compact, steep-spectrum object in an imaging survey (Erickson, 1983) followed quickly by the detection of millisecond pulsations from it (Backer et al., 1982), leading it to be classified as the PSR B1937+21, the first "millisecond pulsar." More recently, an imaging survey serving to find candidate radio pulsars followed by a targeted periodicity search has had considerable success with unidentified *Fermi* sources (e.g., Ray et al., 2012).

Finally, *electron-density and magnetic field models for the Milky Way* will be calibrated and improved by column density and scattering measurements from confirmation observations of new pulsar discoveries in the Galactic plane and bulge.

Coronal Magnetic Activity on Cool Stars

The radio emission from nearby active stars provides a unique probe of accelerated particles and magnetic fields that occur in them, which is useful for a broader understanding of dynamo processes in stars, as well as the particle environment around those stars. The large magnetic field

strengths now known to occur around some brown dwarfs were first detected through their effect on cm-wavelength radio emission (Hallinan et al., 2006) before the signatures were seen through Zeeman splitting of absorption lines at near infrared wavelengths (Reiners & Basri, 2007). The stellar byproduct of exoplanet transit probes like *Kepler* and TESS will yield information on key stellar parameters like rotation, white-light flaring, and asteroseismic constraints on stellar ages. These parameters can be used together to address fundamental questions such as those identified in the *New Worlds, New Horizons* Decadal Survey ("How do rotation and magnetic fields affect stars?"). Unlike other diagnostics of magnetic activity, like coronal emission which displays a maximum value of $L_X/L_{\rm bol} \approx 10^{-3}$ corresponding to the maximum amount of coronal heating a star is able to maintain, incoherent stellar radio emission shows no saturation effects. Thus, the level of radio emission can vary by orders of magnitude depending on the instantaneous particle acceleration events and plasma properties.

The most magnetically active stars will produce detections in VLASS: tidally locked, magnetically enhanced active binary systems, rapidly rotating disked or diskless young stellar objects (YSOs), and fully convective M dwarfs. Non-thermal radio emission from YSOs is attributable to the presence and action of magnetic fields and is seen at all evolutionary classes, providing a unique probe of the beginning of a star's magnetic activity life and its effects on other processes like the star's final formation steps and impact on planetary formation. The fraction of objects detected in legacy VLA pointed centimeter wavelength observations varies with mass and evolutionary phase, but is low, 10–50% (Osten & Wolk, 2009). The increased sensitivity of the JVLA, combined with the large area coverage of the All-Sky component will be able to increase the numbers of radio-detected objects, perhaps up to a factor of 4, based on initial results from Ortiz-Leon et al. (2013). Scaling from the luminosity distribution of currently known active stars, VLASS will be able to detect ultracool dwarfs to 10–20 pc, active dwarf stars to a few tens of parsecs, and active binaries to slightly less than 2 kpc. At the distances to the nearest star forming regions (150–300 pc), VLASS sensitivity limits will probe stellar radio luminosities above 1–4 $\times$ 10^{16} erg s^{-1} Hz^{-1}, enabling studies of particle acceleration at a range of YSO evolutionary stage, from class I–III. All star-forming regions visible from New Mexico will be studied with the VLASS.

Combined with the LSST and eROSITA surveys, the All-Sky component of VLASS will be a foundational aspect of identifying and studying nearby active stars. Particularly powerful will be cross-correlating variable or transient sources identified in LSST surveys with VLASS and vice-versa, enabling unbiased constraints on sources producing extreme magnetic activity. The multi-epoch nature of VLASS will allow for constraints on variability of particle acceleration. Such cross-correlations, as a way of identifying nearby active stars, will allow more robust statistics from which to compare the distribution of optical flares with the efficiency of strong particle acceleration.

Star Formation and Evolution, Distant Thermal Sources, and Galactic Structure

Young, massive stars produce an *H II region*, while intermediate and low-mass stars end their lives by expelling their outer layers into the interstellar medium (ISM) and producing *planetary nebulae* (PNe). In both cases, the hot central star ionizes the surrounding material, which then emits free-free radio emission. Radio observations are a powerful means of identifying these Galactic sources because radio observations are relatively unaffected by dust obscuration that affects visible and near-infrared wavelengths, and centimeter-wavelength surveys have proven to be a powerful means of identifying Galactic thermal sources (e.g., Hoare et al., 2012; Kwitter et al., 2014).

Typical time scales for an H II region or PN to evolve are short. For example, the expansion time scale of an H II region may be only 10^5 yr (Franco et al., 1990; Garcia-Segura & Franco, 1996), and it may take only 10^4 yr for a star to evolve from the asymptotic giant branch (AGB) through the PN phase to become a white dwarf (Kwok, 2005). Indeed, population synthesis models predict a range of expected Galactic planetary nebulae (Sabin et al., 2014) yet the total number of known

nebulae is far lower than even the most conservative expectations. Consequently, large samples of these objects are required to trace evolutionary sequences. Further, as tracers of massive star formation, H II regions are a natural means to identify the spiral structure of the Galaxy.

The VLASS All-Sky component, by virtue of its wide area coverage (§4.1) naturally provides access to a substantial fraction of the Galactic plane. Allowing for degradation in image quality at low declinations, we nonetheless estimate that the Galactic longitude coverage obtained is $-10^\circ \lesssim \ell \lesssim 250^\circ$ ($\approx 70\%$ of the Galactic plane).

Detecting distant thermal sources, such as H II regions and PNe, requires a combination of both angular resolution and adequate brightness temperature sensitivity. An H II region might be several arcseconds in size (0.5 pc at 10 kpc), while surveys of nearby PNe show that they tend to be a few to several arcseconds in size (Aaquist & Kwok, 1990). Given that most H II regions and PNe are not simple spherical shells, but show more compact sub-structure, an angular resolution of a few arcseconds is desirable. Produced by the free-free emission from ionized gas, expected brightness temperatures might be a few hundreds of degrees to of order 10^3 K. Thus, arcsecond angular resolution and a brightness temperature sensitivity of order 10 K or better would be sufficient to detect large numbers of distant thermal sources.

In practice, the VLASS observations by themselves may not be sufficient to identify distant H II regions or PNe, though a combination of spectral information and morphology from the VLASS alone may provide significant filters. However, combining the VLASS with other radio and infrared observations will be able to an expanded sample of H II regions and PNe throughout a significant fraction of the Galactic disk.

3.6 Missing Physics

The radio portion of the spectrum for astrophysical objects provides diagnostics for a whole range of physical processes that are not easily ascertained in other parts of the spectrum. For instance, VLASS will be able to: peer through high columns of dust, finding classes of objects unseen or un-studiable in other parts of the spectrum; characterize the properties of deeply embedded star formation; observe polarized emission from cosmic rays spiraling in magnetic fields; measure spectral indices that elucidate the origin and geometry of emission; and observe variability that both constrains scales of compact sources and reveals wholly new classes of objects.

When multi-wavelength astronomers lack radio information, they are unable to compile a complete picture of the physics of individual objects and the statistical properties of the sky. VLASS, however, will enable the discovery and study of rare classes of objects in the radio, while also allowing the broader astronomical community to determine the radio emitting properties of rare classes of objects that are identified at other wavelengths (e.g., brown dwarfs, γ-ray bursts, or objects from future surveys such as LSST). Additionally, later this decade, the Advanced LIGO and VIRGO gravitational-wave observatories (GWO) are expected to turn on, ushering in a new astronomical land rush across the electromagnetic spectrum to make the first identifications within the large ($\sim 500\mathrm{deg}^2$) error regions of the first events[1]. The existence of high quality dynamic radio images over a substantial region of the sky from the VLASS All-Sky tier will provide future GWO transient hunters a critical baseline from which to discern newly appearing objects from extant static and run-of-the-mill variable sources.

By virtue of having an All-Sky component, VLASS will include portions of the sky for which major investments are already in place to gather optical/NIR spectroscopy, thus allowing meaningful astrophysical investigations of sources. As an example, this will include the entire 14,000 deg^2 area being targeted by the Dark Energy Spectroscopic Instrument (DESI), which will obtain optical spectra for tens of millions of galaxies and quasars, constructing a 3-dimensional map

[1] http://www.ligo.org/science/GWEMalerts.php

spanning the nearby universe to 10 billion light years. As hundreds of thousands of spectra already exist in the proposed area, the radio data from VLASS will immediately enable investigations of stars, stellar remnants, galaxies, clusters, and AGN.

By peering through the dusty Galaxy, the VLASS will enable both individual and statistical studies including the study of the mass-energy-chemical cycle in galaxies, star formation, the influence of rotation and magnetic fields on non-degenerate stars, nailing down the progenitors of type Ia supernovae, the end lives of massive stars, and what controls the parameters of compact stellar remnants.

Unlike any other radio survey to date, VLASS Deep will achieve a depth that is sensitive to the population of star-forming galaxies at the critical epoch of star formation between $1 \lesssim z \lesssim 3$, while simultaneously covering an area that is truly free from the effects of cosmic variance. In doing so, Deep will provide the astronomical community with a critical new dataset to study the evolution of star-forming galaxies as a function of environment. Furthermore, with its subarcsecond resolution, VLASS Deep will remain the only radio survey that will resolve star-forming galaxy disks at $z \gtrsim 1$ over many deg^2 until SKA Phase 1. This aspect of the survey design drives the potentially groundbreaking weak lensing science of Deep, by providing the ability to deliver the first definitive measurement of weak lensing in the radio.

Thus, in a host of ways, VLASS will bring the critical diagnostics provided by observing in the radio part of the spectrum to the broad multi-wavelength astronomical community, enhancing our ability to model and interpret the physics at play.

3.7 A Lasting Legacy into the SKA Era

VLASS will not only deliver unprecedented science as described above, but will also build a lasting legacy well into the SKA era by consciously being designed to highlight the capabilities of the VLA that will remain state of the art well into $>>$2020. Specifically, the survey capitalizes on the exquisite point source sensitivity and high angular resolution that will not be superseded until SKA1-MID begins operating in the Karoo. For comparison, MeerKAT/MIGHTEE (Tier2: $\sim 1\mu$Jy/beam with $\theta_s \approx 5\farcs5$) will be able to detect the same sources as we would with the VLA in the Deep tier, however it will be unable to characterize these sources from a radio perspective or unambiguously associate them with an optical/near-infrared counterpart. This is because the source density at these depths is $\sim$20,000 per deg^2 for the MIGHTEE-Tier2 survey, and the MeerKAT beam is approaching the nominal confusion limit of $\sim$30 beams per source. Another crucial advantage that the VLA has over MeerKAT is its ability to resolve typical star-forming galaxies (and AGN) at all redshifts – MeerKAT will *never* be able to do this. This is a unique science case that will not be superseded until the SKA1-MID is fully operational with $>$100 km baselines. *Consequently, the first generation SKA1 reference radio-continuum surveys, which are in the process of being reviewed, are currently being benchmarked against the Deep imaging component of VLASS (Prandoni & Seymour, 2014).*

In addition to delivering deep, high-resolution imaging, the WIDAR correlator has opened a major new window for spectral index and wideband polarization work, enabling the characterization of the magneto-ionic medium in AGNs and in galaxies across a wide range of redshifts. In combination with SKA precursor surveys at L-band, MeerKAT, ASKAP (POSSUM/EMU) and WODAN, the VLASS will provide 3 GHz of frequency baseline to increase the ability to characterize complex spectral and Faraday structures, opening up new and exciting science that combines the strengths of the VLA and SKA precursors, rather than setting them up to compete. For AGN science, the requirement to morphologically distinguish different types of AGN (e.g., FRI and FRII) from star-forming galaxies and the need for reliable cross-IDs is again the driver for doing this survey with the VLA rather than MeerKAT. However, the synergies between these two facilities can and should be capitalized on. For example, MIGHTEE will provide accurate total flux densities and luminosities for extended AGN, whilst also providing a longer baseline for spectral

index measurement that can be used to infer the physical state of the AGN and the environment in which is resides. Thus, not only will the deep, high resolution imaging from VLASS remain state of the art well into >>2020, the synergy of these observations (in frequency and resolution) with those of the SKA pathfinders coming online over the next ∼5 yr will ultimately enable even more new science than that which is discussed here.

From the point of view of the dynamic radio sky, VLASS will also provide a unique snapshot of the Universe some 20 years after the FIRST survey, and leading up to the advent of the SKA pathfinders and the SKA itself. Current large-area radio transient detection surveys, such as the recent Stripe 82 survey of Mooley et al. (2015, in preparation), successfully utilized the "Epoch 0" provided from FIRST as well as other historical VLA-based surveys, as a starting point for identification of newly appearing objects from the first new Jansky VLA epochs. As the VLA surveys go deeper, the utility of FIRST and other earlier shallow surveys will decrease. VLASS — with its depth, area, and angular resolution — will provide a new launching point for future surveys, taking us into the SKA and LSST eras. This will be the case across the breadth of transient and variability studies touched upon in § 3.3 above, and well beyond.

Finally, it is certainly worth mentioning that experience shows that when telescopes enter unexplored areas of observational phase space, as will be the case with VLASS, they make unexpected discoveries. It has been shown that the most significant discoveries with major telescopes often end up being those that were completely unexpected. As an example, of the "top ten" discoveries with *HST* (as ranked by National Geographic magazine), only one was a key project used in the *HST* funding proposal (e.g., see Norris et al., 2014). Moreover, half of the "top ten" *HST* discoveries were unplanned, including the only *HST* discovery (Dark Energy) to win a Nobel prize. So while specific science goals detailed above have focused the design of VLASS, it may not be surprising if they do not end up being its greatest scientific achievements. It will undoubtedly be the scientific imagination and curiosity of the community that will ultimately drive the best science to come out of VLASS.

4 Survey Strategy

The VLASS science goals drive a survey structured in two tiers. We call the tiers All-Sky (69 μJy bm^{-1}, 33885 deg^2) and Deep (1.5 μJy bm^{-1}, 10 deg^2). A detailed discussion of the survey implementation is presented in § 5.3.

The overall VLASS request is for ∼9000 hours of VLA time. The detailed scheduling (below, and in § 5.2.3) come to a total of 8827 hours. See Table 3 for a summary of the tiers.

Table 3: Summary of VLASS

Component	Resolution (arcsec)	Comb. Depth (μJy bm^{-1} / K)	Area (deg^2)	Epochs (Pass/Epoch)	Time (hr)	Config.	Notes
All-Sky	2.″5	69 / 1.5	33885	3 (1)	5436	B/BnA	
Deep/COSMOS	0.″8	1.5 / 0.32	2	4 (10)	300	A	incl. prev. obs.
Deep/ECDFS	2.″0×0.″8	1.5 / 0.18	4.5	4 (98)	1960	A	
Deep/ELAIS-N1	0.″8	1.5 / 0.13	3.5	4 (39)	1131	A	

Note: Resolution and sensitivities assume robust weighting to achieve near-natural weighted sensitivity with suppressed side lobes.

Sensitivity Assumptions: The sensitivity of the Jansky VLA for mosaicking is computed using the procedure given in the Guide to VLA Observing: Mosaicking[2]. For continuum (Stokes I) at

[2] `https://science.nrao.edu/facilities/vla/docs/manuals/obsguide/modes/mosaicking`

S-band (2–4 GHz) we assume a Survey Speed (SS) of

$$SS = 16.55 \left(\frac{\sigma_I}{100\,\mu\mathrm{Jy/beam}} \right)^2 \mathrm{deg}^2\,\mathrm{hr}^{-1} \quad (1)$$

of on-sky integration time for an assumed image rms of σ_I. This assumes 1500 MHz of useable bandwidth (after RFI excision) and an image averaged over the band using multi-frequency synthesis. The integration time needed to survey a given area to a depth is given by dividing that area by the survey speed.

Overhead Assumptions: In the estimates for total observing time, allowance is made for the overhead for slewing, setup, and calibration that will apply to a given component of the survey. We assume that:

Assumed Overheads for VLASS by Component

Component	Overhead	Comments
Deep/COSMOS, Deep/ECDFS	25%	5–7 hour blocks, contained calibration
Deep/EN1	22%	6–8 hour blocks, contained calibration
All-Sky	17%	long blocks, shared calibration[3]

These numbers are adopted as guidance in the times given below. Note that the overheads actually used for scheduled hours for the Deep fields are close to these, but are rounded to make the schedules of a sensible length (e.g. rounded to nearest 15 minute duration).

For example, for All-Sky the estimated calibration overhead is 17% and thus the required integration time of 4650 hours is multiplied by the factor 1.17 to arrive at a "clock time" of 5439 hours needed to execute the All-Sky component. This in turn is rounded to 5436 hours to allow for distribution between the cycles in which this component is scheduled (§ 5.2.3).

In practice, the exact overhead will depend on exactly how the survey components are scheduled and how much calibration can be shared between blocks. The calculations used to arrive at the overheads are presented in the Technical Implementation Plan (TIP) document, and verification of these assumptions are included in the Test Plan described in § 5.3.5.

4.1 All-Sky

Table 4: Summary of All-Sky (Tier 1)

Parameter	Value
Total Area	33885 deg^2, $\delta > -40^\circ$
Cadence	3 epochs, separated by at least 32 months
Angular Resolution	2.″5 (B/BnA configuration)
Continuum Image rms (Stokes I)	$\sigma_I = 69\,\mu$Jy/beam combined $\sigma_I = 120\,\mu$Jy/beam per-epoch
Integration Time	4650 hr total 1550 hr per epoch,
Scheduled Time (w/ 17% overhead)	5436 hr in total observing, 1812 hr per epoch

[3] As discussed in the TIP, given that shared calibration will take some significant effort to pipeline, overhead for the initial epochs may be closer to 20%.

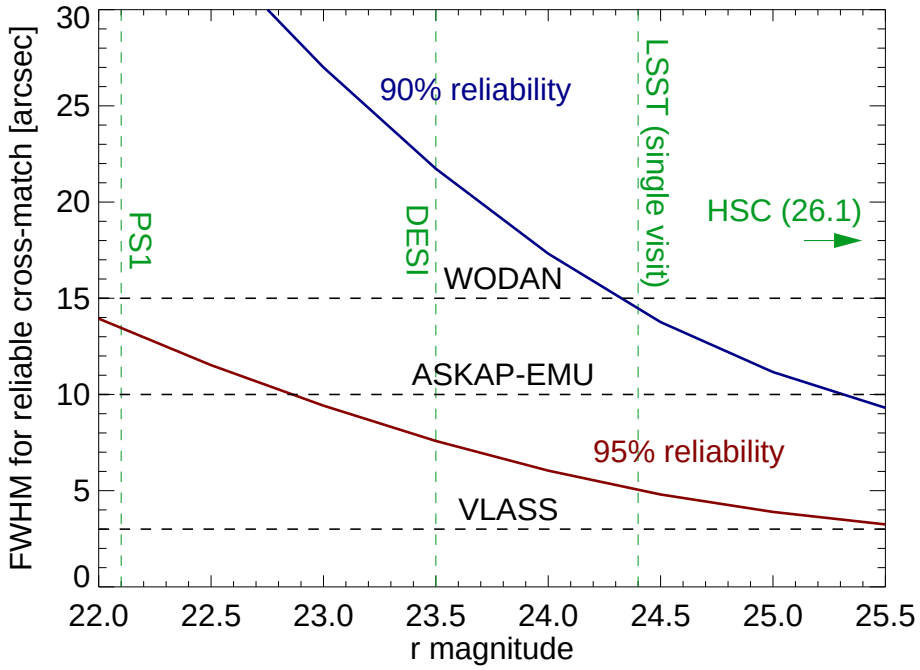

Figure 10: FWHM resolution required to achieve reliable cross-matches at fainter magnitudes using r-band galaxy counts from the CFHTLS-D1 1 deg^2 survey (Jarvis, private communication). Two curves are shown for 90% and 95% reliable identifications, and the resolutions of VLASS, ASKAP-EMU and WODAN are shown. This confirms that the SKA pathfinders are at best marginally sufficient for identifications at SDSS/Pan-STARRS depths, while VLASS is usable all the way to $r = 25$.

4.1.1 Context

The age of survey astronomy is unfolding with the development of sensitive all-sky telescopes in the optical/IR (WISE, Pan-STARRS, PTF, etc.) and at high energies (Swift, Fermi, eROSITA). Ten years from now, LSST will begin constructing the definitive large, deep optical map of the universe. For the past 16 years, the NVSS provided the wider astronomy community with a reliable reference image of the GHz sky. Thanks to the EVLA project upgrades, the VLA is positioned to play a similar role in the next decade of astronomy.

We propose that the first tier of VLASS provide a high-resolution radio reference for the entire northern sky. The All-Sky tier will have an unprecedented combination of resolution and sensitivity with powerful spectral and polarimetric information.

The spatial resolution of this tier (and all tiers of VLASS) will give astronomers a unique ability to robustly identify radio counterparts to sources at other wavelengths. The synthesized beam will have a FWHM of $2\farcs5$, $\sim$ 20 times smaller than NVSS and 4–6 times smaller the SKA pathfinder surveys EMU and WODAN. In Appendix D we provide a detailed analysis (i.e., the "S/N model of positional accuracy") that demonstrates that one-third of the optical counterparts to SDSS depth will be false matches using the 95% confidence matching radius required for WODAN. The false counterparts will obviously be an even bigger problem for deeper optical surveys, such as the ongoing DES and HSC surveys and eventually for LSST (Figure 10). Thus, VLASS will be a unique radio resource for the entire astronomical community.

With a survey depth of 69 μJy bm^{-1}, the All-Sky tier will be $\sim$4 times more sensitive than the

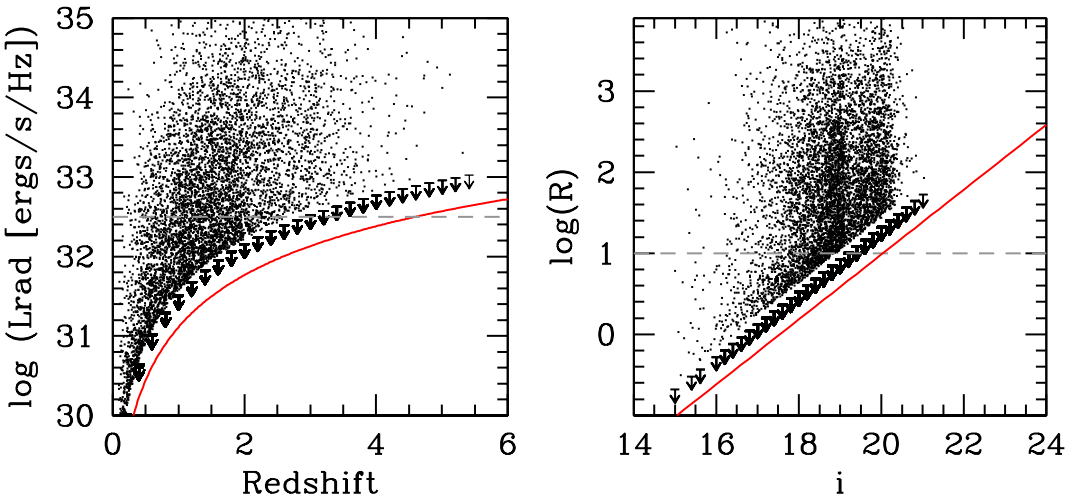

Figure 11: *Left:* Radio luminosity plotted against redshift for SDSS quasars. The dashed line indicates a division between radio- loud and radio-quiet quasars according to the radio luminosity (e.g., Goldschmidt et al., 1999). Radio upper limits are shown by arrows (offset downward slightly from the actual limits and sparse sampled for clarity). The depth of VLASS All-SKy tier (as indicated by the red line) allows us to push the redshift limit of radio-loud completeness from $z = 2.7$ to $z > 4$. *Right:* Radio loudness (as measured by the ratio of radio to optical flux) vs. i-band magnitude. The dashed line shows the traditional division between radio-loud and radio-quiet quasars of log(R)=1. Upper limits are given as arrows (offset downwards slightly and for clarity). The solid red line shows the improvement that results from VLASS All-Sky tier. Not only will we be complete to radio-loud quasars to i = 19.9, combining with the deep optical data will allow us to study the most radio-loud objects to i $\sim$ 24 over a significant fraction ($\sim$30%) of the sky.

NVSS to sources with $\nu \sim -0.7$ radio spectral indices. In a sense, this makes the All-Sky tier an extension of the FIRST survey. However, by virtue of using S-band and its large fractional bandwidth (2–4 GHz), VLASS will produce more reliable images and richer information for each radio source. Spectral indices and full-Stokes spectro-polarimetric properties will constrain the nature of the radio emission and effects of propagation.

4.1.2 Description

Area and Depth: The All-Sky component will cover $\approx$34,000 deg^2 north of declination -40°, which is 82% of the entire celestial sphere down to a 1σ rms depth of 69 μJy, thus covering the entire VLA-visible sky down to FIRST depth.

Angular Resolution: The All-Sky component will be conducted in B and BnA-array, providing a uniform $2\farcs5$ synthesized beam over the entire sky. Such high resolution is necessary for accurate positional matching with existing and forthcoming optical/NIR imaging surveys.

Cadence of Multiple Epochs: The entire sky will be imaged three times down to a depth of 120 μJy, providing 3 epochs of high-resolution maps and catalogs for immediate time-domain science, as well as providing a critical baseline for all future transient surveys and follow-up of multi-wavelength transient events (e.g., gravitational waves, LSST, etc.)

4.1.3 Survey Science – Extragalactic

The All-Sky tier will have impact in many areas of astronomy. Here we highlight the key science enabled by this tier.

Community Science: A prime driver for this tier is to create a set of legacy products that can be used for a very broad range of science by the whole astronomical community. As the entire sky down to -30° declination has already been covered by the Pan-STARRS survey, we can guarantee that the whole VLASS will be utilized for science as soon as it is available, providing this decade's enhanced version of the powerful FIRST+SDSS combination. The 1700 papers citing FIRST cover topics from galaxies to stars, studying individual sources and whole populations, searching for predicted signatures and finding them serendipitously. The VLASS All-Sky tier will become a top-level community resource for almost every area of astronomy.

Quasar Science: The primary demand that quasar science—at high redshifts in particular—places on a radio survey is for a wide area. Quasars are rare, and the radio-loud sources account for only ∼5% of the population as a whole. To SDSS depth, the surface density of optically selected quasars is $\sim 43\ \mathrm{deg}^{-2}$ at $0 < z < 5$ (Richards et al. 2006; Ross et al. 2013), of which only $\sim 1.4\,\mathrm{deg}^{-2}$ are at $z > 3$. Thus only one high-redshift ($z > 6$), radio-loud quasar is detected per $\sim 7\ \mathrm{deg}^2$ of survey area. Building a large statistical sample of radio sources for demographical studies of, for example, the evolution of radio loudness with redshift (Jiang et al., 2007) requires significant sky coverage.

High-resolution is also important for understanding of radio-loud quasars. The typical spectral index for a radio quasar is $\alpha_\nu \sim -0.5$, arguing for lower frequencies in order to achieve higher sensitivity for a given flux limit. In addition, there are hints that compact, steep-spectrum radio emission may be more prevalent at high redshifts (e.g., Frey et al., 2011). Such sources will be easily detected by planned low frequency (< 1 GHz) surveys with excellent sensitivity; however, these surveys will invariably have poor resolution. Efficient matching of radio sources to surveys at other wavelengths (particularly in the optical) requires ∼arcsecond resolution. In this way, a higher frequency VLA survey can provide an essential complement to the low frequency surveys, providing localization of radio sources at a much greater depth than FIRST. This is prerequisite to identifying candidates for spectroscopic campaigns to obtain redshifts, either in the optical/near-IR, or with ALMA.

The FIRST survey detects barely 10% of SDSS quasars, requiring stacking analyses for the vast majority of sources. That is a real problem, as only about 10% of quasars are formally "radio-loud", leaving us with a very biased view of the radio properties of quasars, as well as many unanswered questions. All-Sky will be sensitive to radio-loud quasars down to $i \sim 20$ (Figure 11), which corresponds to a depth of about 40 quasars per deg^2, and an expected number of radio-loud quasars of 40,000. While VLASS will not be as sensitive as FIRST to extended sources, Ivezić et al. (2002) find that complex sources only account for 15% of the SDSS quasar sample. Moreover, Hodge et al. (2011) report on A-array observations (i.e., with better resolution than FIRST) to 3x the depth of FIRST in SDSS Stripe-82 and found that 97% of known SDSS quasars are recovered in the higher resolution data.

Star forming galaxies: Current surveys fail to provide a large sample of low-z galaxies with well-established polarizations over a wide range in starburst luminosities. The All-Sky tier will detect (unresolved at $5\,\sigma$) luminous star forming galaxies (i.e., Luminous Infrared Galaxies; LIRGs) out to $z \sim 0.15$ (LIRGs) and rarer ultra-luminous infrared galaxies (ULIRGs) out to $z \sim 0.5$. By surveying a representative volume of the low-redshift universe, this tier will provide a good baseline sample of relatively nearby objects with which to compare the higher-redshift objects probed by the Deep tier.

Polarization Science: The All-Sky tier provides the first arcsecond-resolution, all-sky survey of polarization at any frequency. By observing at higher frequencies and high spatial resolution, depolarization effects will be dramatically reduced compared to all previous surveys. The uniquely large fractional bandwidth gives sensitivity to larger Faraday depths ($>10^5$ rad m^{-2}) and extended structures in Faraday depth space. This opens the possibility of discovering entirely new populations of polarized sources (e.g., in very turbulent environments: inner regions of jets, starbursts, etc.). The combination of VLASS with the MeerKAT/POSSUM/WODAN surveys will create a powerful lever arm to study magnetic fields in Faraday-complex sources, the Galaxy, and potentially the intergalactic medium.

Time Domain Science: The All-Sky component will be carried out in three distinct epochs, each spanning around 4 months with approximately 32 months in between. This will enable the discovery of emerging long-duration events due to the afterglows from supernova explosions, binary neutron star mergers, and tidal disruption of material falling into supermassive black holes. The VLASS All-Sky tier will also provide a unique snapshot of the Universe some 20 years after the FIRST survey. With its depth, area, and angular resolution, these observations will provide a new launching point for future surveys as well as the targeted follow-up of events triggered by a new suite of multi-wavelength (radio, infrared, optical, X-ray and γ-ray) and multi-messenger (cosmic ray, gravity-wave) facilities.

4.1.4 Survey Science – Galactic

In recent years, IR surveys of the Galaxy have dramatically improved in resolution and sensitivity, which has improved our understanding of the life cycle of stars and gas in the Milky Way. Surveys have been made with *Spitzer* [GLIMPSE: Benjamin et al. (2003); Churchwell et al. (2009) and MIPS-GAL: Carey et al. (2009)], *Herschel* (Hi-GAL: Molinari et al., 2010), and ground-based facilities (Lucas et al., 2008, UKIDSS;). An effort to complement these in the radio domain is the CORNISH survey, a 5 GHz counterpart to GLIMPSE. Recently, a follow up survey to CORNISH, GLOSTAR (VLA/14A-420; PI K. Menten), has begun observing the Galactic plane with the new wideband C-band receiver using multiple configurations and targeting a latitude range of $\pm 1^\circ$ in the Galactic plane. VLASS is an opportunity to systematically survey the *entire* Galactic plane and bulge regions in a way that complements existing IR and radio surveys with high-resolution 3 GHz images.

Searching for Exotic Radio Pulsars: Many exotic classes of radio pulsars—such as compact neutron star binaries, highly scattered millisecond pulsars, and pulsars with spin periods less than a millisecond (should they exist)—suffer significant selection effects in traditional periodicity searches using single dishes. VLASS will enable a hybrid imaging-periodicity search in which relatively simple criteria such as (lack of) source structure and multi-wavelength counterparts are used to winnow the number of sources significantly. The small number of candidate radio pulsars remaining can then be targeted for subsequent, intensive periodicity searches.

Coronal Magnetic Activity on Cool Stars: The radio emission from nearby active stars provides a unique probe of accelerated particles and magnetic fields that occur in them, which is useful for a broader understanding of dynamo processes in stars, as well as the particle environment around those stars. Previous surveys with the legacy VLA have been significantly sensitivity challenged, and the VLASS alone should increase sample sizes by a factor of 4 or more. Moreover, the VLASS will serve as a foundational aspect of probing particle acceleration and magnetic field in nearby active stars when combined with future multi-wavelength observations (e.g., LSST and eROSITA).

Star Formation and Evolution, Distant Thermal Sources, and Galactic Structure: The observing frequency of the VLASS represents a balance between sensitivity for non-thermal and thermal radio sources. A number of Galactic sources are expected to be thermal emitters, most notably H II regions and planetary nebulae (PNe). Both classes of sources have relatively short time scales ($\lesssim 10^5$ yr) and large samples of these objects are required to trace evolutionary sequences. The VLASS All-Sky component—with its combination of wide area coverage, angular resolution, and brightness temperature sensitivity—will be a powerful means for expanding the sample of H II regions and PNe, as well as other thermal sources, throughout a significant fraction of the Galactic disk.

4.2 Deep

Table 5: Summary of Deep (Tier 2)

Field	Parameter	Value
COSMOS		
	Total Area	2 deg^2,
		centered at $10^h00^m28^s$, $+02°12'21''$
	Cadence	4 epochs of 4 month duration spaced by 12 months (approx.)
		10 passes per epoch
	Total Tier 3 Integration Time	234 hr
	Scheduled Time (w/ 25% Overhead)	300 hr
	Per Epoch	75 hr total (7.5 hr per pass)
	Previous data	302 hr of Archival observations (12B-158)
	Continuum Image rms (Stokes I)	$\sigma_I = 1.5\,\mu$Jy/beam combined (w/previous)
		$\sigma_I = 4.5\,\mu$Jy/beam per new epoch
		$\sigma_I = 10\,\mu$Jy/beam per new pass
ECDFS		
	Total Area	4.5 deg^2,
		centered at $03^h32^m28^s$, $-27°48'30''$
	Cadence	4 epochs of 4 month duration spaced by 12 months (approx.)
		92 passes per epoch
	Total Tier 3 Integration Time	1570 hr
	Scheduled Time (w/ 25% Overhead)	1960 hr
	Per Epoch	490 hr total (5 hr per pass)
	Continuum Image rms (Stokes I)	$\sigma_I = 1.5\,\mu$Jy/beam combined
		$\sigma_I = 3\,\mu$Jy/beam per epoch
		$\sigma_I = 30\,\mu$Jy/beam per pass
ELAIS-N1		
	Total Area	3.5 deg^2,
		centered at $16^h08^m44^s$, $+56°26'30''$
	Cadence	4 epochs of 4 month duration spaced by 12 months (approx.)
		39 passes per epoch
	Total Tier 3 Integration Time	937 hr
	Scheduled Time (w/ 22% Overhead)	1131 hr
	Per Epoch	282.75 hr total (7.25 hr per pass)
	Continuum Image rms (Stokes I)	$\sigma_I = 1.5\,\mu$Jy/beam combined
		$\sigma_I = 3\,\mu$Jy/beam per epoch
		$\sigma_I = 19\,\mu$Jy/beam per pass

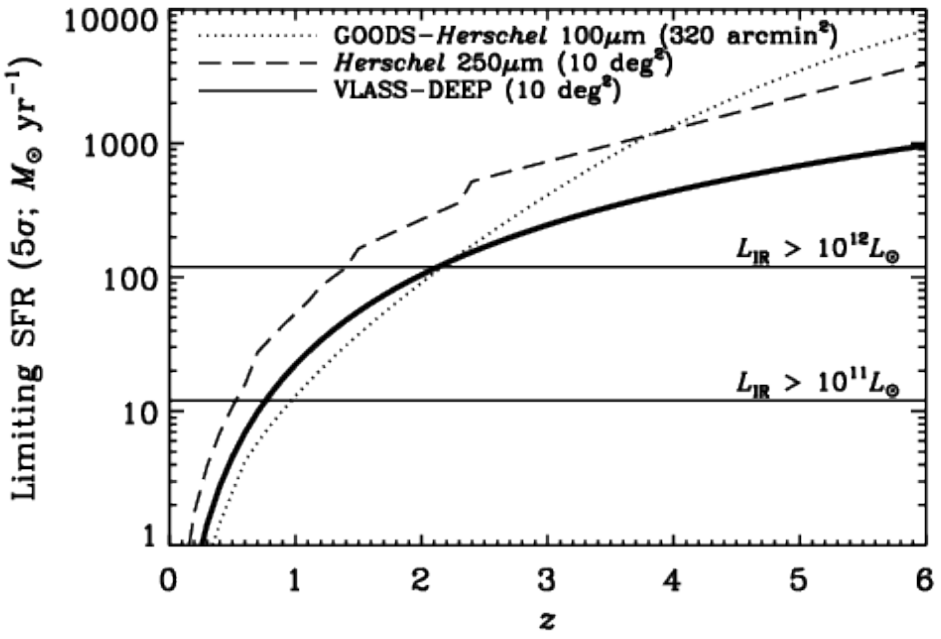

Figure 12: The VLASS-Deep selection function (5σ) for unresolved star-forming galaxies in units of limiting star formation rate (assuming a Kroupa IMF). For comparison, we over plot the selection function (dotted line) of the GOODS-*Herschel* 100 μm (5σ) data, which are some of the *deepest Herschel* far-infrared extragalactic survey data ever taken, covering a total of $\approx$320 arcmin^2 in GOODS-N+S (i.e., more than 100$\times$ less area than VLASS-Deep; Elbaz et al., 2011; Magnelli et al., 2013). Beyond $z \sim 2$, the VLASS data are actually *more* sensitive to star-forming galaxies than the ultra-deep *Herschel* imaging. We additionally show the selection function (dashed line) for *Herschel*/SPIRE 250 μm (5σ) data, as these data are available for the full VLASS-Deep 10 deg^2.

4.2.1 Context

There are three primary reasons why VLASS contains a Deep tier that reaches to much fainter luminosities than the much wider All-Sky tier:

1. A Deep tier allows objects of similar luminosity to those in the complementary, shallower but wider tiers to be observed at much greater distances and larger look-back times. This provides an essential lever arm to disentangle the effects of differing luminosity from the effects of cosmic evolution of the source population being studied. This is particularly relevant in polarization where the Deep tier will provide our first look at the magnetic properties for a large sample of disk galaxies outside of our local universe.

2. The Deep tier will be observed with a higher cadence than the All-Sky tier, allowing studies of variability and transient phenomena on shorter timescales than possible in a wide survey. A Deep survey also enables the study of entirely distinct transient populations than those detected in a wide survey, while additionally allowing transient populations detected in both Deep and All-Sky surveys to be studied at a range of flux density levels to investigate their evolution.

3. The Deep tier provides a reference "truth" image for the All-Sky tier where they overlap, allowing accurate assessment of completeness and reliability.

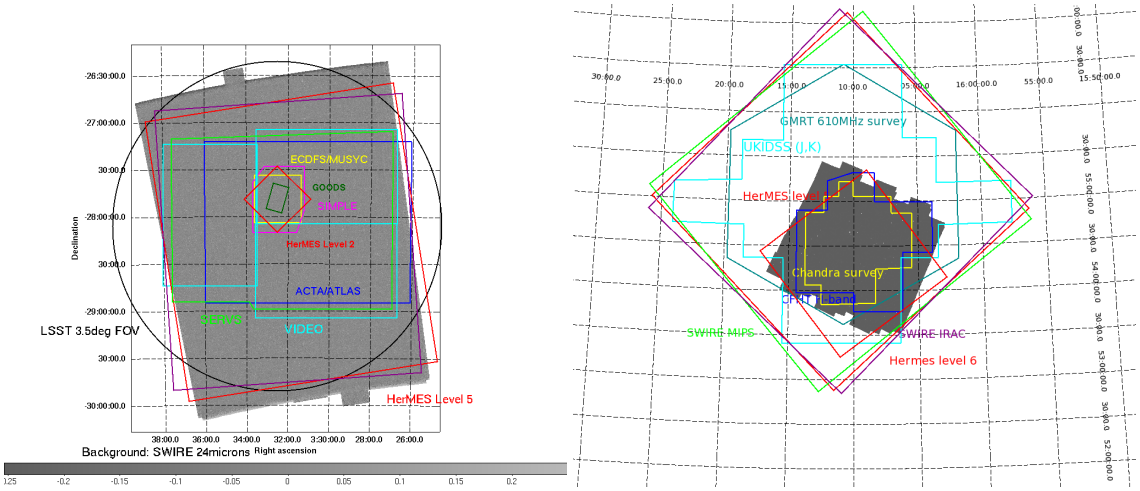

Figure 13: Multi-wavelength coverage maps of ECDFS (left) and EN1 (right), showing the wealth of degree-scale imaging over each field.

To date, the combined area of all extragalactic deep fields at $\lesssim 2\mu$Jy at S-band (or equivalent) constitutes <3 deg^2. Given that star formation is environmentally dependent, any investigation of the evolution of star-forming galaxies requires that we be able to probe them over the full range of cosmic environments (e.g., from rich clusters to voids). And, by having multiple fields covering such large areas, such a survey will be able to overcome/test any remaining cosmic variance effects. VLASS Deep, like the LSST Deep Drilling Fields, SERVS, and VIDEO surveys, lies in parameter space that sits between the ultra deep *HST* surveys and the wide, DES-like surveys. However, sampling this portion of survey parameter space is extremely important as it allows us to fully probe the epoch in the Universe which is most active, taking into account the rarer AGN, powerful starbursts, along with the moderate luminosity AGN and star-forming galaxies and their environment. The extremely wide-area surveys do not have the depth to do this, while ultra-deep surveys simply do not sample the requisite volume and are limited by cosmic variance (e.g., Moster et al., 2011).

As already discussed above, we have chosen 10 deg^2 as the full survey area of Deep as this is the only way to enable the chance for a statistically significant detection of weak lensing in the radio (see Figure 4), reduce the Poisson uncertainty for deriving statistically meaningful luminosity functions for star-forming galaxies (see Figure 2), as well as to reduce sample variance due to large-scale structure (see Figure 3), which is critical for developing our understanding of the link between star formation, galaxy mass and environment. Furthermore, it is worth stressing that the Deep tier provides the only means for non-radio experts working on either galaxy evolution and cosmology to readily incorporate meaningful radio data into their investigations. It would be impossible for such a survey to be executed and reduced/imaged via a PI program(s) – the needs (time/effort/computing power/disk space) far exceed what can be expected by a typical member of the astronomical community.

4.2.2 Description

Area and depth: The Deep component of VLASS will cover 10 deg^2 to an rms depth of 1.5 μJy in three well-separated fields to help mitigate against cosmic variance effects. This combination of area and depth was primarily chosen as it is the minimum requirement for VLASS Deep to potentially deliver a statistically significant detection of weak lensing; this is a primary science

Table 6: Current/Scheduled 1–10 deg^2 Multi-Wavelength Coverage of the ECDFS

Band	Survey Name and Solid-Angle Coverage	Comments
Radio	Australia Telescope Large Area Survey (**ATLAS**; 3.7 deg^2)[a]	15 μJy rms depth at 1.4 GHz
	MIGHTEE Survey (Scheduled; 4.5 deg^2)[b]	1 μJy rms depth at 1.4 GHz
FIR	*Herschel* Multi-tiered Extragal. Survey (**HerMES**; 0.6–11 deg^2)[c]	5–60 mJy depth at 100–500 μm
MIR	*Spitzer* Wide-area InfraRed Extragal. Survey (**SWIRE**; 6.6 deg^2)[d]	3.6–160 μm
NIR	*Spitzer* Extragal. Representative Volume Survey (**SERVS**; 4.5 deg^2)[e]	2 μJy depth at 3.6 and 4.5 μm
	VISTA Deep Extragal. Observations Survey (**VIDEO**; 4.5 deg^2)[f]	$ZYJHK_s$ to $m_{\rm AB} \approx$ 23.5–25.7
Optical Photometry	Dark Energy Survey (**DES**; 9 deg^2 in 3 ECDFS fields)[g]	Multi-epoch *griz*; $m_{\rm AB} \approx 28$ co-added
	Pan-STARRS1 Medium-Deep Survey (**PS1MD**; 7 deg^2)[h]	Multi-epoch *grizy*; $m_{\rm AB} \approx 26$ co-added
	VST Optical Imaging of CDF-S and ES1 (**VOICE**; 4.5 deg^2)[i]	Multi-epoch *ugri*; $m_{\rm AB} \approx 26$ co-added
	SWIRE optical imaging (6.6 deg^2)[d]	
	LSST deep-drilling field (Planned; 10 deg^2)[j]	*ugrizy*; 20 000 visits total
Optical/NIR Spectroscopy	Carnegie-*Spitzer*-IMACS Survey (**CSI**; 6 deg^2)[k]	40 000 redshifts, 3.6 μm selected
	PRIsm MUlti-object Survey (**PRIMUS**; 1.95 deg^2)[l]	20 800 redshifts to $i_{\rm AB} \approx 23.5$
	VLT **MOONS** Survey (Scheduled; 4.5 deg^2)[m]	80 000 redshifts
	Spectroscopy of $\approx$ 900 radio and IR-luminous galaxies in ATLAS[n]	
UV	*GALEX* Deep Imaging Survey (7 deg^2)[o]	Depth $m_{\rm AB} \approx 25$

References: [a] Norris et al. (2006); Banfield et al. (2014a,b); [b] `http://public.ska.ac.za/meerkat/meerkat-large-survey-projects`; [c] Oliver et al. (2012); [d] Lonsdale et al. (2003); [e] Mauduit et al. (2012); [f] Jarvis et al. (2013); [g] Bernstein et al. (2012); [h] Tonry et al. (2012); [i] `http://people.na.infn.it/~covone/voice/voice.html`; [j]`http://www.lsst.org/News/enews/deep-drilling-201202.html`; [k] Kelson et al. (2014); [l] Coil et al. (2011); [m] `http://www.roe.ac.uk/~ciras/MOONS/VLT-MOONS.html`; [n] Mao et al. (2012); [o] `http://galexgi.gsfc.nasa.gov/docs/galex/surveys/index.html`

goal of the SKA, for which the VLA has the ability to make this first definitive measurement of weak lensing in the radio years before hand. As shown by the right panel of Figure 4, existing PI surveys come nowhere near the required depth over large enough areas to make a statistically significant detection.

By requiring a depth of 1.5 μJy, Deep will also be sensitive to L* galaxies out to $z \sim 2$ (e.g., Gruppioni et al., 2013, see Figure 12). *At this depth, VLASS-Deep is as sensitive to obscured star formation as the deepest Herschel survey data taken (i.e., GOODS-Herschel; Elbaz et al., 2011; Magnelli et al., 2013), but will cover more than 100$\times$ the area with 10$\times$ better angular resolution.* Furthermore, a 7.5 μJy/beam (5σ detection threshold) corresponds to a star-formation rate of $\sim$50 solar masses per year at $z = 1.5$. Given that the luminosity function for star-forming galaxies is relatively steep, the increase in source density is significant when compared to the current VLA survey over the COSMOS field: e.g. in the redshift slice $z = 1.4 - 1.5$, there are $\sim$250 vs $\sim$450 star-forming galaxies per deg^2 for 2.5 μJy rms vs 1.5 μJy rms, respectively.

Angular Resolution: Sub-arcsecond resolution (A-array in S-band) is needed in order to both make reliable identifications of faint star-forming galaxies, and measure the sizes of star-forming galaxy disks to enable weak-lensing science, as well as for a comparison with optical sizes. We note that in addition to robustly-weighted maps, we will take advantage of the centrally-dense A-array to investigate completeness issues, by making *uv*-tapered versions of our maps that should improve the brightness temperature sensitivity by a factor of $\approx$3.

Cadence of multiple epochs: Deep will have $\approx$4 epochs, each reaching an rms of $\sim$3 μJy.

Choice of fields: After a long and thoughtful debate among a large constituent of the extragalactic working group members, our final field selection for Deep includes 4.5 deg^2 in the Extended Chandra Deep Field South (ECDFS), 3.5 deg^2 in the ELAIS-N1 (EN1) field and 2 deg^2 in the COSMOS field. Other fields that were seriously considered in this debate include: XMM-LSS, the Lockman Hole, the Boötes NOAO Deep Wide-Field Survey region, and the North Ecliptic Pole (NEP).

The choice of these fields was made by a combination of available ancillary data on the angular scales relevant to the Deep key science goals, along with more logistical/practical considerations, including scheduling concerns.

While many sorts of ancillary data are valuable in support of the VLASS radio observations, deep *Spitzer* IRAC and ground-based near-infrared data were considered to be essential for identifying galaxy counterparts to faint, high redshift radio sources. We initially prioritized southern and equatorial fields due to visibility to ALMA (and potentially CCAT). COSMOS (equatorial) and the ECDFS (declination -27°) were natural choices, due to the richness of their ancillary data. The southern declination of ECDFS does introduce drawbacks in terms of VLA beam shape and schedulability, but these were deemed to be outweighed by other advantages. The 4.5 deg^2 footprint for ECDFS was primarily defined by the relatively deep Spitzer IRAC data from SERVS (Mauduit et al., 2012) and near-infrared imaging from VIDEO (Jarvis et al., 2013), whereas VLASS coverage in COSMOS was restricted to the standard 2 deg^2 footprint defined by most other multi-wavelength data in that field.

Our second-choice equatorial field, XMM-LSS, has somewhat better IRAC/NIR/optical data than the northern EN1 field, and more extant spectroscopy. However, XMM-LSS, at declination -2°, appears to be impractical for S-band observations due to RFI issues as it sits in the Clarke satellite belt. We considered, but ruled out, using L-band for that field (only), concluding that the resulting VLA frequency non-uniformity was unacceptable.

It was also thought that having a northern field would both help significantly with practical VLA scheduling constraints, and deliver a better behaved beam for comparison with ECDFS imaging. Among the four candidate northern fields (EN1, Lockman Hole, Boötes, NEP), the NEP was discarded for having the poorest ancillary data. Boötes has good multi-wavelength data but those observations were designed to cover 9 deg^2 and are generally shallower than those in other, smaller fields. In particular, the *Spitzer* IRAC and *Herschel* far-infrared data are shallower than those in EN1, Lockman Hole, ECDFS or COSMOS. Lockman Hole has good data including relatively deep *Spitzer* IRAC from SERVS, but its right ascension ($10^{\rm h}$ $49^{\rm m}$) is similar to that of COSMOS ($10^{\rm h}$ $00^{\rm m}$), leading to significant VLA scheduling conflicts.

This process of elimination led to the selection of EN1 as the third VLASS field. EN1 has *Spitzer* IRAC data from SERVS, albeit covering only 2 deg^2 of the 3.5 deg^2 planned for VLASS (there are shallower SWIRE IRAC data over the full area), and deep NIR imaging from the UKIDSS DXS, which can be supplemented with future proposals to 4m-class telescopes.

One goal of VLASS Deep is to relate the radio sources to the underlying dark matter distribution through halo occupation modeling. This requires having enough continuous area to reach the halo-halo clustering term (not just how satellites cluster around central dominant galaxies - usually called the single halo term). Therefore, one needs to enter the linear regime, while retaining the requisite depth to also model the single halo term. This turnover from the single halo to the two-halo term occurs at around $2'$. However, to obtain the pair statistics at this scale with the expected number density of radio sources requires a linear scale of around 2° (e.g., Lindsay et al., 2014b), which is achieved by two of our chosen fields (i.e., ECDFS & EN1).

The chosen footprints for ECDFS and EN1 are largely based on the available deep NIR/VIDEO and warm *Spitzer*/SERVS data (see Figure 13). Figure 13 illustrates the coverage of multi-wavelength ancillary data available for the ECDFS and EN1 fields, and Table 6, provides a detailed list of the available ancillary data for our largest field, ECDFS. All three fields have medium-deep multi-wavelength data in X-ray through infrared bands, with typical 5σ depths of $r_{AB} \sim 25$ and $K_{AB} \sim 23$ in the optical/near-IR, mid-infrared depths of $S_{4.5} \approx 2\mu$Jy and $S_{24} \approx 300\mu$Jy, and *Herschel* SPIRE data to $S_{250} \approx 30$mJy. Much of multi-wavelength COSMOS data (imaging/cutouts, catalogs, etc.) are already readily available from IPAC/IRSA[4]. In addition, COSMOS has an existing S-band VLA survey to 2 μJy, which will be augmented with VLASS-Deep imaging. While we plan

[4]http://irsa.ipac.caltech.edu/Missions/cosmos.html

to use the existing COSMOS data for VLASS-Deep, it is worth stressing that the existing COSMOS data alone (2 deg^2) does not enable any of our key science goals such as mapping out large-scale structure or providing a statistically significant weak-lensing detection. EN1 has 0.1deg^2 to 1μJy sensitivity in C-band, 1.1deg^2 to 7μJy at 610 MHz, and is completely covered by the LOFAR EoR experiment at 110–190 MHz (and WSRT at 310–380 MHz), allowing us to obtain extended spectral coverage for some fraction of the survey objects.

4.2.3 Survey Science

Star-forming galaxies: While the All-Sky tier will detect luminous star forming galaxies out to $z \sim 0.15$ (LIRGs) or ~ 0.5 (ULIRGs), we need the Deep tier to find them at $0.5 < z < 4$ to study the evolution of the radio properties. The proposed Deep fields have *Herschel* data that are sensitive to ULIRGs at $z \sim 2$, but which have low spatial resolution, making unambiguous identifications difficult. Radio data with good angular resolution are required as the bridge to cross-identify the *Herschel* sources with the deep near-infrared data in these fields (from *Spitzer* and VISTA surveys). The primary beam of ALMA (e.g., $\approx 1'$ in diameter at Band 3/90 GHz relative to $15'$ at S-band/3 GHz) is too small to make it an efficient survey instrument, so the VLA is needed. The Deep component of VLASS will allow us to answer key questions about the evolution of the luminous starburst population as a function of redshift and environment, in particular magnetic field evolution (through both polarization studies and a careful comparison of the far-infrared-radio correlation for objects of equivalent luminosity).

Clustering and large-scale structure at high redshifts: Determining the mass of dark matter haloes in which both AGN and star-forming galaxies occupy requires robust measurements of the angular two-point correlation function to angular scales that reach well into linear regime (from $3 - 10$ co-moving Mpc) at the redshift of interest. To accurately measure the two-point correlation function to a given scale depends on the number of galaxy pairs of a given type at that particular angular separation. For highly-clustered sources, which are generally the most massive and rare, many of which host AGN, this means that a relatively large linear dimension to the survey is required to ensure that the measurement is not completely washed out by shot noise. A general rule-of-thumb to ensure that the angular correlation function can be measured accuratly in a given $\delta z \sim 0.5$ bin, is that the survey dimension has to be approximately 1 order of magnitude larger than the scales of interest (see e.g. Figure A1 in Lindsay et al., 2014b). Therefore at $z \sim 1$, 6 Mpc corresponds to $\sim 0.2^\circ$, which means that one needs to survey with *linear* dimension of around 2 deg (i.e., which is not achieved even by COSMOS), and preferable with a geometry that maximizes the number of pairs at these scales (i.e. almost square). As the angular diameter distance does not change substantially between $z = 1$ and 2, then similar scales are required for the key redshift range of interest for VLASS Deep.

Weak lensing: The two crucial observational parameters that determine the quality of weak lensing measurements are the survey depth and angular resolution. An angular resolution $\theta_{\rm res} < 1''$ is required in order to facilitate the accurate measurement of typical galaxy shapes at redshifts $z \sim 1$. The choice of A-array at S-band ($\theta_{\rm res} = 0\farcs8$) is therefore well suited for weak lensing. Although ECDFS does not achieve this in both axes of the synthesized beam, the weak lensing predictions for Deep still suggest a statistically significant detection. In terms of survey area, a simple optimization procedure designed to maximize the signal-to-noise of the weak lensing measurement yields an optimal survey area of order $\sim$10 deg^2. Thus the array configuration and survey area envisaged for the Deep component is extremely well suited for weak lensing science.

AGN and implications for galaxy formation: Radio jets are probably the key to understanding feedback processes in galaxy formation. Although strong "quasar mode" feedback is easy to find in the form of winds and powerful jets powered by the most luminous AGN, the duty cycle of such activity is so small ($\sim 10^{-2}$ even in massive objects at the epoch of peak of quasar activity). Jets and winds of relatively low kinetic luminosity are probably responsible for providing the bulk of AGN feedback outside of quasar outbursts in a "maintenance mode", whose characteristics are currently poorly understood. Measuring the AGN radio luminosity function down to the lowest AGN luminosities, where it merges with the radio luminosity function of starbursts is therefore essential. While the All-Sky tier will allow us to obtain a good baseline at low redshifts, the Deep component is needed to push out to $z \sim 1-2$, where feedback needs to be most active to prevent galaxy growth.

Quasar science: Although SDSS-III/BOSS targeted FIRST sources nearly 3 magnitudes deeper in the optical than the main SDSS survey, a paltry 4% of BOSS quasars appear in the FIRST catalog (Pâris et al., 2014). Clearly, a next-generation survey is needed to explore the radio properties of these large quasar samples. While All-Sky substantially increase the number of SDSS quasars detected in the radio (not just radio loud), only with the Deep tier will we detect the vast majority of radio-quiet quasars in the radio. Not only will Deep provide truth tables that will inform what limitations the All-Sky tier has, but achieving this greater depth is important to determining whether this (quiet) radio flux is intrinsic to the AGN or is due to star formation (e.g., Kimball et al., 2011b; Condon et al., 2013b; Zakamska & Greene, 2014). As with the flux densities, spectral indices measured in the Deep tier will provide truth tables for interpreting the spectral indices measured in the the All-Sky tier. At the rms of Deep, we can hope to measure relatively accurate spectral indices for quasars as faint as 52μJy, which generally represents a radio-quiet quasar. At the limit of the good spectral indices for All-Sky, the error on the Deep spectral indices will have statistical errors as small as $\Delta\alpha \pm 0.003$. The Deep tier will provide a small area where we are complete to SDSS quasars at all redshifts and to the depth of the imaging data. The Deep fields have also been targeted as part of a spectroscopic survey of luminous mid-infrared selected AGN (Lacy et al., 2013), so radio luminosities of dust reddened AGN and quasars will also be obtained to compare to the normal quasar population.

Time Domain Science: The Deep Tier fields will be observed in 40–392 passes (see Table 5) in each of four A-configuration cycles spread throughout the 5-year span of the survey, sampling the transient and variable radio sky in these areas with cadences from days to years. This in turn will enable the measurements of the variability of the AGN population on these timescales, probing both intrinsic and propagation induced dynamic phenomena. The Deep data stream will also open up the deep radio sky for the discovery and characterization of intermediate and long duration transients from lower luminosity events or at greater distances than in the All-Sky tier in fields that are and will continue to be well-studied throughout the wavelength spectrum.

5 Data Products, Observing, and Implementation Plan

Here we present an overview of the data products, observing strategy, and implementation plan. *Details of the data products, observations, and implementation plan for carrying out and processing the survey are given in the VLASS Technical Implementation Plan (TIP) document.* The TIP includes risk assessment and estimated resources required. We provide here only a high-level summary of the most salient issues. The TIP has been reviewed internally by NRAO prior to the VLASS Community Review. The NRAO technical report will be provided to the community review panel.

5.1 Data Products

The VLASS data products described below are broken into classes of "Basic" and "Enhanced". The Basic Data Products (BDP) for VLASS are those that will be produced by NRAO using standard (or soon to be standard) data processing systems, or modest extensions thereof. NRAO will assume responsibility for producing and providing the basic products and will carry out the necessary quality assurance. The BDP have been defined to be a set of products from which the community can derive the science outlined in this proposal, requiring modest post-processing on the user's part. Enhanced Data Products require extra resources or involve specialized domain expertise, so they will be left for community members to define and produce. These would clearly enhance the utility of the survey and enable further science, but are beyond the anticipated resources of NRAO to carry out.

5.1.1 Basic Data Products

The Basic Data Products of VLASS consist of

1. raw visibility data;
2. calibration data and process to generate calibration products (current best version as well as past released versions maintained in Archive);
3. quick-look continuum images;
4. single-epoch images and image cubes;
5. single-epoch basic object catalogs;
6. cumulative VLASS images and image cubes; and
7. cumulative VLASS catalog.

The resources for processing, curating, and serving the BDP will be provided by NRAO (§5.1.3). Teams led by NRAO, but including external community members where possible, will carry out the activities required for the processing and Quality Assurance (QA) of the products. Table 7 summarizes the components of each data product and the timescale for their production. Specific details of individual BDP are described below.

Raw Visibility Data: The raw visibility data for VLASS will be stored in the standard VLA archive. These data will be available immediately after observation with no proprietary period. As VLASS is being observed using standard data rates (25 MBps maximum) there are no special resources required for the storage and distribution of these data.

Calibrated Data: VLASS data will be processed using a modified version of the normal CASA-based VLA calibration pipeline. By the time of the VLASS observations, the VLA pipeline will have the requisite functionality to process VLASS data (full polarization, many individual target fields generated in OTF mode). The VLA pipeline is currently run on most VLA observations and is well tested. VLASS will use a version specifically tested on VLASS pilot observations.

Once the pipeline has run and after QA assessment, users will gain access to the calibrated data from the Archive. Archiving the calibrated visibility data themselves would double the required data volume, which is too costly. Instead, VLASS will archive calibration products and maintain scripts to generate the calibrated dataset. Scripts to apply calibration products will be based on CASA. Upon first processing of a Scheduling Block, the calibrated data will be available for a short time for transfer to subsequent processing teams.

Table 7: VLASS Basic Data Products

Data Product	Components	Production Time Scale
Raw Visibility Data	standard VLA data	Immediate
Calibrated Data	Final Calibration Tables Pipeline Control Script Flagging Commands QA Reports & Plots *Calibration Sky Models*	1 Week after Observation
Quick-Look Images	Stokes I Images Stokes I Noise Images	48 hrs.
Single-Epoch Images	Stokes IQU continuum images, & noise images Stokes IQU spectral cubes, & noise cubes Stokes I Spectral Index, and uncertainty images (generated using Multi-Frequency Synthesis)	6 mos. I 12 mos. QU & cubes
Single-Epoch Basic Object Catalog	Position, and uncertainty (centroid of Stokes I emission) Peak Brightness in Stokes IQU and uncertainty Flux Density in Stokes IQU and uncertainty Spectral Index at Peak Brightness (I) and uncertainty Integrated Spectral Index (I) and uncertainty Integrated IQU spectrum (bright sources) Basic Shape information for IQU	With Single-Epoch Images
Cumulative VLASS Images	Stokes IQU continuum images, & noise images Stokes IQU spectral cubes, & noise cubes Stokes I Spectral Index, Curvature, and uncertainty images	12 mos. I 16 mos. QU & cubes
Cumulative VLASS Catalog	Position, and uncertainty (centroid of Stokes I emission) Peak Brightness in Stokes IQU and uncertainty Flux Density in Stokes IQU and uncertainty Spectral Index, Curvature at Peak Brightness (Stokes I) and uncertainty Integrated Spectral Index (Stokes I) and uncertainty Integrated IQU spectrum (bright sources) Basic Shape information for IQU	With VLASS Images

Quick-Look Images: The identification of transient and variable objects is a key VLASS science goal. The Transient Working Group has set the requirement to generate images within 48 hr of data acquisition, with a goal of 24 hr. The Quick-Look Stokes I images will be constructed through mosaicking, and there will also be a corresponding rms sensitivity (noise) image.

Single-Epoch Images: These fully calibrated and quality-assured images will be produced using a specialized CASA-based Imaging Pipeline and served from the Archive. This pipeline will be developed by the NRAO staff, with the involvement and guidance of active community members. Continuum images (averaged over band) will be produced for intensity (Stokes I) and linear polarization (Stokes QU), plus images of the rms noise in intensity and polarization. For Stokes I continuum, multi-frequency synthesis (MFS) will be used to generate spectral index images (and uncertainty maps). In addition, spectral image cubes will be generated for Stokes IQU. Due to limited archive resources, compression (reduced frequency resolution, cutouts around bright sources only) will used as necessary (see the TIP for details).

Single-Epoch Basic Object Catalogs: Results from previous analyses (e.g., Huynh et al., 2012) and tests on the VLASS images will be used to determine the optimal means to identify sources within the VLASS images. The software (or software packages) that produce the optimal results will be used to produce a Basic Object Catalog from the VLASS images.

Cumulative VLASS Images: These images will be produced in a similar manner as for the Single-Epoch Images, but using all epochs, and would serve to be the final set of VLASS images. Sufficiently strong variable sources will be taken into account during the imaging. In addition to the image and cube products listed above for the single-epoch images, an additional MFS continuum spectral curvature image will be produced. Compression will be used as necessary on the spectral image cubes.

Cumulative VLASS Catalog: These would be produced in a manner similar to the Single-Epoch Basic Object Catalog but would serve to be the complete catalog for VLASS.

5.1.2 Enhanced Data Products

The Enhanced Data Products (EDP) are those that require additional resource and/or more domain expertise, and so will be defined and produced by the VLASS community outside the NRAO. These data products will require external support to define, produce, and validate. However, these products are seen as essential to the VLASS science case, so both BDP and EDP (where practical) will be curated and served by the NRAO. Enhanced Data Services (EDS, § 5.1.3) will be required for curation and distribution of EDP beyond the capabilities of NRAO to support.

Some examples of EDP include (but are not restricted to):

1. Transient Object Catalogs and Alerts
2. Rotation Measure Images and Catalogs
3. Full spectral resolution image cubes
4. Improved Object Catalogs
5. Light curves (intensity and polarization) for objects and/or image cutouts
6. Catalogs of multi-wavelength associations to VLASS sources

Beyond requiring extensive domain expertise, these areas are also ideal for nucleating multi-wavelength community groups and resources to work with and enhance VLASS.

A special case is the support for commensal observing at P-band (230–470 MHz) using the VLA Low Band Ionospheric and Transient Experiment (VLITE[5]) system, which became operational in November of 2014. This system provides 64 MHz of bandwidth centered at 352 MHz with 100 kHz spectral resolution and 2 s temporal resolution for nearly all PI-driven Cassegrain observations. Modifications to VLITE to permit OTF mapping are required [see VLASS White Paper by Clarke et al. (2014)[6]], but are not expected to require substantial effort. There is no NRAO processing or archive support currently budgeted for VLITE data products, and thus use of VLITE with VLASS should be considered as a EDP (and EDS) provided in partnership with the Naval Research Laboratory (NRL). All raw VLITE data are archived by NRL and data processing pipelines are available. The natural expansion of the VLITE system into a full 27 antenna wideband commensal system, called the Low Band Observatory (LOBO), may occur during the VLASS program. LOBO is expected to be fully integrated into NRAO archiving.

Other areas for EDP will undoubtedly become apparent. Once the survey is approved, we will take proposals for new EDP to be included in the list above. Criteria for including EDP in the VLASS archive will be relevance to the VLASS science case and cost of curating and serving the products. As an incentive to include EDP in the VLASS archive, we ask that the NRAO encourage authors that use EDP to acknowledge groups that produced them.

[5] `vlite.nrao.edu`

[6] `https://science.nrao.edu/science/surveys/vlass/Wilson_WP_r0.pdf`

5.1.3 Enhanced Data Services and the VLASS Archive

A comprehensive survey like VLASS will produce a diverse set of data products and will require a full-featured archive to serve it to the public. A baseline plan is to serve products from a website hosted by the NRAO. This site will feature basic search capabilities of catalogs and products, as has been done for FIRST[7] and NVSS[8]. Previous VLA surveys only provided catalogs and images, so at a minimum VLASS will extend that search capability to visibility data, calibration products, and deep/multi-epoch images. The NRAO will also provide data analysis scripts to apply calibration to raw data.

However, astronomy is increasingly a multi-wavelength discipline with a diverse set of tools for comparing observations from different observatories. If the VLASS archive exists only as a stand-alone NRAO-hosted service, it would not be as useful as one integrated with the tools available at places like IPAC[9] or the Virtual Observatory [10].

We are investigating options for having catalogs and/or images served by organizations outside the NRAO. This would extend the reach of VLASS outside the radio community and open access to powerful tools for multi-wavelength analysis. The VLASS community, including the co-authors of the VLASS proposal, will be writing an NSF proposal to support VLASS data analysis and a more effective archive. These Enhanced Data Services will greatly augment the utility of VLASS and its basic and enhanced data products to the wider astronomical community.

Another area that would be greatly improved through EDS is the capability for "processing on-demand" (POD) of images or image cubes. This would alleviate storage volume concerns, and enable more flexible angular and spectral resolution of the resulting products. We expect to utilize the NSF XSEDE network for modest use of POD-like processing for the pipeline. Fully enabled POD for VLASS could be carried out through partnerships with NSF supercomputing centers or with DOE science labs. Exploration of these options will commence upon approval by NRAO of VLASS.

As noted above, data archive and distribution support for commensal observing at P-band using the VLITE system is not currently budgeted for support by NRAO. Archive serving of VLASS should be considered as a EDS provided in partnership with NRL. NRL staff are involved in the VLASS planning and are eager to work with the community to enable access to VLITE data products as part of the archival system.

5.2 Observing

Here we present a brief overview of the observing strategy and related logistics. As stated above, details of the observations and observing plan are given in the VLASS TIP.

5.2.1 Mosaic Observing Patterns

In order to carry out the VLASS, we will need to observe the sky using a large number of mosaicked pointings of the VLA. At 2–4 GHz, the VLA has a field-of-view given by the primary beam response of the 25-meter diameter antennas. This approximately follows a Gaussian response, with a full-width at half-maximum (FWHM) given by

$$\theta_{FWHM} \approx 45' \left(\frac{1\,\mathrm{GHz}}{\nu} \right) \tag{2}$$

[7] `http://sundog.stsci.edu/cgi-bin/searchfirst`

[8] `http://www.cv.nrao.edu/nvss/postage.shtml`

[9] `http://www.ipac.caltech.edu`

[10] `http://www.us-vo.org`

at observing frequency ν, and thus over the S-band the FWHM varies from 22.5′ at 2 GHz to 11.25′ at 4 GHz, with FWHM of 15′ at 3 GHz mid-band. In order to optimally cover a given sky area in an efficient manner, the array must either conduct a raster scan using "On-The-Fly" mosaicking (OTFM), or tile the area with a number of discrete pointings in a hexagonal packed configuration ("Hex-pattern Mosaicking"). The choice between these techniques is determined by the extent to which the extra overhead (from 3 to 7 seconds) needed to move the array and settle at each pointing in the discrete hex-pattern mosaic becomes a burden on the observations, and thus OTFM is favored.

The techniques of OTFM and Hex-pattern Mosaicking and the calculations and procedures needed to set these up are described in the *Guide to VLA Observing: Mosaicking*[11] section. The salient features are:

OTFM: There is very little move-and-settle overhead as the array is in continuous motion over a row of a raster with only a small startup ($\sim$10–15 sec) at the start of a row. In OTFM the phase center of the array is discretely stepped on timescales of a few seconds or longer, so no phase smearing of the images results. However, because the primary beam response pattern is moving with respect to the sky, there are errors introduced in the amplitudes by the moving beam in a single visibility integration time. Short correlator "dump" times are required, ideally 10% or less of the time it takes to cross the FWHM of the primary beam (0.45 seconds or less for All-Sky). This in turn increases data rates from those that might otherwise be required to avoid time smearing. OTFM has been used successfully in the S-band Stripe 82 program of 13B-370 (PI: Gregg Hallinan), and has produced Stokes I images of comparable quality to those using a traditional hex-mosaic, and is under test for polarimetry. For VLA S-band, the calculated exposure time is 5.4 seconds at a rms image sensitivity of 120 μJy/beam (the depth of an All-Sky epoch), and thus efficient All-Sky observations require OTFM.

Hex-pattern Mosaicking: It takes the VLA 3–7 s (depending on the direction of motion in azimuth-elevation coordinates, usually around 6–7 s if not optimized) to move and settle between nearby pointings. In order to keep the overhead from this motion to be 25% or less, one needs to spend at least 28 s integrating on each pointing. For a hex-pattern, each field gets 67% of the total integration time desired on-sky, so observations where the VLA Exposure Calculator[12] indicates an on-source time of 42 seconds (around 43 μJy/beam) or less will incur significant overhead if not done with OTFM. Thus, the DEEP observations (single-pass depth $< 30\,\mu$Jy/beam) can be carried out with straightforward Hex-pattern Mosaicking.

5.2.2 Scheduling Considerations

The Jansky VLA is normally operated using a "Dynamic Scheduling Queue" where the individual Scheduling Blocks (SBs) are created in the VLA Observing Preparation Tool (OPT) to be able to be executed in a prescribed range of LST, and submitted to the VLA Scheduler software (OST) to be queued up for observation by the array in a manner dictated by weather and priority. It is our intent that the DEEP observations, where possible for each pass, be observable using standard Dynamic Scheduling. This requires that these blocks contain sufficient calibration to stand alone or be boot-strapped from other VLASS SBs executed nearby in time.For All-Sky, it will be advantageous to construct the schedules to be observed at specific LST start times. This would allow maximum efficiency in calibration and control of slewing (e.g., telescope wraps), as well as repeatable u-v coverage to mitigate source variability.

To carry out the day to day scheduling and monitoring of VLASS, we propose an "Astronomer on Duty" (AoD) who will keep track of what SBs are ready to observe, make sure they are submitted, make sure that they run, and make any modification necessary (e.g., due to TOO or weather

[11] `https://science.nrao.edu/facilities/vla/docs/manuals/obsguide/modes/mosaicking`

[12] `https://science.nrao.edu/facilities/vla/docs/manuals/propvla/determining/source`

interrupts). This duty would be rotated and would be the point of contact with the NRAO Data Analysts who would be handling the general logistics of scheduling, data transfer, and pipeline processing.

Target-of-Opportunity Interrupts: For the VLASS, provision will be made for the possibility that observations will be interrupted for time critical TOO programs (e.g., for triggered transient observations). There is currently no mechanical provision in the way schedules are constructed or executed for the suspension and restarting of schedule blocks. Therefore, the most straightforward implementation is to break all schedules into blocks of 2–3 hours in length, and to allow TOO interrupts to simply stop the execution of the current schedule and possibly pre-empt the execution of the following one or more SBs. After TOO observations are complete, the VLASS schedule would resume with the next appropriate block. The AoD would be informed of this interruption, and would examine the archive record to determine the missing observations and construct a "make-up" SB to be run at the first appropriate opportunity. The plan for the construction of schedules (see below) will take this need into account.

5.2.3 Overall Observing Schedule

VLASS as proposed requires just under 9000 hours of scheduled observing time, which we propose will be carried out over the course of 6 cycles of VLA in its A and B configurations, spanning a total of around 7 years (84 months). We assume the array follows the current standard cycle order of B followed by A. We also assume that each configuration is the current 4-month duration, but note that accommodating VLASS could involve extending some of the durations in the more loaded sessions.

Cycle	Config	All-Sky	COSMOS	ECDFS	ELAIS-N1	Total
1	B	906	0	0	0	906.0
1	A	0	60	325	188.5	573.5
2	B	906	0	0	0	906.0
2	A	0	60	325	188.5	573.5
3	B	906	0	0	0	906.0
3	A	0	60	325	188.5	573.5
4	B	906	0	0	0	906.0
4	A	0	60	325	188.5	573.5
5	B	906	0	0	0	906.0
5	A	0	60	325	188.5	573.5
6	B	906	0	0	0	906.0
6	A	0	0	335	188.5	523.5
Tot		5436	300	1960	1131	8827.0

Note: The All-Sky allocation is placed into the relevant B configuration, but we plan to observed the southernmost regions of the survey in the BnA hybrid to form a more circular synthesized beam comparable to that for higher declinations. This will require a total of 1871 hours (for Declination $-40^\circ < \delta < -10^\circ$), or approximately 312 hours (13 days) per configuration cycle if split evenly between them.

This starts in May 2016 and follows the standard cycle schedule (BADC), completing in 2023. We assume that each configuration is the current 4-month duration, but note that accommodating VLASS could involve extending some of the durations in the more loaded sessions. The B-configuration All-Sky has three epochs per field with the sky split into two parts that get 3 passes each.

5.3 Implementation Plan

Here we present an overview of the implementation plan. As stated above, a more in depth discussion of the survey implementation strategy can be found in the VLASS TIP.

5.3.1 Calibration

The goal of the VLASS Calibration process is to determine, on the basis of *a priori* factors and from observations of standard calibration sources, the corrections to the raw data amplitude, phase, and visibility weights to be applied to the data. This process also determines the flags that are needed to remove bad data due to instrumental faults, RFI, and other causes of error. When applied to the VLASS data, this calibration will allow the production of images in the next processing stage. This process only includes the derivation of the complex gain and bandpass calibration factors known through previous measurements or determined by the observations of calibrators and transferred to the VLASS target observations. The self-calibration of VLASS data is included in the Imaging stage of processing.

5.3.2 Imaging

VLASS is at its heart a wide-band continuum imaging survey. The science goals of the survey are predicated on the ability of the instrument and data processing to deliver images of sufficient quality to be able to identify objects and measure the salient properties (e.g., flux density, position, spectral index, polarization, light curve). In order to keep up with the observing, the VLASS Imaging Pipeline must be able to process and image the data at a rate commensurate with the observing rate. This will be effected through the parallel image processing of sub-mosaics on NRAO-based clusters or externally provided systems (e.g., through XSEDE).

There are three imaging processes that need to be handled by the pipeline:

- Quick Look (QL) imaging triggered after every scheduling block is observed (e.g., for transient identification)
- per-epoch imaging triggered after the last observation in each configuration
- cumulative imaging triggered after each epoch beyond the first, incorporating all previous data

For each of these, there are three kinds of images that may be produced:

- Wide-band (2–4GHz) continuum images
- Full-resolution (2MHz channels) image cubes
- Reduced-resolution (e.g. 128MHz) spectral image cubes

Imaging is done in all Stokes parameters (IQUV) for polarimetry capability, except in the QL imaging which only processes Stokes I.

Continuum imaging will include higher-order Taylor terms in the spectral dimension (e.g., spectral index, spectral curvature) depending on image depth (e.g., for processing beyond the Quick Look). CASA has Multi-Frequency Synthesis (MFS) algorithms for this that have been used in past programs, and further development of these capabilities is underway. Full-polarimetric imaging is a key part of VLASS, and the use of accurate polarized "primary beam" maps of the VLA field-of-view during imaging and analysis are critical to the production of science ready images. Self-calibration (through the use of previous sky models as well as true self-calibration from iterative imaging) is also an integral part of the image processing.

We assume for all image size calculations that in the ideal case the images will be pixellated at a sampling level 0.4 of the (robust weighted) resolution at the highest frequency of the band (4 GHz), rounded to a convenient value. For A-configuration, this is 0.2″ (resolution 0.49″ at 4GHz), giving 324 Mpix per square degree. For B-configuration, this is 0.6″ (resolution 1.58″ at 4GHz), or 36 Mpix per square degree.

The image cubes are needed as input to more advanced processing for polarization studies, Rotation Measure determination, spectral line surveys, and more detailed SED modeling of sources. Most of these would be provided as Enhanced Data Products and Services. Note that the storage and distribution of the large full-resolution cubes is not possible under BDP for the archive (see § 5.3.4), and thus compressed cubes (at reduced spectral resolution or as cutouts only around sufficiently bright source emission) will only be provided. Options for external hosting and "on-demand" image processing should be explored (e.g., as an Enhanced Data Service).

5.3.3 Image Analysis and Sky Catalogs

The main image analysis task for VLASS is the production of the basic object catalogs for the Quick-Look and standard images.

A good study of the performance of radio continuum image source finders is Hancock et al. (2012), which considers the available options in the context of ASKAP. Also available as a proof of concept is the source finding carried out for the VLA Stripe-82 surveys by Mooley et al. (2014, in preparation). There is also a comprehensive discussion in Mooley et al. (2013) on the analysis of archival VLA ECDFS multi-epoch data. It is our current assessment that one or more of these methods will be suitable for the basic catalogs from VLASS.

Note that inclusion of the spectral index images and polarimetric images from VLASS will likely require some extensions to these source finders, investigation of which is included in the Test & Development Plan. More advanced catalogs and source finding algorithms could be developed and produced as an Enhanced Data Product.

5.3.4 Archiving and Data Distribution

The primary interface that the user community will have to VLASS is through the archive and data distribution system. Raw data will be served via the normal VLA archive, available with no proprietary period as soon as it has been ingested into the archive system.

The archive, or at least some archive, will have to also serve the VLASS data products as described above. It is the responsibility of NRAO and VLASS to make the Basic Data Products available through this archive mechanism. Storage in the JVLA archive for VLASS products is limited. Details of the amount of storage needed and available are given in the TIP. Due to these limitations, compressed versions of the spectral image cubes will be provided as BDP.

Enhanced Data Products may or may not be made available through the NRAO-hosted VLASS archive, this will need to be negotiated and is largely dependent upon resources required and available in the community. The VLASS products, either in basic form or further processes, may also be made available via alternative Enhanced Data Services.

5.3.5 Test & Development Plan

There are a number of issues related to VLASS that must be addressed before the survey can be observed on the telescope. As part of the TIP, we propose a VLASS Test & Development Program leading up to and through the survey start, for example through small test observations or through larger pilot observations, or through analysis of archival data from previously observed projects such as Stripe-82 (13B-370) and the COSMOS (12B-158) surveys. These will require significant astronomer resources to carry out, and thus we are unable to fully execute this program

before submission of the VLASS proposal — approval for the observation of VLASS would be necessary before allocating the resources to carry out this test program. There would be a final critical technical design review before survey observations commence, and at that point we will have dealt with the high and medium risk issues sufficiently to proceed.

Many of the key items are currently being carried out by VLA staff and resident observers as part of the normal development and science support, and by the user community in their research activities. However, new resources (additional staff, post-doc, or student time, computing, and telescope test time) will be required to fully implement this plan before the start of VLASS.

6 Education and Public Outreach

The activities of communication, education and outreach cover a very large, and often overlapping, sets of activities, which, however, present interesting opportunities for dissemination. We discuss how VLASS science, results and data will be publicized and made available to interested persons. Wherever possible, we leverage off existing infrastructure and resources, adopting and adapting as necessary. The overall objective is to disseminate VLASS science, results and data to the widest audiences.

6.1 Audiences

We identify these unique audiences for VLASS, each with its own style of communication and interaction, and grouped into 4 categories:

6.1.1 Scientists

- Experienced radio astronomers, experts at analyzing radio data
- Novice radio astronomers, content experts but who many have little to no experience with retrieving and analyzing radio data

This audience comprises professional astronomers who are primarily interested in how VLASS products can be used to further their research objectives.

For expert radio astronomers, access to the data and calibrated products is relatively easy, as is the analysis. For astronomers who are familiar with other methods of data acquisition (optical telescope spectra and images) or delivery methods (e.g., calibrated HST or Chandra data products) figuring out how to obtain, manipulate and understand and integrate unaccustomed data structures can be challenging. Thus, the first group is likely satisfied with access to a cataloged database. The second group would prefer to have calibrated data products in a form they can use with their familiar tools, for example a FITS image of the M87 Halo in 90 cm continuum halo (Image courtesy of NRAO/AUI and F.N. Owen, J.A. Eilek and N.E. Kassim). This group is keenly interested in timely updates - for example, the most recent data release. Methods of communication include email newsletters, the Astronomers Facebook Group, The American Astronomical Society, and similar venues.

6.1.2 Staffers, Managers

- NRAO directorate and upper management
- AUI officers and board of trustees
- Funding agency program officers

- Congressional staff

Members of this audience are probably most interested in receiving encapsulated information e.g., progress reports, press releases, summary of results.

6.1.3 Educators

- Teachers in accredited K-12 schools, 2 and 4 year colleges
- Informal science educators, e.g., after school programs, science centers, planetaria and so forth
- Disseminators of information, e.g., journalists, bloggers

This grouping has teachers who serve a variety of demographics, namely pre-college and undergraduate students in formal educational institutions, subject to curriculum requirements. Informal science educators serve students, but also include families as well as the general public. The needs for this group as a whole are easily accessible materials, with appropriate pedagogical backing.

6.1.4 General public

The broadest category is the general public, which includes people of all ages, interest level and residency (US, international and so forth). The public is far from monolithic, with very wide range in age, education level, socioeconomic status and preferred means of obtaining information.

6.2 Social media and communication

Interest in science and astronomy among the general public has been on the rise and is at least partly facilitated by the ease of sharing information and engaging with scientists using social media. The Very Large Array Sky Survey can build on the existing audience and practices of NRAO social media and rely on the breadth of expertise and personalities working with the project.

Examples of active NRAO social media accounts (as of 7/9/2014):

- Facebook - https://www.facebook.com/TheNRAO - 40,041 likes
- Twitter - https://twitter.com/thenrao - 5186 followers
- Google Plus - https://plus.google.com/117435324254706605576/posts - 235 followers, 22,378 views

A sound social media project includes defining clear goals for the communications, picking which specific platforms to use, and ensuring regular posting and interaction with the community (Bohon et al. 2013). Though some of the work of VLASS can be worked into the existing framework of NRAO social media projects, work from VLASS's many participants would be appreciated as well. This would particularly be true of the NRAO's Facebook presence, which is by far its largest audience.

One model for additional participation is to have a weekly "host" of a twitter account that uses the week to communicate their particular aspect of the science being done with VLASS. Examples of such accounts already in use are @realscientists (https://twitter.com/realscientists), @WetheHumanities (https://twitter.com/WetheHumanities), and @astrotweeps (https://twitter.com/astrotweeps). Other collaboration members who are already active on social media can use a specific hashtag to join the conversation. To date, we have adopted the simple hashtag #VLASS.

Another outlet for VLASS news and communication would be in blog form so that long format stories can be told. Such a blog would be modeled after the CANDELS Blog (http://candels-collaboration.blogspot.com/). This site has two editors who ensure that new and relevant content is posted on a regular basis. These editors invite members of the collaboration to submit posts on their specific science, their role in the survey, biographical profiles, or explainer articles on broad and basic scientific concepts. A blog hosted by Wordpress.com is free and is easy to use for collaborative projects. The URL vlass.org is also available (that is, has been privately reserved) for use for either this blog or for a broader public website if desired.

Although it is now considered an "old" form of web communication, email lists are still a popular method of communication as it ties directly into the users daily email routine and does not require visiting an external app or site. Email lists can also be audience specific (as in separate lists for teachers, general public, and professional astronomer) and are opt-in by the user. At the very least, a periodic email list should be made available for professional astronomers interested in the status of the survey and its data products.

All of these methods of communication have little to no cost for the accounts but incur costs in the person-hours to develop content and communicate with the community.

6.3 Examples of Community Educational Outreach Activities

6.3.1 Picture of the Week

Each epoch of VLASS data acquisition lasts approximately 8-12 weeks. Starting with the first week, VLASS should release a picture of an interesting object, along with explanatory material and a press release delivered through as many channels as possible to maximize exposure. The very first image could be simply a 'pretty picture' just to get started, though thereafter in addition to being good looking, the POTW should be of scientific interest, whether as a unique object or one that demonstrates a specific instrument capability. In this category are the "most": distant, brightest, faintest, dusty, nearest, resolved etc. VLASS scientists pick the targets ahead of time, reduce the data and generate the 'picture'. Someone expert in visualization will need to work with VLASS scientists on these pictures. This is very similar to the way HST among others, generate interest in its surveys (PHAT, Frontiers Fields) and attract attention.

6.3.2 Citizen Science

Public participation in science has grown in the last few years with access to new technologies and data sharing techniques. Projects range in participant involvement from collection of data (e.g., variable star observations) to web-enabled classification and data analysis (e.g., Galaxy Zoo, CosmoQuest) to passive use of computing resources (e.g., SETI@home). With the exception of projects that just use computing resources with no human intervention, citizen science projects tied to large surveys such as VLASS are best suited for problems that need human interaction through simple tasks that cannot be handled automatically by a computer. Searching for transients that might be missed by traditional source finding techniques is one such application of a citizen science task.

Audiences: general public, with access to the internet. Can also tie into K-12 education with appropriate teacher materials.

6.3.3 Science Stories

An ongoing VLASS blog, where VLASS personnel contribute individual entries, can generate and sustain interest in the survey. Individual stories could include descriptions (by the parties involved) of the deliberations undertaken to arrive at the final survey plan, life of an astronomer

during the week of, and the like. New postings are advertised via social media apps, email, on the web page. Readers can post comments (moderated, of course).

Audiences: all

6.3.4 Education Activities

Here, the objective is to take advantage of existing resources at NRAO, its partner institutions (e.g., RIT, CalTech) and extant networks (e.g., NightSky Network), to share VLASS science in ways that are compatible with the objectives of formal and informal educators. Partnerships with other national and international institutions with experience in this area (International Astronomical Union's Office for Astronomy Development, Galileo Teacher Training Program) would be helpful as well.

Audiences: K-12 and Higher Education

7 Summary

The proposed VLASS comprises a cohesive and aggressive science program that will benefit the entire astronomical community, deliver unique forefront scientific discovery, and keep its legacy value well into the SKA-era. The scientific legacy, impact, and efficiency of deep and all sky surveys have by now been clearly established. Surveys such as the Hubble Deep Fields, GALEX, NVSS/FIRST, Sloan, and the future LSST give credence to their importance and impact. The astronomical community has embraced the scientific importance of surveys and the need for mechanisms, outside of the normal PI proposal review process, to enable large survey programs to be approved for telescope time. These programs then, by definition, must be carried out in a way that produces data that is accessible to and impacts a large swatch of the astronomical community.

The proposed VLASS finds its place within this tried and true tradition of modern astronomy. Analysis of the statistics from NVSS and FIRST (as with the Hubble Deep Fields) clearly indicate that the impact on PI science from radio community surveys is as positive as those from Hubble. This is true not only in terms of the extensive usage of these data by wide sections of the community, but also due to the new inquiry driven PI science they enable, that could not otherwise have been conceived or survived the proposal process without the critical enabling data and demonstration science from the surveys. Lastly, while unquestionably delivering forefront science, the proposed VLASS will also accelerate the integration of radio astronomical data into the multi-wavelength astronomical community, putting the U.S. broad astronomical community in an optimum position to make substantial use of the SKA when it comes online.

References

Aaquist, O. B., & Kwok, S. 1990, Astronomy & Astrophysics, Supplement Series, 84, 229

Aguirre, A., Hernquist, L., Schaye, J., et al. 2001, Astrophysical Journal, 561, 521

Antonova, A., Hallinan, G., Doyle, J. G., et al. 2013, Astronomy & Astrophysics, 549, A131

Antonucci, R. 1993, Annual Reviews of Astronomy and Astrophysics, 31, 473

Appleton, P. N., Fadda, D. T., Marleau, F. R., et al. 2004, Astrophysical Journal Supplement, 154, 147

Arshakian, T. G., Beck, R., Krause, M., & Sokoloff, D. 2009, Astronomy & Astrophysics, 494, 21

Backer, D. C., Kulkarni, S. R., Heiles, C., Davis, M. M., & Goss, W. M. 1982, Nature, 300, 615

Banfield, J. K., Schnitzeler, D. H. F. M., George, S. J., et al. 2014, Monthly Notices of the Royal Astronomical Society, 444, 700

Beck, R., Brandenburg, A., Moss, D., Shukurov, A., & Sokoloff, D. 1996, Annual Reviews of Astronomy and Astrophysics, 34, 155

Becker, R. H., White, R. L., & Helfand, D. J. 1995, Astrophysical Journal, 450, 559

Begelman, M. C., & Cioffi, D. F. 1989, Astrophysical Journal Letters, 345, L21

Behroozi, P. S., Wechsler, R. H., & Conroy, C. 2013, Astrophysical Journal, 770, 57

Benaglia, P. 2010, in Astronomical Society of the Pacific Conference Series, Vol. 422, High Energy Phenomena in Massive Stars, ed. J. Martí, P. L. Luque-Escamilla, & J. A. Combi, 111

Benjamin, R. A., Churchwell, E., Babler, B. L., et al. 2003, Publications of the ASP, 115, 953

Berger, E., Rutledge, R. E., Phan-Bao, N., et al. 2009, Astrophysical Journal, 695, 310

Bernet, M. L., Miniati, F., & Lilly, S. J. 2013, Astrophysical Journal Letters, 772, L28

Bernet, M. L., Miniati, F., Lilly, S. J., Kronberg, P. P., & Dessauges-Zavadsky, M. 2008, Nature, 454, 302

Bernstein, J. P., Kessler, R., Kuhlmann, S., et al. 2012, Astrophysical Journal, 753, 152

Best, P. N., & Heckman, T. M. 2012, Monthly Notices of the Royal Astronomical Society, 421, 1569

Best, P. N., Kaiser, C. R., Heckman, T. M., & Kauffmann, G. 2006, Monthly Notices of the Royal Astronomical Society, 368, L67

Best, P. N., Kauffmann, G., Heckman, T. M., et al. 2005, Monthly Notices of the Royal Astronomical Society, 362, 25

Bicknell, G. V., Cameron, R. A., & Gingold, R. A. 1990, Astrophysical Journal, 357, 373

Bîrzan, L., McNamara, B. R., Nulsen, P. E. J., Carilli, C. L., & Wise, M. W. 2008, Astrophysical Journal, 686, 859

Blanton, E. L., Gregg, M. D., Helfand, D. J., Becker, R. H., & White, R. L. 2000, Astrophysical Journal, 531, 118

Bonafede, A., Feretti, L., Murgia, M., et al. 2010, Astronomy & Astrophysics, 513, A30

Bonfield, D. G., Jarvis, M. J., Hardcastle, M. J., et al. 2011, Monthly Notices of the Royal Astronomical Society, 416, 13

Bouwens, R. J., Illingworth, G. D., Oesch, P. A., et al. 2012, Astrophysical Journal, 754, 83

Bower, G. C., Saul, D., Bloom, J. S., et al. 2007, Astrophysical Journal, 666, 346

Bower, R. G., Benson, A. J., Malbon, R., et al. 2006, Monthly Notices of the Royal Astronomical Society, 370, 645

Braun, R., Heald, G., & Beck, R. 2010, Astronomy & Astrophysics, 514, A42

Brown, M. L., & Battye, R. A. 2011, Monthly Notices of the Royal Astronomical Society, 410, 2057

Brown, M. L., Taylor, A. N., Hambly, N. C., & Dye, S. 2002, Monthly Notices of the Royal Astronomical Society, 333, 501

Brown, M. L., Abdalla, F. B., Amara, A., et al. 2013, ArXiv e-prints

Burn, B. J. 1966, Monthly Notices of the Royal Astronomical Society, 133, 67

Camera, S., Santos, M. G., Bacon, D. J., et al. 2012, Monthly Notices of the Royal Astronomical Society, 427, 2079

Carey, S. J., Noriega-Crespo, A., Mizuno, D. R., et al. 2009, Publications of the ASP, 121, 76

Carretti, E., Crocker, R. M., Staveley-Smith, L., et al. 2013, Nature, 493, 66

Catelan, P., Kamionkowski, M., & Blandford, R. D. 2001, Monthly Notices of the Royal Astronomical Society, 320, L7

Cenko, S. B., Kulkarni, S. R., Horesh, A., et al. 2013, Astrophysical Journal, 769, 130

Chang, T.-C., & Refregier, A. 2002, Astrophysical Journal, 570, 447

Chang, T.-C., Refregier, A., & Helfand, D. J. 2004, Astrophysical Journal, 617, 794

Churchill, C., Steidel, C., & Kacprzak, G. 2005, in Astronomical Society of the Pacific Conference Series, Vol. 331, Extra-Planar Gas, ed. R. Braun, 387

Churchwell, E., Babler, B. L., Meade, M. R., et al. 2009, Publications of the ASP, 121, 213

Coil, A. L., Blanton, M. R., Burles, S. M., et al. 2011, Astrophysical Journal, 741, 8

Coleman, P. H., & Condon, J. J. 1985, Astronomical Journal, 90, 1431

Condon, J. J., Cotton, W. D., Greisen, E. W., et al. 1998, Astronomical Journal, 115, 1693

Condon, J. J., Kellermann, K. I., Kimball, A. E., Ivezić, Ž., & Perley, R. A. 2013a, Astrophysical Journal, 768, 37

—. 2013b, Astrophysical Journal, 768, 37

Cowie, L. L., Songaila, A., Hu, E. M., & Cohen, J. G. 1996, Astronomical Journal, 112, 839

Croston, J. H., Pratt, G. W., Böhringer, H., et al. 2008, Astronomy & Astrophysics, 487, 431

Croton, D. J., Springel, V., White, S. D. M., et al. 2006, Monthly Notices of the Royal Astronomical Society, 365, 11

Darnley, M. J., Bode, M. F., Kerins, E., et al. 2006, Monthly Notices of the Royal Astronomical Society, 369, 257

de Zotti, G., Massardi, M., Negrello, M., & Wall, J. 2010, Astronomy and Astrophysics Reviews, 18, 1

Dressing, C. D., & Charbonneau, D. 2013, Astrophysical Journal, 767, 95

Elbaz, D., Dickinson, M., Hwang, H. S., et al. 2011, Astronomy & Astrophysics, 533, A119

Erickson, W. C. 1983, Astrophysical Journal Letters, 264, L13

Farnes, J. S., Gaensler, B. M., & Carretti, E. 2014a, Astrophysical Journal Supplement, 212, 15

Farnes, J. S., O'Sullivan, S. P., Corrigan, M. E., & Gaensler, B. M. 2014b, ArXiv e-prints

Farnsworth, D., Rudnick, L., & Brown, S. 2011, Astronomical Journal, 141, 191

Feretti, L., Giovannini, G., Govoni, F., & Murgia, M. 2012a, Astronomy and Astrophysics Reviews, 20, 54

—. 2012b, Astronomy and Astrophysics Reviews, 20, 54

Fong, W., Berger, E., Margutti, R., et al. 2012, Astrophysical Journal, 756, 189

Frail, D. A., Kulkarni, S. R., Ofek, E. O., Bower, G. C., & Nakar, E. 2012, Astrophysical Journal, 747, 70

Franco, J., Tenorio-Tagle, G., & Bodenheimer, P. 1990, Astrophysical Journal, 349, 126

Frey, S., Paragi, Z., Gurvits, L. I., Gabányi, K. É., & Cseh, D. 2011, Astronomy & Astrophysics, 531, L5

Furlanetto, S. R., & Loeb, A. 2001, Astrophysical Journal, 556, 619

Gal-Yam, A., Fox, D. B., Price, P. A., et al. 2006, Nature, 444, 1053

Garcia-Segura, G., & Franco, J. 1996, Astrophysical Journal, 469, 171

Ghirlanda, G., Burlon, D., Ghisellini, G., et al. 2014, Publications of the ASA, 31, 22

Giacintucci, S., O'Sullivan, E., Clarke, T. E., et al. 2012, Astrophysical Journal, 755, 172

Goldschmidt, P., Kukula, M. J., Miller, L., & Dunlop, J. S. 1999, Astrophysical Journal, 511, 612

Gruppioni, C., Pozzi, F., Rodighiero, G., et al. 2013, Monthly Notices of the Royal Astronomical Society, 432, 23

Hales, C. A., Norris, R. P., Gaensler, B. M., & Middelberg, E. 2014a, Monthly Notices of the Royal Astronomical Society, 440, 3113

Hales, C. A., Norris, R. P., Gaensler, B. M., et al. 2014b, Monthly Notices of the Royal Astronomical Society, 441, 2555

Hallinan, G., Antonova, A., Doyle, J. G., et al. 2006, Astrophysical Journal, 653, 690

—. 2008, Astrophysical Journal, 684, 644

Hallinan, G., Bourke, S., Lane, C., et al. 2007, Astrophysical Journal Letters, 663, L25

Hammond, A. M., Robishaw, T., & Gaensler, B. M. 2012, ArXiv e-prints

Hancock, P. J., Murphy, T., Gaensler, B. M., Hopkins, A., & Curran, J. R. 2012, Monthly Notices of the Royal Astronomical Society, 422, 1812

Hardcastle, M. J., Evans, D. A., & Croston, J. H. 2007, Monthly Notices of the Royal Astronomical Society, 376, 1849

Hardcastle, M. J., & Worrall, D. M. 2000, Monthly Notices of the Royal Astronomical Society, 319, 562

Heavens, A., Refregier, A., & Heymans, C. 2000, Monthly Notices of the Royal Astronomical Society, 319, 649

Heckman, T. M., & Best, P. N. 2014, Annual Reviews of Astronomy and Astrophysics, 52, 589

Helou, G., Soifer, B. T., & Rowan-Robinson, M. 1985, Astrophysical Journal Letters, 298, L7

Herbert, P. D., Jarvis, M. J., Willott, C. J., et al. 2010, Monthly Notices of the Royal Astronomical Society, 406, 1841

Hessels, J. W. T., Ransom, S. M., Stairs, I. H., et al. 2006, Science, 311, 1901

Heywood, I., Jarvis, M. J., & Condon, J. J. 2013, Monthly Notices of the Royal Astronomical Society, 432, 2625

Hirata, C. M., & Seljak, U. 2004, Physical Review D, 70, 063526

Hoare, M. G., Purcell, C. R., Churchwell, E. B., et al. 2012, Publications of the ASP, 124, 939

Hodge, J. A., Becker, R. H., White, R. L., Richards, G. T., & Zeimann, G. R. 2011, Astronomical Journal, 142, 3

Hopkins, A. M., & Beacom, J. F. 2006, Astrophysical Journal, 651, 142

Hopkins, P. F. 2012, Monthly Notices of the Royal Astronomical Society, 420, L8

Huynh, M. T., Hopkins, A., Norris, R., et al. 2012, Publications of the ASA, 29, 229

Hyman, S. D., Lazio, T. J. W., Kassim, N. E., & Bartleson, A. L. 2002, Astronomical Journal, 123, 1497

Hyman, S. D., Lazio, T. J. W., Kassim, N. E., et al. 2005, Nature, 434, 50

Hyman, S. D., Wijnands, R., Lazio, T. J. W., et al. 2009, Astrophysical Journal, 696, 280

Ivezić, Ž., Menou, K., Knapp, G. R., et al. 2002, Astronomical Journal, 124, 2364

Ivison, R. J., Magnelli, B., Ibar, E., et al. 2010, Astronomy & Astrophysics, 518, L31

Janssen, R. M. J., Röttgering, H. J. A., Best, P. N., & Brinchmann, J. 2012, Astronomy & Astrophysics, 541, A62

Jarvis, M. J., & Rawlings, S. 2004, New Astronomy Review, 48, 1173

Jarvis, M. J., Smith, D. J. B., Bonfield, D. G., et al. 2010, Monthly Notices of the Royal Astronomical Society, 409, 92

Jarvis, M. J., Bonfield, D. G., Bruce, V. A., et al. 2013, Monthly Notices of the Royal Astronomical Society, 428, 1281

Jiang, L., Fan, X., Ivezić, Ž., et al. 2007, Astrophysical Journal, 656, 680

Kacprzak, G. G., Churchill, C. W., Ceverino, D., et al. 2010, Astrophysical Journal, 711, 533

Kalberla, P. M. W., Burton, W. B., Hartmann, D., et al. 2005, Astronomy & Astrophysics, 440, 775

Kalfountzou, E., Jarvis, M. J., Bonfield, D. G., & Hardcastle, M. J. 2012, Monthly Notices of the Royal Astronomical Society, 427, 2401

Kalfountzou, E., Stevens, J. A., Jarvis, M. J., et al. 2014, Monthly Notices of the Royal Astronomical Society, 442, 1181

Kelson, D. D., Williams, R. J., Dressler, A., et al. 2014, Astrophysical Journal, 783, 110

Khodachenko, M. L., Ribas, I., Lammer, H., et al. 2007, Astrobiology, 7, 167

Kimball, A. E., Kellermann, K. I., Condon, J. J., Ivezić, Ž., & Perley, R. A. 2011a, Astrophysical Journal Letters, 739, L29

—. 2011b, Astrophysical Journal Letters, 739, L29

Kramer, M., Stairs, I. H., Manchester, R. N., et al. 2006, Science, 314, 97

Kratzer, R. M. 2014, PhD thesis, Drexel University

Kulkarni, S. R., & Phinney, E. S. 2005, Nature, 434, 28

Kwitter, K. B., Méndez, R. H., Peña, M., et al. 2014, Revista Mexicana de Astronomia y Astrofisica, 50, 203

Kwok, S. 2005, Journal of Korean Astronomical Society, 38, 271

Lacy, M., Ridgway, S. E., Gates, E. L., et al. 2013, Astrophysical Journal Supplement, 208, 24

Lammer, H., Lichtenegger, H. I. M., Kulikov, Y. N., et al. 2007, Astrobiology, 7, 185

Lazio, J., Bloom, J. S., Bower, G. C., et al. 2009, in ArXiv Astrophysics e-prints, Vol. 2010, astro2010: The Astronomy and Astrophysics Decadal Survey, 176

Lewis, I., Balogh, M., De Propris, R., et al. 2002, Monthly Notices of the Royal Astronomical Society, 334, 673

LIGO Scientific Collaboration, Virgo Collaboration, Aasi, J., et al. 2013, ArXiv e-prints

Lilly, S. J., Le Fevre, O., Hammer, F., & Crampton, D. 1996, Astrophysical Journal Letters, 460, L1

Lindsay, S. N., Jarvis, M. J., & McAlpine, K. 2014a, Monthly Notices of the Royal Astronomical Society, 440, 2322

Lindsay, S. N., Jarvis, M. J., Santos, M. G., et al. 2014b, Monthly Notices of the Royal Astronomical Society, 440, 1527

Lonsdale, C. J., Smith, H. E., Rowan-Robinson, M., et al. 2003, Publications of the ASP, 115, 897

Lovell, B. 1963, Nature, 198, 228

Lucas, P. W., Hoare, M. G., Longmore, A., et al. 2008, Monthly Notices of the Royal Astronomical Society, 391, 136

Lyne, A. G., Burgay, M., Kramer, M., et al. 2004, Science, 303, 1153

Magnelli, B., Popesso, P., Berta, S., et al. 2013, ArXiv e-prints

Mao, M. Y., Sharp, R., Norris, R. P., et al. 2012, Monthly Notices of the Royal Astronomical Society, 426, 3334

Margutti, R., Soderberg, A. M., Wieringa, M. H., et al. 2013a, Astrophysical Journal, 778, 18

—. 2013b, Astrophysical Journal, 778, 18

Mauduit, J.-C., Lacy, M., Farrah, D., et al. 2012, Publications of the ASP, 124, 714

Miller-Jones, J. C. A., Jonker, P. G., Maccarone, T. J., Nelemans, G., & Calvelo, D. E. 2011, Astrophysical Journal Letters, 739, L18

Molinari, S., Swinyard, B., Bally, J., et al. 2010, Publications of the ASP, 122, 314

Mooley, K. P., Frail, D. A., Ofek, E. O., et al. 2013, Astrophysical Journal, 768, 165

Mooley, K. P., Myers, S. T., Hallinan, G., et al. 2014, in American Astronomical Society Meeting Abstracts, Vol. 223, American Astronomical Society Meeting Abstracts 223, 236.02

Moster, B. P., Somerville, R. S., Newman, J. A., & Rix, H.-W. 2011, Astrophysical Journal, 731, 113

Murphy, E. J. 2009, Astrophysical Journal, 706, 482

Muxlow, T. W. B., Richards, A. M. S., Garrington, S. T., et al. 2005, Monthly Notices of the Royal Astronomical Society, 358, 1159

Nakar, E., & Piran, T. 2011, Nature, 478, 82

National Research Council. 2010, New Worlds, New Horizons in Astronomy and Astrophysics (Washington, DC: The National Academies Press)

Norman, C. A., Bowen, D. V., Heckman, T., Blades, C., & Danly, L. 1996, Astrophysical Journal, 472, 73

Norris, R. P., Basu, K., Brown, M., et al. 2014, ArXiv e-prints

Norris, R. P., Afonso, J., Appleton, P. N., et al. 2006, Astronomical Journal, 132, 2409

Oliver, S. J., Bock, J., Altieri, B., et al. 2012, Monthly Notices of the Royal Astronomical Society, 424, 1614

Ortiz-Leon, G. N., Loinard, L., Mioduszewski, A. J., et al. 2013, in Protostars and Planets VI Posters, 4

Osten, R. A., & Bastian, T. S. 2006, Astrophysical Journal, 637, 1016

Osten, R. A., Hawley, S. L., Allred, J. C., Johns-Krull, C. M., & Roark, C. 2005, Astrophysical Journal, 621, 398

Osten, R. A., & Wolk, S. J. 2009, Astrophysical Journal, 691, 1128

O'Sullivan, S. P., Brown, S., Robishaw, T., et al. 2012, Monthly Notices of the Royal Astronomical Society, 421, 3300

O'Sullivan, S. P., Feain, I. J., McClure-Griffiths, N. M., et al. 2013, Astrophysical Journal, 764, 162

Pâris, I., Petitjean, P., Aubourg, É., et al. 2014, Astronomy & Astrophysics, 563, A54

Peng, Y.-j., Lilly, S. J., Renzini, A., & Carollo, M. 2012, Astrophysical Journal, 757, 4

Peng, Y.-j., Lilly, S. J., Kovač, K., et al. 2010, Astrophysical Journal, 721, 193

Peterson, J. R., & Fabian, A. C. 2006, Physics Reports, 427, 1

Planck Collaboration, Ade, P. A. R., Aghanim, N., et al. 2014, Astronomy & Astrophysics, 571, A19

Prandoni, I., & Seymour, N. 2014, ArXiv e-prints

Quider, A. M., Nestor, D. B., Turnshek, D. A., et al. 2011, Astronomical Journal, 141, 137

Raccanelli, A., Bonaldi, A., Negrello, M., et al. 2008, Monthly Notices of the Royal Astronomical Society, 386, 2161

Raccanelli, A., Zhao, G.-B., Bacon, D. J., et al. 2012, Monthly Notices of the Royal Astronomical Society, 424, 801

Ransom, S. M., Stairs, I. H., Archibald, A. M., et al. 2014, Nature, 505, 520

Ray, P. S., Abdo, A. A., Parent, D., et al. 2012, ArXiv e-prints

Reiners, A., & Basri, G. 2007, Astrophysical Journal, 656, 1121

Rosario, D. J., Trakhtenbrot, B., Lutz, D., et al. 2013, Astronomy & Astrophysics, 560, A72

Route, M., & Wolszczan, A. 2012, Astrophysical Journal Letters, 747, L22

Rubin, V. C., Burley, J., Kiasatpoor, A., et al. 1962, Astronomical Journal, 67, 491

Rudnick, L., & Owen, F. N. 2014, Astrophysical Journal, 785, 45

Runnoe, J. C., Brotherton, M. S., Shang, Z., Wills, B. J., & DiPompeo, M. A. 2013, Monthly Notices of the Royal Astronomical Society, 429, 135

Sabin, L., Parker, Q. A., Corradi, R. L. M., et al. 2014, Monthly Notices of the Royal Astronomical Society, 443, 3388

Sargent, M. T., Schinnerer, E., Murphy, E., et al. 2010, Astrophysical Journal Supplement, 186, 341

Schmidt, M., & Green, R. F. 1983, Astrophysical Journal, 269, 352

Schnitzeler, D. H. F. M. 2010, Monthly Notices of the Royal Astronomical Society, 409, L99

Silk, J. 2013, Astrophysical Journal, 772, 112

Soderberg, A. M., Brunthaler, A., Nakar, E., Chevalier, R. A., & Bietenholz, M. F. 2010, Astrophysical Journal, 725, 922

Sokoloff, D. D., Bykov, A. A., Shukurov, A., et al. 1998, Monthly Notices of the Royal Astronomical Society, 299, 189

Stil, J. M., Keller, B. W., George, S. J., & Taylor, A. R. 2014, Astrophysical Journal, 787, 99

Stil, J. M., Krause, M., Beck, R., & Taylor, A. R. 2009, Astrophysical Journal, 693, 1392

Sun, X. H., & Reich, W. 2012, Astronomy & Astrophysics, 543, A127

Sun, X. H., Rudnick, L., Akahori, T., et al. 2014, ArXiv e-prints

Tasse, C., Best, P. N., Röttgering, H., & Le Borgne, D. 2008, Astronomy & Astrophysics, 490, 893

Taylor, A. R., Stil, J. M., & Sunstrum, C. 2009, Astrophysical Journal, 702, 1230

Tonry, J. L., Stubbs, C. W., Kilic, M., et al. 2012, Astrophysical Journal, 745, 42

Tribble, P. C. 1991, Monthly Notices of the Royal Astronomical Society, 250, 726

Urry, C. M., & Padovani, P. 1995, Publications of the ASP, 107, 803

Wade, G. A., Grunhut, J. H., & MiMeS Collaboration. 2012, in Astronomical Society of the Pacific Conference Series, Vol. 464, Circumstellar Dynamics at High Resolution, ed. A. C. Carciofi & T. Rivinius, 405

White, R. L., Becker, R. H., Helfand, D. J., & Gregg, M. D. 1997, Astrophysical Journal, 475, 479

Wills, B. J., & Browne, I. W. A. 1986, Astrophysical Journal, 302, 56

Wilman, R. J., Jarvis, M. J., Mauch, T., Rawlings, S., & Hickey, S. 2010, Monthly Notices of the Royal Astronomical Society, 405, 447

Wilman, R. J., Miller, L., Jarvis, M. J., et al. 2008, Monthly Notices of the Royal Astronomical Society, 388, 1335

Windhorst, R. A., Miley, G. K., Owen, F. N., Kron, R. G., & Koo, D. C. 1985, Astrophysical Journal, 289, 494

Wing, J. D., & Blanton, E. L. 2011, Astronomical Journal, 141, 88

Xu, J., & Han, J. L. 2014, Monthly Notices of the Royal Astronomical Society, 442, 3329

Zakamska, N. L., & Greene, J. E. 2014, Monthly Notices of the Royal Astronomical Society, 442, 784

Zhu, G., & Ménard, B. 2013, Astrophysical Journal, 770, 130

Zweibel, E. G., & Heiles, C. 1997, Nature, 385, 131

Appendix

A Motivation and Process

In July 2013 NRAO announced that it would consider a new radio sky survey using the Karl G. Jansky Very Large Array (VLA), after several members of the community approached the NRAO Director suggesting that it was time to think about a follow-on from NVSS and FIRST. These two surveys were ground-breaking in their time, but in the twenty years since their execution both the capabilities now available on the VLA following the Expanded VLA (EVLA) Construction Project, and the wealth of surveys, extant and planned, at other wavelengths that require *arcsecond* localization of associated radio emission, make necessary the consideration of a new radio survey. In particular, the availability of On-The-Fly (OTF) mosaics and the wide fractional bandwidth of the VLA provide the fast mapping speed, increased continuum sensitivity, and instantaneous spectral index information that would simply not have been possible prior to the improvements provided by the EVLA.

Given the potential impact a large survey would have on the use of the telescope, both in terms of the large-scale survey science that is simply not possible through the regular peer-review process, and on the resulting reduction in the availability of time for regular PI science should a large survey proceed, the survey science and definition had to be proposed and reviewed by the community. A process was therefore defined that would result in a community-led recommendation being provided to the NRAO Director, with NRAO facilitating the process. The process included, from the start, open *international* participation in the development of a VLA Sky Survey (VLASS) Proposal, with the final deliverables being public data and data products. Should the Proposal pass its Community Review, NRAO would implement the survey, deliver basic data products, and support the community with higher-level data products as resources allow.

In preparation for a VLASS Science Planning Workshop held January 5, 2014 at the 223$^{\rm rd}$ American Astronomical Society meeting in Washington, D.C., White Papers (WPs) were solicited from the community through the NRAO eNews, and a Scientific Organizing Committee (SOC) was convened to review the WPs and define the agenda of the Workshop. A total of 22 WPs were received, with contributions from 180 unique authors (see Table 8). It is interesting to note that of these authors, approximately 20% were *not* users of NRAO telescopes, and do not appear in the NRAO User Database (i.e., they have never been on a proposal to use an NRAO instrument, either as co-I or PI, nor have they registered in the User Database for any other reason). Therefore, the act of soliciting the WPs, in and of itself, already attracted interest from a broader community than the "traditional" radio astronomy community. The Workshop attracted $\approx$50 attendees, and comprised morning talks followed by afternoon discussion. Areas for debate became apparent, and some possible avenues for the survey began to be ruled out (such as a large-scale, high-frequency survey).

Following the Workshop, the SOC was responsible for defining the process by which the VLASS Proposal would be developed. In February 2014 the Survey Science Group (SSG) was formed comprising several working groups (WGs), open to the entire community, and advertised in multiple eNews articles. The WGs topics were:

- Galactic
- Extragalactic
- Transients and Variability
- Programmatics
- Communication/Education/Outreach
- Technical

Table 8: VLASS Proposal Contributors, Including VLASS White Paper Authors

F. Abdalla, Jose Afonso, A. Amara, David Bacon, Julie Banfield, Tim Bastian, Richard Battye, **Stefi A. Baum**, Tony Beasley, Rainer Beck, Robert Becker, Michael Bell, Edo Berger, Rob Beswick, Sanjay Bhatnagar, Mark Birkinshaw, V. Boehm, Geoff Bower, **Niel W. Brandt**, A. Brazier, Sarah Bridle, Michael Brotherton, Alex Brown, Michael L. Brown, Shea Brown, Ian Browne, Gianfranco Brunetti, Sarah Burke Spolaor, Ettore Carretti, Caitlin Casey, Sayan Chakraborti, **Claire J. Chandler**, Shami Chatterjee, **Tracy Clarke**, Julia Comerford, **Jim Cordes**, Bill Cotton, Fronefield Crawford, Daniele Dallacasa, Constantinos Demetroullas, **Susana E. Deustua**, **Mark Dickinson**, Klaus Dolag, Sean Dougherty, Steve Drake, Alastair Edge, Torsten Ensslin, Andy Fabian, Xiaohui Fan, Jamie Farnes, Luigina Feretti, Pedro Ferreira, Dale Frail, Bryan Gaensler, Simon Garrington, Joern Geisbuesch, Simona Giacintucci, Adam Ginsburg, Gabriele Giovannini, Eilat Glikman, Federica Govoni, Keith Grainge, Meghan Gray, Dave Green, Manuel Guedel, **Nicole E. Gugliucci**, Chris Hales, **Gregg Hallinan**, Martin Hardcastle, Ian Harrison, Marijke Haverkorn, Martha Haynes, George Heald, Sue Ann Heatherly, Alan Heavens, Joe Helmboldt, C. Heymans, Ian Heywood, Julie Hlavacek-Larrondo, **Jackie Hodge**, Michael Hogan, Assaf Horesh, C.-L. Hung, Zeljko Ivezic, Neal Jackson, Matt Jarvis, B. Joachimi, Atish Kamble, David Kaplan, Namir Kassim, S. Kay, Amy Kimball, T.D. Kitching, Roland Kothes, Diederik Kruijssen, Shri Kulkarni, Mark Lacy, **Cornelia Lang**, **Casey Law**, **Joe Lazio**, J.P. Leahy, Jeff Linsky, Xin Liu, Britt Lundgren, R. Maartens, Antonio Mario Magalhaes, Minnie Mao, **Sui Ann Mao**, Maxim Markevitch, Walter Max-Moerbeck, Ian McGreer, Brian McNamara, Lance Miller, Elisabeth Mills, Kunal Mooley, Tony Mroczkowski, **Eric J. Murphy**, Matteo Murgia, Tom Muxlow, **Steve Myers**, Bob Nichol, Shane O'Sullivan, Niels Oppermann, **Rachel Osten**, Pat Palmer, P. Patel, Wendy Peters, Emil Polisensky, Ed Prather, J. Pritchard, Cormac Purcell, A. Raccanelli, Scott Ransom, Urvashi Rao, Paul Ray, A. Refregier, **Gordon Richards**, Anita Richards, C. Riseley, Tim Robishaw, Anish Roshi, Larry Rudnick, Michael Rupen, Helen Russell, Elaine Sadler, M. Santos, Anna Scaife, B.M. Schafer, Richard Schilizzi, Dominic Schnitzeler, Yue Shen, Kartik Sheth, Lorant Sjouwerman, Ian Smail, Oleg Smirnov, Vernesa Smolcic, Alicia Soderberg, Dmitry Sokolov, Tim Spuck, Judy Stanley, J.-L. Starck, Jeroen Stil, John Stoke, **Michael Strauss**, Meng Su, Xiaohui Sun, R. Szepietowski, A.N. Taylor, Russ Taylor, Valentina Vacca, Reinout van Weeren, Tiziana Venturi, Andrew Walsh, Wei-Hao Wang, Dave Westpfahl, Robert Wharton, **Rick White**, Stephen White, L. Whittaker, Peter Williams, Kathryn Williamson, Tony Willis, Tom Wilson, Maik Wolleben, Nicholas Wrigley, **Ashley Zauderer**, J. Zuntz

Note: Members of the SSG are listed in **bold**.

Each working group was led by two co-chairs, with the co-chairs comprising the SSG Governing Council. The SSG Governing Council itself had two co-chairs (Stefi Baum and Eric Murphy). Contributions to the WG discussions were enabled through the NRAO Science Forum,[13] with material also posted on the NRAO Public Wiki, [14] along with other methods of group communication such as Google Groups, as defined by the co-chairs of the individual WGs. In this way, contributions to the discussion on these WGs was expanded well beyond the original authorship of the WPs.

The process by which the VLASS survey definition proceeded from this point is worth documenting, as it may serve to guide the development of future surveys. Initially, the three scientific WGs (Galactic, Extragalactic, and Transients/Variability) were asked by the SSG Council co-chairs to specify their "ideal" survey designs, supported by key science goals. A "virtual face-to-face" meeting was then used to assess areas of commonality between the elements of the proposed surveys (frequency band, array configuration) and to identify areas that needed further discussion (number of epochs, depth of each epoch, monolithic vs. tiered). At this stage, the focus of the

[13]https://science.nrao.edu/forums/viewforum.php?f=59

[14]https://safe.nrao.edu/wiki/bin/view/VLA/VLASS

Galactic working group on thermal science, and therefore on higher frequencies than the Extragalactic or Transient WGs and with much less baseline understanding of the nature of the Galactic sky at those frequencies, led to difficulties defining a coherent survey that would justify being part of VLASS rather than being proposed as a Large program through the regular NRAO proposal process. In all three cases, the "ideal" survey (for each WG) would have far exceeded a reasonable time request. For example the Galactic WG wanted both high and low frequency, while transients wanted many more epochs than possible. Extragalactic ideally would like 5 tiers of decreasing area, but increasing depth (the areas being roughly categorized as All-sky, SDSS/FIRST/DESI footprint, DES+HSC footprint, SDSS Stripe-82, a few of the LSST deep drilling fields, and an Ultra-deep field) from the depth of FIRST down to $\sim$0.5 μJy. With this lack of consensus, the SSG Council co-chairs proposed a baseline all-sky, S-band, B-config, survey of $\sim$8500 hours, with the WGs proposing tradeoffs in time/area coverage needed to achieve their key science goals. The VLASS Proposal is the outcome of this process, and represents contributions from more than 200 astronomers over a 12 month period from November 2013 through October 2014.

B The Impact of VLASS on Overall VLA Science: The High Impact of Surveys

The time committed to the proposed VLASS will reduce the time available for other VLA programs. However, we argue that the time spent on large VLA surveys has effects that increase the net science coming from the VLA:

1. VLA sky surveys have a science impact per observing hour that is demonstrably greater than the average VLA observing program. This is at least partly because surveys expand the usage of radio data beyond the usual radio astronomy community.

2. Once VLA sky survey products are available, many science projects that require pointed observations of a sample of objects (e.g., to measure spectral indices for a sample of quasars) can be carried out directly from the catalogs rather than requiring an observing proposal. That reduces the time requested for such observing proposals and so increases the time available for other projects.

3. The sky survey products themselves will become a key resource for radio astronomers in identifying targets and projects for followup proposals. That also leads to an increase in the science done by enabling projects that are not possible without the inputs from a sky survey.

The existing VLA sky surveys, NVSS (Condon et al., 1998) and FIRST (Becker et al., 1995; White et al., 1997), provide powerful evidence that the telescope time dedicated to these surveys repays the investment many times over. Below we present some statistics on the usage of the FIRST survey data and on the impact of FIRST and NVSS as measured by publications and citations.

B.1 FIRST survey data usage

The FIRST image server[15] provides JPEG or FITS cutouts extracted from the FIRST survey at user-specified positions. Here are some statistics about its usage:

- During the last 18 months the FIRST cutout server has delivered on average more than 7,500 image cutouts every day.

[15] `http://third.ucllnl.org/cgi-bin/firstcutout`

- Each image served is equivalent to a three-minute VLA observation (the exposure time required to reach the FIRST depth); thus, our image server issues the equivalent of a 3-minute VLA observation every 12 seconds.
- Every 10 days the FIRST cutout server distributes snapshots with a total exposure time equal to the entire 4000 hours invested in the FIRST survey.

By creating a legacy dataset that covers as much of the sky as possible, we can vastly expand the user community (and scientific productivity) of the VLA. This is the single most important reason to do an all-sky survey.

B.2 NVSS/FIRST publications & citations

Publications and citations are the best objective measures we have of scientific impact. While there are lots of caveats (e.g., papers in fashionable fields collect more citations), every other measure of productivity is even less objective and harder to evaluate. In this section we discuss the publication statistics for the FIRST and NVSS surveys. The results strongly support the value of these surveys both in absolute terms and in comparison to other VLA projects.

There are three basic papers that define the FIRST and NVSS survey data products:

- FIRST images: (Becker et al., 1995)
  - 1311 citations
- FIRST catalogs: (White et al., 1997)
  - 587 citations
  - 1722 citations combined with Becker et al.
- NVSS images & catalogs: (Condon et al., 1998)
  - 2675 citations

Combining the FIRST and NVSS papers, there are a total of 3550 citations (3132 refereed citations). These 3 papers are ranked #1, #2, and #11 in citations among all VLA publications.

These papers are highly cited not just among VLA publications, but among all astronomy papers. Of the most-cited papers published since 1995, the NVSS paper is #16 and the Becker et al. paper is #67. Other than WMAP papers, the only other "radio astronomy" papers to crack the top 100 are #29 (Urry & Padovani, 1995, "Unified Schemes for Radio-Loud Active Galactic Nuclei") and #63 (Kalberla et al., 2005, "The Leiden/Argentine/Bonn (LAB) Survey of Galactic HI").

There are a few exceptions, but we can generally treat the list of citing papers as an indication of the usage of VLA survey data. The 3522 papers in ADS that cite NVSS and/or FIRST (as of 2014 March 29) have a total of 9086 unique authors. There could be some double-counting here, since some authors publish using more than one version of their name/initials; but even if we compare only last names, there are still 6925 unique authors among these papers. There are 1876 unique first authors on these papers, or 1666 unique first authors using unique last names only. So, if anything, these citation numbers underestimate the usage of the survey data.

The NRAO database includes a total of $\sim$6200 users (G. Hunt, private communication). That includes almost everyone who has ever been on a radio proposal. It is clear that the community using NVSS/FIRST data is considerably larger than the community of radio telescope users. By every measure, the impact of FIRST plus NVSS is large. According to the NRAO publications database, there were 192 refereed VLA papers per year over the decade 2000–2009. (We used those years because the VLA publication rate has dropped a little since 2010.) For comparison, over

that same period there were 262 refereed publications per year that cited FIRST and/or NVSS. While these two numbers (the NRAO publication database and the FIRST/NVSS citations) are self-evidently collected in different ways (the former PI provided to NRAO, the second through ADS), nevertheless it provides an interesting comparison. Thus, there is strong evidence against the argument that the science out of the VLA is negatively impacted when surveys displace regular proposals. It is our expectation that VLASS will enhance science at the VLA, just as major surveys have been clearly demonstrated to enhance science at many other modern observatories using even more rigorous statistical citation comparisons (e.g., data collected by STScI, *Spitzer*, Sloan, etc.).

It is our expectation that VLASS will enhance science at the VLA, as has been clearly demonstrated at every other modern observatory using even more rigorous statistical citation comparisons (e.g., data collected by STScI, NASA etc.). That is why more and more time at all major observatories is being dedicated to large surveys.

B.3 Will VLASS have the same impact as FIRST & NVSS?

Both the publications and data usage provide extremely strong support for the proposition that time invested in VLASS will be repaid many times over. The impact of NVSS and FIRST is demonstrably much greater than the impact of the displaced VLA science proposals. Moreover, after a few years the time invested in the survey pays for itself by freeing up observing time that would otherwise have been spent on survey-like observations of samples of objects or of small sky areas. And the survey data multiplies the value of other VLA observations by providing ancillary data at a different epoch, frequency, and resolution that can be used in conjunction with new observations. Many current VLA proposals begin with samples that are derived from the existing surveys. From every point of view, the investment of time in VLASS increases the overall scientific productivity of the VLA.

Some have argued that FIRST and NVSS were unique, and that a new VLA sky survey will not have the same impact because it will not have the unique and long-lasting legacy value in the face of the oncoming SKA pathfinders (and the SKA itself). We see two strong counter-argument to this view. First, the resolution of the VLASS is an essential difference that puts VLASS in a class by itself (§D). WODAN and ASKAP-EMU will surely spawn some great science on radio source properties. However, astronomers attempting to identify radio sources with even moderately deep observations at visible or infrared wavelengths will use VLASS.

Secondly, we have a clear counter-example to the argument that the survey must be "absolutely unique" compared to any existing or planned future survey. Consider the NVSS and FIRST themselves: They were carried out at the same time, with the same telescope and receivers. They observed at the same frequency. The sky covered by FIRST was also completely covered by NVSS. FIRST is only about 2.5 times deeper than NVSS for point sources, and the sensitivity difference is even less for extended sources. And yet both FIRST and NVSS have thrived, and both have had a demonstrably large impact on radio and multi-wavelength science. How can that be?

The answer is that the higher resolution of FIRST (with a beam 8 times smaller than NVSS) is essential in doing cross-matches to SDSS and other deep imaging observations. Science with NVSS depends on its larger sky coverage and good sensitivity to large-scale emission that come from a low-resolution survey. Even though these surveys were carried out and released essentially simultaneously, and even though they had many characteristics in common, it took only one difference — resolution — to distinguish them and make them both widely used to this day.

While we agree that it is important to consider VLASS in the context of current planned surveys and not to duplicate those surveys, we definitely do not agree that it is necessary to push to the extreme limits of the VLA parameter space (e.g., very high frequencies and the highest possible spatial resolution) in order to distinguish it from coming low-frequency, low-resolution surveys by the SKA pathfinders. NVSS and FIRST have had a huge impact on astronomy, and they have

succeeded in vastly expanding the community of users of radio data. VLASS will surely have a comparable impact.

C Additional Science Enabled by VLASS

Below we identify science that will be enabled by VLASS in addition to the key science themes discussed in the main text of the proposal.

C.1 Extragalactic Science & Cosmology

The Physics of Galaxy Clusters:
Clusters of galaxies are the largest gravitationally bound systems in the universe, and are dominated by dark matter ($\sim$80%). Clusters are thought to form hierarchically, with smaller galaxy clusters merging to form bigger ones. This process continues at the present time. Only a tiny fraction of a cluster's mass is in the form of stars in galaxies ($\sim$3–5%), while the rest ($\sim$15–17%) comprises the intracluster medium (ICM), which is a diffuse hot (10^7–10^8 K) gas detected in X-ray observations by its thermal bremsstrahlung and highly-ionized line emission. Radio observations play a key role in understanding the physics of galaxy clusters and the role of the intracluster environment in galaxy evolution. The proposed VLASS observations are particularly suited to (i) Study the interaction and feedback between the ICM and relativistic plasma from AGN, (ii) Determine the properties of cluster-wide magnetic fields, and (iii) probe cluster weather and turbulence through tailed radio galaxies. In addition, the high-resolution VLASS observations will enable the removal of compact sources from lower resolution images that are used to study large-scale diffuse radio emission in clusters (Feretti et al., 2012b).

AGN Feedback The hot gas in the center of relaxed clusters has a relatively high density ($\sim 10^{-2}$ cm^{-3}), which implies short radiative cooling times that should lead to strong cooling flows. However, only weak cooling is observed and thus some feedback source to heat the cool core is required. At present, it is hypothesized that the source of heating in cool-core clusters is the AGN activity of the brightest cluster galaxy at the center (e.g., Peterson & Fabian, 2006). The details of this process are still far from being understood.

The radio feedback is thought to work through radio lobes which inflate bubbles (X-ray cavities) in the thermal gas, driving weak shocks and sound waves through the ICM. These bubbles are expected to detach and buoyantly rise through the ICM after the central AGN activity decreases. In addition to the energy injection, these rising bubbles provide a means of seeding the ICM with magnetic fields and relativistic particles. X-ray observations are only able to easily detect small cavities near the plane of the sky at relatively small distances from the cluster core. Larger cavities farther from the core, where the ICM is more diffuse, as well as those at small angles from the line of sight do not provide sufficient contrast for detection in even moderately deep X-ray observations. On the other hand, radio observations provide methods to place observational limits on the energy injected into the ICM by AGN feedback by tracing the complete kinetic feedback history of the ICM over multiple AGN outburst cycles. Despite the many uncertainties, the study of the radio spectrum in the aged and active components provides critical information on the cycles of activity of, and the total energy output delivered into the ICM throughout the cluster lifetime (e.g., Giacintucci et al., 2012).

ICM Magnetic Fields The study of polarized radio emission from cluster and background sources indicates that magnetic fields are ubiquitous in clusters. However, very little is known about the strength and structure of these fields and the origin of these fields is still being debated.

Studies of the polarization fraction through Rotation Measures of both cluster and background sources provide a way to determine the properties of ICM magnetic fields (e.g., Bonafede et al., 2010). Such a study is difficult to perform for individual clusters given the limited amount of polarized sources available. VLASS will provide a very large sample of polarized sources allowing binning the results for a large number of clusters.

Cluster Weather and High-z Clusters Narrow and Wide Angle Tailed radio galaxies (NATs and WATs, respectively) are the most spectacular examples of radio emission from elliptical galaxies. Their shape is the signature of galaxy cluster membership, and is explained as the combination of motion of the hosting galaxy within the cluster and ICM bulk gas motion (e.g., Blanton et al., 2000). Spectral studies along the tails provide estimates of the age of the radio plasma, which in turn can be used to infer the galaxy velocity within the cluster, and information on the dynamical state of the cluster and the ICM. Due to their unique association with dense environments, NATs and WATs can readily be used to identify high-z galaxy clusters (Wing & Blanton, 2011). High-z clusters require significant observational efforts for detection in the X-ray and optical bands, while they are fairly accessible with high resolution (arcsecond scale) radio observations. In this way, wide radio surveys that discover WATs and NATs nicely complement the ongoing surveys that exploit the redshift-independent surface brightness of the Sunyaev-Zel'dovich effect, which is now being used to locate previously-unknown clusters at high-z.

The Integrated Sachs-Wolfe Effect:
The Integrated Sachs-Wolfe (ISW) effect is manifested as a correlation induced between the Cosmic Microwave Background (CMB) radiation and the gravitational potentials of large-scale structure in the Universe. The ISW is generated as the CMB photons traverse time-varying potentials. The ISW signal is only detectable in cosmologies where the co-moving frame gravitational potentials of large-scale structure evolve, such as those dominated by Dark Energy (ΛCDM). Thus, a strong detection of the ISW effect is an important test of the ΛCDM model.

The Planck mission recently reported results correlating their CMB measurements with optical and radio surveys (Planck Collaboration et al., 2014). The strongest detection of ISW was between Planck and NVSS survey, which had a source density of $48.25\,\mathrm{deg}^{-2}$ and covered 73% of the sky. The VLASS ALL-SKY tier will reach a source density of $290\,\mathrm{deg}^{-2}$ and cover 82% of the sky (Table 2), and should provide stronger detections of constraints on the ISW when combined with Planck data. This high-resolution selected sample will be differently biased compared to the existing and future low-resolution radio samples (NVSS,EMU,WODAN), and will be an independent new test of this important cosmological cornerstone.

C.2 Time Domain Science

Below we identify a number of additional scientific opportunities in time domain science that will be addressed by VLASS, and expand on some of the themes already discussed in Section 3.3.

Supernovae A comparison of the star formation rate and supernova discovery in the local universe implies that as many as half of the supernovae remain undetected in the traditional optical searches, largely due to extinction via dust obscuration. This has far reaching consequences for models of stellar and galaxy evolution. Synoptic radio surveys, unaffected by dust obscuration, offer a means to reveal the radio afterglows of the core collapse supernovae population (type II, Ib and Ic) (Gal-Yam et al., 2006). Furthermore, Soderberg et al. (2010) and Margutti et al. (2013b) have confirmed that the nearby, subluminous class of GRBs may generate relativistic ejecta yet lack high-energy mission, implying an additional population of energetic radio afterglows detectable in radio surveys, occupying the

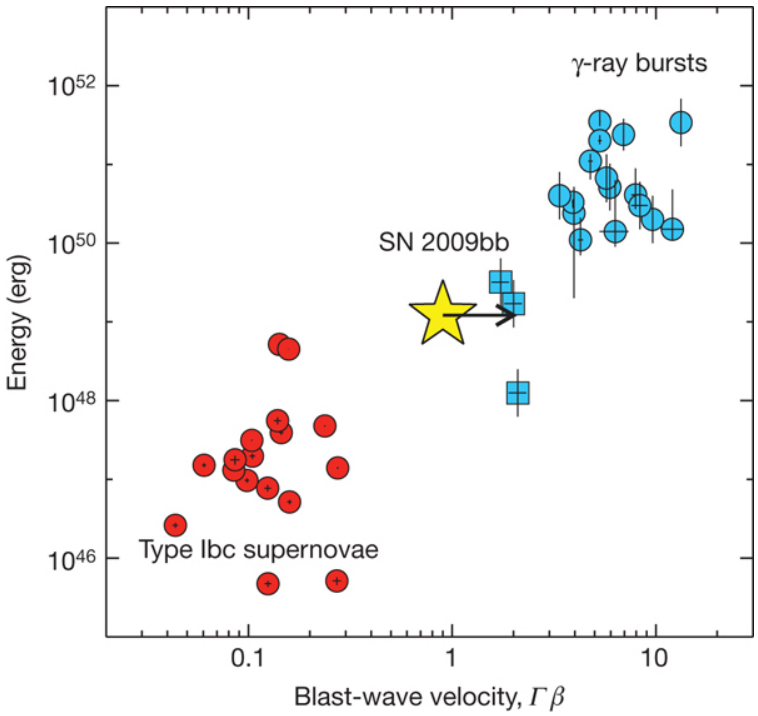

Figure 14: Kinetic energy in the fastest moving ejecta is plotted against shock wave speeds and compared for SNe and GRBs. It can be seen that the normal supernova shock wave carries a few orders of magnitude less energy than a GRB shock wave. Similar to the velocity space, the energy distribution of SN and GRBs also appear bimodal. Events similar to SN 2009bb populating this parameter space remain to be discovered Margutti et al. (2013a); Soderberg et al. (2010)).

gap in energy and ejecta velocity between supernovae and GRBs (Figure 14). Conversely, deep follow-up observations of type Ia supernovae suggest that population does not produce bright radio afterglows, likely reflecting the distinct environment of such events. As Figure 5 shows, VLASS will probe sufficient volume to rigorously constrain the rate of core collapse radio supernovae in the local universe.

Orphan Afterglows of Long Gamma-Ray Bursts: Long duration GRBs are a sub-class of type Ibc supernovae that produce a highly relativistic, collimated outflow powered by a central engine, thought to be an accreting black hole or neutron star. As might be inferred by their name, GRBs are predominantly discovered by space-based wide-field gamma-ray observatories. Detailed follow-up of exemplar candidates is carried out from X-ray to radio wavelengths, with radio observations, once again, key to establishing calorimetry of the explosion. Due to the highly collimated nature of the emission at gamma-ray wavelengths, only those bursts that are collimated in the direction of Earth are detected. Best estimates suggest this corresponds to a small fraction of the true GRB event rate, dependent on the typical opening angle of the collimated jet, with very poor constraints on the latter. The late time radio afterglow of such events, on the other hand, is largely symmetric, providing a means to directly constrain the true rate of GRBs (Cenko et al., 2013). Detection of a population of such "orphan afterglows" would provide an observational measure of the beaming fraction of GRBs. Indeed, given the current degree of uncertainty, even upper limits on this value would be a powerful constraint on models. In assessing the potential impact of VLASS is broaching this problem, we note that a very large degree of uncertainty in the true rate pre-

cludes a meaningful prediction, although we include an estimate for the expected rate based on the recent work of Ghirlanda et al. (2014) in Figure 5.

Stellar Flares and Coronal Mass Ejections: Many classes of stars produce flares that are several orders of magnitude more luminous and frequent than any produced on the Sun, including young stellar objects, active M dwarfs and certain classes of tight binaries (e.g., RS CVn systems). Such activity dominates the star's output over much of the electromagnetic spectrum, governs its angular momentum evolution and can also have a profound impact on the planetary systems orbiting such stars. In the latter case, higher X-ray and ultraviolet irradiation can lead to heating of the upper planetary atmosphere, resulting in photochemical reactions leading to significant atmospheric loss. In particular, studies of terrestrial planets in the habitable zone of M dwarfs, possibly the most abundant Earth-like planets in the solar neighborhood (Dressing & Charbonneau, 2013), suggest that large flares and coronal mass ejections (CMEs) may potentially lead to catastrophic loss of the atmosphere of such planets (Khodachenko et al., 2007; Lammer et al., 2007).

Radio bursts are a powerful means to detect and characterize flares and CMEs on the Sun and studies of radio bursts from nearby active stars can be similarly used to probe the local environment of impulsive flare and CME events with the potential for groundbreaking insight into the bulk motion of plasma in stellar coronae. Extremely bright bursts up to 1 Jy (Lovell, 1963) have been detected for decades from nearby M dwarfs, at luminosities that are up to 5 orders of magnitude more intense than any equivalent solar bursts. In more recent years, dynamic spectroscopy of stellar radio bursts has been carried out using the Very Large Array (VLA), Effelsberg, Jodrell Bank and Arecibo radio observatories (Osten & Bastian, 2006, and references therein). In the case of the detected stellar radio bursts, the luminosities are orders of magnitude brighter than anything detected from the Sun, highlighting that the coronae possessed by active stars are very different to the solar corona. The radio emission properties clearly indicate coherent processes, probably associated with plasma radiation or electron cyclotron maser emission, the former providing direct measurement of plasma densities and the latter direct measurement of magnetic field strengths, while broadband dynamic spectra of bursts provide information of the size and extent of the associated stellar coronae. Studying the coronae of such active stars provides a laboratory to investigate physical regimes unavailable with spatially detailed studies of our low-activity Sun. Furthermore, such bursts potentially provide direct insight on the density, velocity and energetics of mass ejection from stellar coronae and the associated impact on planetary atmospheres.

Active stars also produce large incoherent flares (Osten et al., 2005), due to gyrosynchrotron radiation associated with the same nature of magnetic reconnection events that produce bright coherent bursts. Insufficient data exists on the relationship between the incoherent and coherent flare emission, but this can be probed by VLASS and VLITE/LOBO with the former probing the higher frequency incoherent emission and the latter probing the coherent emission more frequently confined to lower frequencies. The degree of circular polarization is often a good distinguishing characteristic between the incoherent and coherent emission. The measured rate of flares from active stars in previous surveys (Mooley et al., 2014) suggests that flares from M dwarfs in particular will prove to be one of the most frequent transient events detected by VLASS, with potentially 100s of events recovered in the All-Sky and Wide tiers of the survey.

Substellar Auroral Emissions: A dozen or so low mass stars and brown dwarfs have been found to be radio sources in the last decade (Antonova et al., 2013, and references therein). A subset of these objects have been the subject of lengthy follow-up campaigns that have revealed the presence of 100% circularly polarized, periodic pulses, with the pulse period typically 2-3

hours and consistent with rotation (Hallinan et al., 2007, 2008; Berger et al., 2009). This radio emission is thought to be electron cyclotron emission produced at the electron cyclotron frequency, in the same fashion as that detected from the auroral regions of the magnetized planets in our solar system. As is the case for such planets, it enables very accurate measurement of magnetic field strengths and rotation periods and has led to the confirmation of kilogauss magnetic fields in large-scale configurations for ultracool dwarfs. Indeed, radio observations have been the only method thus far capable of direct magnetic field measurements for L dwarfs; Zeeman broadening measurements are inhibited by the difficulty in obtaining high resolution spectra of these cool, dim objects (Reiners & Basri, 2007).

Most recently Route & Wolszczan (2012) found the coolest radio brown dwarf yet detected, with the detection of radio pulses from the 900K T6.5 dwarf, 2MASS J10475385+2124234. Individual pulses were detected from this object in multiple short duration observations with the Arecibo observatory, resulting in a confirmed magnetic field strength of at least 1.7 kG near the surface of this extremely cool object. This significant discovery highlights the unparalleled diagnostic potential of radio observations of brown dwarfs, and their importance in constraining dynamo theory in the mass gap between planets and stars. VLASS will be the first survey with the depth to blindly detect brown dwarfs in both quiescence and outburst. The detection of late L, T and Y dwarfs would be of particular significance for ongoing empirical measurements of magnetic fields in this regime.

Galactic Center Radio Transients: Blind surveys of the Galactic Center region with the VLA have been used to search for radio transients with a considerable degree of success (Hyman et al. (2002, 2005, 2009), see Figure 15). Most notably, a blind search program using the Very Large Array (VLA) at 330 MHz (90 cm) identified a mysterious, bright, pulsing source towards the Galactic Center inconsistent with any known class of radio source, labeled GCRT J1745-3009 (Hyman et al., 2005). 100% circularly polarized 1 Jy bursts of duration ten minutes each, reoccurring with period of 77 minutes, were detected in a 7 hours of VLA data taken in September 2002. In multiple follow-up observations, the transient was detected in two more epochs of observations with the Giant Metre-Wave Radio Telescope (GMRT) in 2003 and 2004, with flux levels greatly reduced relative to the original detection. At the last known epoch of emission detected in 2004, the source exhibited an unusually steep spectrum with $\alpha = -13 \pm 3$ ($S(\nu) \propto \nu^{\alpha}$). Very high circular polarization has also been reported. GCRT J1745-3009 may be as close as 180 pc to the Galactic Center but limits on distance, and thus brightness temperature, are otherwise weak. For distances d $<$ 70 pc from the Earth, the radio flux density constrains its brightness temperature to exceed the limit for incoherent synchrotron radiation thus requiring a coherent emission mechanism. The high circular polarization, spectral characteristics and intrinsic beaming of the emission support the assertion of coherent radio emission for this new class of radio source, christened "burper" (Kulkarni & Phinney, 2005). We note that the 100% circularly polarized nature of the bursts from GCRT J1745-3009 favors parallel searches for transients in Stokes V where the galactic contribution will be reduced by many orders of magnitude relative to unpolarized Stokes I images.

No counterpart was identified in observations at other wavelengths, largely due to the poor localization of the position of the transient in radio data. It remains unclear whether GCRT J1745-3009 is intrinsically close to the Galactic Center or rather simply lies in the direction of the Galactic Center; the latter case being feasible due to the biased nature of the survey, for which blind searches for transients were restricted to the Galactic Center. Proposed counterparts include a nulling pulsar, a double pulsar, a transient white dwarf pulsar, a precessing radio pulsar or a nearby pulsing brown dwarf or low mass flare star.

A second Galactic Center radio transient source (GCRT J1742-3001) was detected in multiple epochs of a 235 MHz transient monitoring program with the GMRT in 2006 and 2007 (Hy-

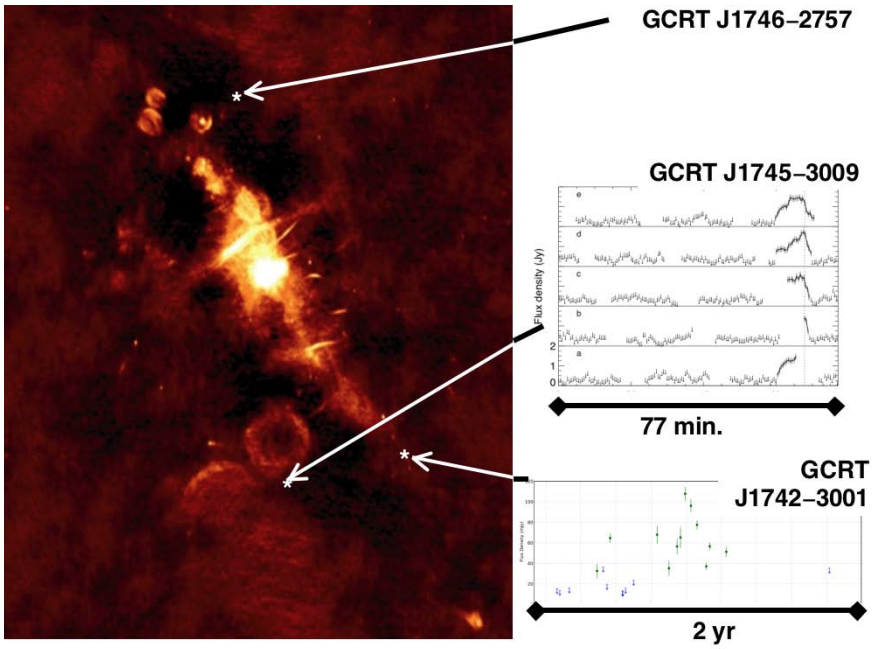

Figure 15: The diversity of the light curves for transients toward the Galactic center Hyman et al. (2002, 2005, 2009). The transient GCRT J1745-3009 burst several times (duration ∼10 minutes) during a 6-hr observation, with subsequent bursts detected over the next 1.5 yr; GCRT J1742-3001 brightened and faded over several months, preceded 6 months earlier by intermittent bursts; and GCRT J1746-2757 was detected in only a single epoch. None of these objects has been identified nor has a multi-wavelength counterpart been found. The background image is the Galactic center at 330 MHz. Figure taken from Lazio et al. (2009).

man et al., 2009). This was a very different class of radio transient, observed to brighten over a period of a month to a maximum of 100 mJy before fading in the subsequent 6 months. Once again, a very steep spectrum ($\alpha = -2$) was inferred. Discovering the frequency, nature and progenitors of these new classes of radio transients will open up new population of exotic objects to astrophysical study with the possibility of such transients being due to previously undetected populations of neutron stars being a particularly exciting possibility. The detection of two new classes of transient in very limited blind searches towards the Galactic Center speaks to the huge potential for discovery associated with monitoring this region of the sky. VLASS will easily probe much deeper than any previous Galactic Center transient surveys. In particular, considering the steep negative spectrum confirmed for GCRT J1745-3009 and GCRT J1742-3001, the possible inclusion of VLITE/LOBO will be key to probing these particular populations as results from previous surveys suggest that the rate of detected transients would be ~ 0.2/hr with the upgraded VLA (Hyman et al., 2009).

C.3 Galactic Science

The following classes of sources are likely to be found by VLASS, but are not considered to drive the survey design.

Thermal Emission from Stellar Winds The thermal emissions from massive stars exhibit rising spectra, with $F_\nu \propto \nu^\alpha$, with $\alpha \sim 0.6$ for free-free emission from an ionized wind. For massive stars, this wind emission is formed further out in the wind than other diagnostics like

Hα or X-ray emission, so has different sensitivities to wind clumping and porosity. While the overall effect of this mass loss from hot stars is also important to a better understanding of how this matter interacts with its environment, the radio wind emission diagnostic is important to a detailed investigation of the wind flows of individual stars, particularly for comparison with measurements at other wavelengths. There are fewer radio-detected massive stars than the total number known: Rubin et al. (1962) cataloged $\sim$ 1300 O–B5 stars within 3 kpc of the Sun within $\pm 5^\circ$ in Galactic latitude. There are only about 65 O–B2 stars with radio detections (Benaglia, 2010), and $\approx$70% of these show thermal emission. It is likely that radio-detected hot thermal wind sources will be among the sources detected in VLASS.

Symbiotic Stars The outflows associated with accreting white dwarf systems (novae, symbiotic systems) produce thermal radio emission, but radio emission has not traditionally been the vehicle for detecting these objects. VLASS can identify additional candidates in these two classes; radio measurements are key to constraining the ejected mass and thus the characteristics of the explosion and the evolution of the white dwarf.

Thermally-Emitting Novae Approximately 35 Galactic novae explode each year, with about half of them occurring in the Galactic bulge (Darnley et al., 2006). Most novae are detected in the optical, and due to the effects of dust and optical incompleteness, usually only about a quarter of the total number are detected.

Radio Emission from Massive Star Stellar Winds About 30% of hot stars with radio detections display evidence of non-thermal spectra, with $\alpha \lesssim 0$; the non-thermal emission is interpreted to be synchrotron emission from colliding winds of a massive star binary (Benaglia, 2010). There is no concensus about formation mechanisms to produce non-thermal radio emission from single OB stars. Recent results indicate that magnetic fields play a heretofore unrealized role in channeling wind emission (Wade et al., 2012), with 6.5% of O and B stars surveyed exhibiting evidence of magnetic fields in their optical spectra.

X-ray Binaries (XRBs) Radio and X-ray measurements of stellar-mass black hole and neutron star binaries in a variety of states reveal a power-law relationship ($L_R \propto L_X^{0.6}$) between these emissions (Miller-Jones et al., 2011), illustrating the fundamental coupling between accretion processes (revealed by the X-ray emission) and the presence and action of a jet (probed by radio emission). More generally, there is also a "fundamental plane" relation for black holes, relating their X-ray emission, radio emission, and the mass of the black hole. New XRBs are identified when they go into an outbursting state, and VLASS will provide an immediate measure (or constraint) on the properties of system.

D The "S/N model" of Positional Accuracy

A long-standing notion has been that as the signal-to-noise ratio (S/N) increases, much better positional accuracy is obtained, so that high angular resolution is not needed for reliable identifications at visible or near-infrared wavelengths. The prediction of what we will call the "S/N model" is that as the flux density increases, the positional error will decrease as $1/S/N$, allowing the optical counterpart to be matched. Specifically, the NVSS catalog description (Condon et al., 1998) gives this formula for the noise in RA or Dec for point sources:

$$\sigma_{1D} = \theta/(S/N\sqrt{2\ln 2}) \quad . \tag{3}$$

Here θ is the resolution FWHM (45″ for NVSS) and S/N is the signal-to-noise ratio. Note that this noise equation already has been increased by an emprical factor of $\sqrt{2}$ compared with the

theoretical equation "to adjust the errors into agreement with the more accurate FIRST positions" (quoting the NVSS catalog description[16]). This predicts $\sigma_{1D} \sim 7.6''$ at the catalog detection limit ($S/N = 5$) and $\sigma_{1D} \sim 1''$ at a flux density of 18 mJy/beam.

The positional scatter in Equation (3) is a 1-dimensional uncertainty, giving the error in either RA or Dec. In a 2-D distribution, many values will scatter outside the 1σ circle. The 90% confidence separation limit σ_{90}, which is typically more appropriate for catalog matching, is a constant factor $\sqrt{2 \ln 10}$ times larger than σ_{1D}:

$$\sigma_{90} = \frac{\theta}{S/N} \sqrt{\frac{\ln 10}{\ln 2}} \quad . \tag{4}$$

With that increase it is necessary for the NVSS flux density to exceed 40 mJy/beam ($S/N = 85$) to reduce the predicted separation error to $1''$.

The above positional accuracy applies to perfect point sources (and perfect data). But how well does it work for real data? We assess the accuracy of the S/N model using a comparison of the FIRST and NVSS data. The NVSS resolution is $45''$ FWHM. The FIRST resolution is $5\farcs4$ FWHM. As a large-scale test, we selected a sample of all the FIRST sources that have an SDSS match within $0\farcs7$ and that have an NVSS match within $100''$. We restricted the sample to sources with FIRST peak flux densities greater than the 2.5 mJy NVSS detection limit. For all these $\sim 95,000$ sources, we computed the distance to the nearest NVSS source. The important thing about this sample is that the FIRST source matches the optical source position. That means that if NVSS is to identify the same counterpart, it needs to have a position close to the FIRST source position. There may be several FIRST source components associated with a single NVSS source, but only the FIRST sources that match optical counterparts are included.

How do the positional errors of the S/N model compare with reality? To test this, Figure 16 shows the distance between the NVSS and FIRST positions as a function of the NVSS flux density. The positional differences do tend to decrease as the flux densities increase. The blue line shows the 90% confidence separation limit σ_{90} from Equation (4), simply assuming that all objects are point sources with the median NVSS rms value. The red histogram shows the empirical 50, 90, 95, and 99% confidence separation limits as a function of flux density, computed by determining the relevant percentile of the actual separations in each bin. The computed separation has been corrected for the effects of chance nearby NVSS associations. *The actual 90% confidence radius is flat all the way past 100 mJy, and it is much larger than the predicted 90% curve.* The empirical separation distribution has many more distant outliers than expected from a Gaussian distribution.

In short, to find 90% of these counterparts using the NVSS positions, it is necessary to use a matching radius of approximately $7''$ ($\sim 0.15\,\theta$) even for sources that are 100 times the rms noise level. The theoretical S/N model predicts that the positions ought to be much more accurate than that ($\sigma_{90} = 0.8''$). To include 95% of the counterparts requires a matching radius of $15''$ ($\sim 0.3\,\theta$), while getting 99% of the counterparts requires matching out to $39''$ ($\sim \theta$).

Why are the low-resolution positions so inaccurate? — Why are the inaccuracies in the positions so much greater than the S/N model predictions? Real radio sources are not symmetrical objects. They have lobes, jets, cores; star-forming galaxies have spiral arms; and there can be confusion where multiple radio sources get mixed together in the low resolution beam. A low resolution survey does indeed provide a measurement, with high accuracy, of the mean flux-weighted position as the S/N increases. **However, the flux-weighted centroid is often not where the optical counterpart lies.** In many cases, the counterpart is associated with some sharp structure within the radio source, and that structure may be far from the flux-weighted center.

Effect on optical identifications — This analysis shows that matching at the $45''$ resolution of NVSS requires a matching radius of $7''$ = 15% of the NVSS FWHM resolution. Our experience

[16] `http://www.cv.nrao.edu/nvss/catalog.ps`

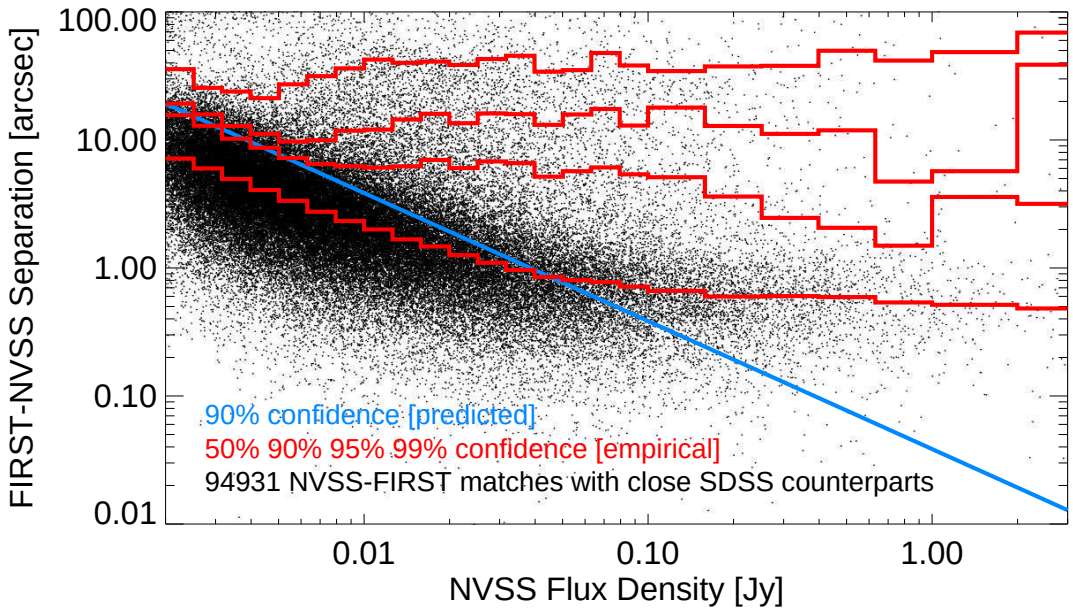

Figure 16: Position difference between NVSS and FIRST positions as a function of NVSS flux density. The sample includes only objects that have a close SDSS counterpart to the FIRST source position (within 0.7″). *Blue line:* Theoretical 90% confidence separation limit computed using the S/N model. *Red histograms:* (from bottom to top) the 50, 90, 95, and 99% confidence limits, computed by determining the actual separations in each bin. While the 50% curve behaves approximately as expected, the tail of the distribution is clearly non-Gaussian and has many more distant outliers than expected based on the 90% prediction.

with the FIRST survey is that an even larger radius is required: to get a reasonably complete list of optical identifications we had to use a matching radius of 2″ $\sim$ 40% of the FIRST FWHM resolution. We argue that is a universal requirement for radio sources: at least for sources down to the sub-mJy regime, the matching radius that is required for realistic radio source morphologies is at least 15% of the FWHM resolution. Achieving 95% complete identifications requires a radius 30% of the FWHM resolution. The resolution for WODAN (which will survey the northern sky accessible to the VLA) is of order 15 $\times$ 17″, while the resolution for ASKAP-EMU is 10″. For 95% completeness, WODAN will therefore require an optical matching radius of 4.8″ and ASKAP-EMU will require 3″.

A cross-match between SDSS and FIRST shows that 19% of FIRST sources have a *false* (chance) SDSS counterpart within 4.8″. For comparison, 33% of FIRST sources have a true match within 2″. The conclusion is that *one-third* of the optical counterparts at SDSS depth will be false matches when using a 4.8″ matching radius.

The number of false matches can be reduced somewhat by doing a careful analysis of the likelihood of association as a function of separation, but when the starting point is contaminated by 33% of false matches, the final list of identifications will not be complete or reliable. The false matching problem will only get worse for deeper optical/IR data. For example, Pan-STARRS is about 1 magnitude fainter than SDSS in the red and also goes into the Galactic plane where the source density is much higher, so it demands better resolution. We have used the measured density of PS1 sources on the sky to compute the likelihood of false identifications in PS1 as a function of Galactic latitude. The left panel of Figure 17 compares the WODAN and VLASS (S-band B-configuration) surveys. For WODAN, 10% of sources even in the extragalactic sky ($|\delta| >$

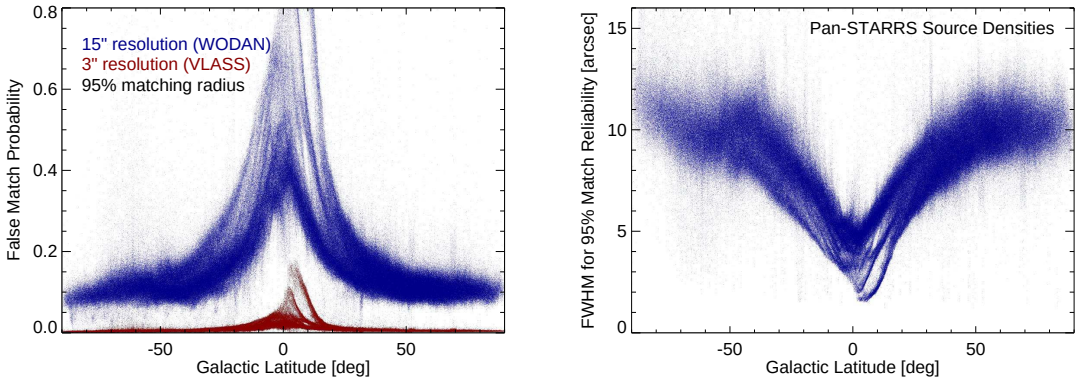

Figure 17: *Left:* Probability of a false match in Pan-STARRS as a function of Galactic latitude. The actual density of PS1 objects was used to calculate the likelihood of a false counterpart within the 95% confidence radius. The plot shows probabilities both for the WODAN 15″ resolution (blue) and VLASS S-band 3″ resolution (red). Over most of the extragalactic sky $\sim$ 10% of WODAN-PS1 cross-matches will be chance coincidences, compared with $<$ 1% of VLASS-PS1 matches. VLASS positions are sufficient for reliable identifications even close to the Galactic plane. *Right:* FWHM resolution required to achieve 95% cross-match reliability in Pan-STARRS as a function of Galactic latitude. In the extragalactic sky ($|\delta| > 30°$) a resolution better than 10″ is required. WODAN does not have the required resolution; ASKAP-EMU just reaches this limit but will not cover most of the northern sky. The VLASS S-band survey easily meets this requirement.

30°) will have a spurious counterpart in PS1. For many purposes that is an unacceptable level of contamination. In contrast, VLASS has only a $<$ 1% contamination rate in the extragalactic sky, and is usable even in the densest parts of the Galactic plane. The right panel of Figure 17 turns this around and asks what FWHM resolution is required to achieve a 95% reliability ($\sim 2\sigma$) in matches to the PS1 catalog. At $|\delta| > 30°$ a FWHM resolution of 11″ is required. That is significantly higher resolution than WODAN and slightly higher than ASKAP-EMU will achieve, but is easily satisfied by VLASS. In fact, VLASS with a resolution of 3″ has 95% confident PS1 matches over 99% of the current PS1 catalog area, with only the most crowded areas of the Galactic plane requiring higher resolution.

The next generation of optical/IR surveys will be deeper than Pan-STARRS. Figure 10 shows the resolution required as a function of magnitude using the *r*-band galaxy counts from the CFHTLS-D1 1 deg^2 survey (Jarvis, private communication). Since this does not include stars or redder galaxies, it is more optimistic (and less realistic) at the Pan-STARRS limit, but it shows the resolution required for deeper identifications. For 90% reliable identifications, VLASS can be used to $r = 27.2$, ASKAP-EMU to $r = 25.3$, and WODAN to $r = 24.3$. For 95% reliable identifications, the magnitude limits are 25.7 (VLASS), 22.9 (ASKAP-EMU), and 21.8 (WODAN). The SKA-precursor surveys are usable at the depth of SDSS and Pan-STARRS in the extragalactic sky, but fall well short of the required resolution at fainter magnitudes and in the crowded Galactic plane. VLASS, by contrast, is useful at least to $r = 26$.

The bottom line is that we need high resolution to get the accurate positions required for optical identifications. Deeper radio imaging is not a substitute for the necessary resolution. VLASS will be the survey of choice for multi-wavelength science, and an all-sky VLASS will have a long and useful life even after the SKA-precursor surveys are complete.